[illegible]

[illegible]

Prepared for

AIR FORCE TECHNICAL APPLICATIONS CENTER
Washington, D.C.

By

[illegible]
SEISMIC DATA LABORATORY

Under

Project VELA UNIFORM

Sponsored by

ADVANCED RESEARCH PROJECTS AGENCY
Nuclear Monitoring Research Office
ARPA Order No. 624

APPROVED FOR PUBLIC RELEASE; DISTRIBUTION UNLIMITED.

Unclassified
Security Classification

DOCUMENT CONTROL DATA - R&D

(Security classification of title, body of abstract and indexing annotation must be entered when the overall report is classified)

1. ORIGINATING ACTIVITY (Corporate author) TELEDYNE GEOTECH ALEXANDRIA, VIRGINIA	2a. REPORT SECURITY CLASSIFICATION Unclassified 2b. GROUP

3. REPORT TITLE

RADIATION OF RAYLEIGH WAVE ENERGY FROM NUCLEAR EXPLOSIONS AND EARTHQUAKES IN SOUTHERN NEVADA

4. DESCRIPTIVE NOTES (Type of report and inclusive dates)

Scientific

5. AUTHOR(S) (Last name, first name, initial)

Massé, Robert P.

6. REPORT DATE 30 March 1971	7a. TOTAL NO. OF PAGES 116	7b. NO. OF REFS 32
8a. CONTRACT OR GRANT NO. F33657-70-C-0941 b. PROJECT NO. VELA T/0706 ARPA Order No. 624	9a. ORIGINATOR'S REPORT NUMBER(S) 266 9b. OTHER REPORT NO(S) (Any other numbers that may be assigned this report)	

APPROVED FOR PUBLIC RELEASE; DISTRIBUTION UNLIMITED.

ns-
nly

ADVANCED RESEARCH PROJECTS AGENCY
NUCLEAR MONITORING RESEARCH OFFICE
WASHINGTON, D. C.

13 ABSTRACT

Amplitudes of Rayleigh waves generated by some southern Nevada nuclear explosions and cavity collapses were analyzed. The Rayleigh amplitude radiation patterns for all the explosions and collapses investigated were found to be similar within the expected variation of 30% due to calibration and measurement errors. The primary factor affecting the Rayleigh amplitude radiation patterns of the explosions was found to be the effect of the earth structure along the travel paths from source to receivers, with the effect of any tectonic strain release being small. The amplitude correction for the travel path to each recording station was determined, and used in the evaluation of the source mechanisms of four southern Nevada earthquakes. Use of the amplitude corrections can improve the estimate of surface wave magnitude.

14. KEY WORDS

Surface wave
Radiation
Magnitude
Attenuation

Unclassified
Security Classification

RADIATION OF RAYLEIGH WAVE ENERGY
FROM NUCLEAR EXPLOSIONS AND EARTHQUAKES
IN SOUTHERN NEVADA

SEISMIC DATA LABORATORY REPORT No. 266

AFTAC Project No.:	VELA T/0706
Project Title:	Seismic Data Laboratory
ARPA Order No.:	624
ARPA Program Code No.:	9F10
Name of Contractor:	TELEDYNE GEOTECH
Contract No.:	F33657-70-C-0941
Date of Contract:	01 April 1970
Amount of Contract:	$ 1,828,736
Contract Expiration Date:	30 June 1971
Project Manager:	Royal A. Hartenberger (703) 836-7647

P. O. Box 334, Alexandria, Virginia

APPROVED FOR PUBLIC RELEASE; DISTRIBUTION UNLIMITED.

This research was supported by the Advanced Research Projects Agency, Nuclear Monitoring Research Office, under Project VELA-UNIFORM and accomplished under technical direction of the Air Force Technical Applications Center under Contract F33657-70-C-0941.

ABSTRACT

Amplitudes of Rayleigh waves generated by some southern Nevada nuclear explosions and cavity collapses were analyzed. The Rayleigh amplitude radiation patterns for all the explosions and collapses investigated were found to be similar within the expected variation of 30% due to calibration and measurement errors. The primary factor affecting the Rayleigh amplitude radiation patterns of the explosions was found to be the effect of the earth structure along the travel paths from source to receivers, with the effect of any tectonic strain release being small. The amplitude correction for the travel path to each recording station was determined, and used in the evaluation of the source mechanisms of four southern Nevada earthquakes. Use of the amplitude corrections can improve the estimate of surface wave magnitude.

TABLE OF CONTENTS

LIST OF FIGURES

LIST OF FIGURES (Cont'd.)

LIST OF FIGURES (Cont'd.)

LIST OF FIGURES (Cont'd.)

LIST OF FIGURES (Cont'd.)

LIST OF FIGURES (Cont'd.)

LIST OF TABLES

INTRODUCTION

The importance of reaching a full understanding of the nature of earthquake and explosion source mechanisms has prompted many source function studies. To investigate the source function, these studies have utilized various properties of seismic waves such as: the first motion of body phases (see the review by Honda, 1962), the phase of surface waves (Aki, 1960a, 1960b, 1960c, 1964a, 1964b; and Ben-Menahem and Toksöz, 1963), and the amplitude of surface waves (Aki, 1964b; Brune and Pomeroy, 1963; Smith, 1963, Toksöz et al, 1964, 1965; and Toksöz and Clermont, 1967).

In the present study, the source mechanisms of some southern Nevada nuclear explosions, cavity collapses, and earthquakes were investigated using amplitudes of long period Rayleigh waves. The amplitudes were measured in the time domain, with usually the cycle with the largest amplitude being selected for measurement. Southern Nevada was chosen as the source area for this study, because it includes the Nevada Test Site (NTS) at which many nuclear explosions have been detonated, and because it is a moderately active seismic region, with most of the earthquakes being of shallow focus. This source area is centered in the western United States, which is a region of great structural complexity.

To employ amplitudes of seismic waves in a study of seismic sources, the effects of the earth's structure between the source and each receiver first must be determined. These effects were found to be considerable, and they indicate variations in the crustal and upper mantle structure between the source area and the stations used in this study.

Source radiation patterns were determined using Rayleigh wave

amplitudes corrected for the source-to-receiver path effect. These source radiation patterns and their implications for magnitude computations are discussed.

RAYLEIGH RADIATION PATTERNS FOR NTS EXPLOSIONS AND COLLAPSES

Rayleigh waves from some NTS explosions recorded by a network of seismic stations were examined to determine if the Rayleigh wave amplitudes measured in the time domain could be represented by the product of an event (source) amplitude factor and a station (total path effect) amplitude factor. This product may be written in the form:

$$A_{ij} = E_i S_j \qquad (1)$$

where A_{ij} is the measured amplitude of a seismic phase recorded at the j'th station for the i'th nuclear explosion, E_i is an event amplitude factor and S_j is a station amplitude factor representing the effect on the measured amplitude of the earth structure along the entire travel path from source to station. If the amplitudes of seismic signals from a set of nuclear explosions satisfy equation (1), it is implied that the explosions will all have essentially <u>the same source radiation pattern</u>, and will differ from each other only in the total amount of energy released. If this radiation pattern which is common to all the explosions is not circular, the station amplitude factors will represent both the path effect due to earth structure and the variation with azimuth in the amount of energy propagating from the source. The magnitudes (m_b) of the explosions and collapses investigated differ from each other by less than 1.5. Therefore spectral changes associated with source yield changes are not significant in the period range being considered (greater than eight seconds). To employ equation (1), the amplitude of the same cycle in the signal need not be measured at all stations for a given explosion, but for a given station the same cycle of

motion must be measured for all explosions.

Amplitudes of Rayleigh waves from the NTS explosions AUK, BILBY, BRONZE, CUP, KLICKITAT, and WAGTAIL were analyzed to determine if equation (1) could be applied. The epicenter coordinates and magnitude (m_b) of each of these explosions are listed in Table I, and their relative locations are shown in Figure 1.

The recording stations used were in the distance range 294 km to 2343 km. Seismic data from stations closer than 294 km were not included in the analysis because the instruments at these close stations were found to be frequently overdriven by the surface waves, with the result that amplitude and period measurements are very unreliable.

The amplitude and period values for the Rayleigh waves were obtained from station films. Figures 2 and 3 give an example of Rayleigh signals from each of the seismic stations used in this study with the cycle measured at each station indicated. At any given station, the Rayleigh signals were found to be similar for all explosions which were of sufficient magnitude to be recorded with a high signal-to-noise ratio. (The only possible exception we have found is Hardhat at HL-ID which is discussed in a later section.) The similarity in signal waveform is shown in Figure 4 for the seismic stations DR-CO and WO-AZ. The signals given in Figures 2 and 3 therefore serve as an example of the Rayleigh signal from an NTS explosion recorded at each of the stations used in this study. Because of the similarity of the Rayleigh signals, the difference between periods measured for all explosions at any given station was usually less than two seconds as shown by the tabulated measurements for each event given in the appendix.

Errors in amplitude and period measurement of the Rayleigh

signals can be quite large, and can arise from several sources. The field calibration of the instruments is usually not claimed to be better than ± 15%, and may be worse. Reading errors and errors due to the presence of seismic noise also contribute to the total measurement error. It was found that only a small amount of seismic noise was sufficient to cause an error in the measured period of one or more seconds. The correction for the amplitude response of the seismograph system can be greatly in error if the measured period is in error. The percent error in the instrument-corrected amplitude value due to a ± 1.0 second error in the period is shown in Figure 5 for the LRSM long-period system. The importance of obtaining accurate period measurements is evident. von Seggern (1969) also noted the errors introduced in making period measurements. Based on Figure 5, we consider the uncertainty in the calculated amplitudes to be ± 30 per cent for most stations. Calculation of spectral amplitudes from calibrated seismic data would eliminate some of this uncertainty, but this process is very time consuming if many signals are to be analyzed.

All Rayleigh amplitudes were scaled by $(\sin\Delta)^{1/2}$ where Δ is the great circle distance between epicenter and station. The factor $(\sin\Delta)^{1/2}$ is an amplitude correction for spreading of surface waves over a sphere. This correction is not necessary for the determination of the Rayleigh wave radiation patterns if the present analysis technique is used, and so application of this scale factor is arbitrary.

To determine event amplitude factors E_i and station amplitude factors S_j from a set of measured amplitudes A_{ij}, equation (1) was written in logarithmic form:

$$\ln A_{ij} = \ln E_i + \ln S_j \qquad (2)$$

Using equation (2) for each station recording each event considered, the least squares solution for the terms $\ln E_i$ and $\ln S_j$

was determined. The stations used in the analysis for each explosion are shown in Figures 6 through 11. These figures also show the total number of stations recording long period data in the distance range under consideration and indicate why some data was not available for measurements. Each station had to record at least two of the explosions being analyzed to be included in the station amplitude factor determination procedures. Because of the error introduced in the measurement of the periods, equations (2) were not only solved using values of A_{ij} corrected for the instrumental (period) response but also using values of A_{ij} with no correction for instrumental response (the amplitudes were of course still corrected for the gain of the seismograph system at its calibration period of 25 seconds). This procedure is valid since the instrumental response remained the same at each station and since there is an obvious similarity of signals from all explosions recorded at any given station.

The event amplitude factors E_i and station amplitude factors S_j determined with equation (2) were scaled by arbitrarily setting the station amplitude factor for DR-CO to a value of 50. The scaled event amplitude factors for the cases of A_{ij} both corrected and not corrected for instrumental response are presented in Table II along with the corresponding Rayleigh wave station amplitude factors.

For each nuclear explosion, the adjusted amplitudes A'_{ij} were formed, where

$$A'_{ij} = A_{ij}/E_iS_j \tag{3}$$

The adjusted amplitude patterns for the explosions are shown in Figures 12 through 17 for A_{ij} corrected for instrumental response and in Figures 18 through 23 for A_{ij} not corrected for instrumental response.

The patterns computed using station amplitudes corrected for instrumental response (Figures 12 through 17) do not deviate from a unit circle to an extent greater than that which can be attributed to the measurement and calibration errors. This indicates that the Rayleigh wave source radiation patterns of the explosions investigated are identical to within the expected error in amplitude and so application of equation (1) is legitimate. One dominant type of source mechanism seems to be generating most of the observed Rayleigh wave energy for the nuclear explosions studied. As noted previously, this common radiation pattern may not be circular.

Employing station amplitudes not corrected for instrumental response in the calculation of amplitude radiation patterns (Figures 18 through 23) decreases the deviation of the data points from the unit circle. The consistency of this reduction of scattering about the unit circle for each explosion is in agreement with the observation of the similarity of Rayleigh signals at each station and is a further indication that errors are being introduced in making the period measurements.

The same analysis technique used to investigate the radiation patterns of the nuclear explosions AUK, BILBY, BRONZE, CUP, KLICKITAT, and WAGTAIL was next applied to two events: BILBY and the BILBY collapse. Since these two events were analyzed using a least squares procedure with equation (2), only those stations receiving signals from both BILBY and the BILBY collapse with a usable signal-to-noise ratio could be included in the determination of the event and station amplitude factors. These stations are shown in Figures 24 and 25.

Rayleigh signals from the collapse of a nuclear explosion are known to be 180° out of phase with the Rayleigh signals generated by the explosion itself (Brune and Pomeroy, 1963;

Smith, 1963; and Toksöz et al, 1964). Examples of this phase relationship are shown in Figure 26 for three nuclear explosion-collapse pairs with the collapse signal shifted 180°. Measurements of all collapse signals were made therefore only after first shifting these signals through 180°. The same cycle of motion as measured for the signal from a nuclear explosion at any given station was then also measured for the signal from a collapse. The similarity of the Rayleigh explosion and collapse signals as shown in Figure 26 indicates a similarity in the spectra of the two events in the period range of ten to twenty seconds. At periods shorter than ten seconds, explosions generate relatively more energy than collapses.

Using equation (2), event amplitude factors E_i and station amplitude factors S_j were determined and scaled by setting the station amplitude factor for DR-CO to a value of 50. The scaled event amplitude factors for BILBY and the BILBY collapse determined by solving equation (2) using first A_{ij} values corrected and then A_{ij} values not corrected for instrumental response are given in Table III together with the corresponding Rayleigh wave station amplitude factors. Comparison of these station amplitude factors with those given in Table II shows agreement to within the expected error, with better agreement existing between the amplitude factors computed with no correction for instrumental response.

The event amplitude factors and station amplitude factors were used to determine the adjusted amplitude values A'_{ij} defined by equation (3). These values were then plotted giving amplitude patterns which are shown in Figures 27 and 28 for A_{ij} corrected for instrumental response and in Figures 29 and 30 for A_{ij} not corrected for instrumental response. These patterns do not deviate from a unit circle more than the expected error in the individual

amplitudes, and so the radiation pattern of the explosion can be considered to be the same as that of the collapse to within the measurement error. This similarity between the explosion and the collapse radiation patterns indicates that very little tectonic strain release in the form of Rayleigh wave energy occurred during the nuclear explosion since cavity collapses are believed to release little if any tectonic strain energy. The tectonic component of energy in the Rayleigh waves from the BILBY explosion must then be less than 40%. This agress with the observed similarity in the waveform between signals generated by BILBY and signals generated by the BILBY collapse (shifted 180°). Argument for a tectonic strain component in the Rayleigh wave signals generated by BILBY would be principally for the purpose of explaining the observed Love waves generated by the explosion (e.g. Toksöz and Clermont, 1967, Lambert et al, 1970c). The tectonic component in the Rayleigh wave signals for the BILBY explosion was found to be approximately 33% by Toksöz and Clermont (1967) and Lambert et al (1970c) using theoretically computed Love to Rayleigh amplitude ratios. It is not known at present whether tectonic strain release is the mechanism producing the Love waves (Kisslinger et al, 1961; Press and Archambeau, 1962; Kim and Kisslinger, 1967; Geyer and Martner, 1969; and Archambeau and Sammis, 1970).

The similarity previously found between the radiation pattern of BILBY and the AUK, BRONZE, CUP, KLICKITAT, and WAGTAIL radiation patterns indicates that the Rayleigh wave signals from these explosions also had little if any tectonic component. This is in agreement with the similarity in waveform of Rayleigh waves from all these explosions as recorded at any given station. Therefore the station amplitude factors S_j determined for these explosions can be considered to represent primarily the effect of

earth structure along the travel path on the observed amplitudes with the effect of an azimuthally dependent source radiation pattern being minor. The variation in these station amplitude factors is evidence then for the strong influence of a complex earth structure on the amplitudes of Rayleigh waves in the nine to twenty second period range. Computation of the true amplitude response of the earth along a given path by theoretical means through the use of an earth model (e.g. Toksöz et al, 1964) thus becomes very difficult and will probably fail to predict many of the observed amplitude variations. In particular, there are observations in the western United States of apparent negative Q (where amplitudes increase with distance, probably due to refracted energy), which are not predicted by most models. An example of such apparent negative Q may be found along the eastern profile from the RULISON explosion detonated in western Colorado. (Lambert and Ahner, 1970a.)

An explosion believed to be accompanied by a large release of tectonic strain is the HARDHAT explosion (Brune and Pomeroy, 1963; Aki, 1964b; and Toksöz et al, 1964). Although a large number of LRSM stations recorded the HARDHAT explosion, many of these stations did not record any other large NTS explosions. The nuclear explosion AARDVARK was recorded by a number of the same stations which recorded HARDHAT (Figures 31 and 32) and so AARDVARK and HARDHAT were selected to be analyzed together, following the same procedure as previously described. Unfortunately the signal to noise ratios for AARDVARK and HARDHAT Rayleigh signals are not as high as for many of the larger events (see the HARDHAT Rayleigh signals in Figure 33).

In the analysis the station amplitude factor for DR-CO was again set equal to 50. The event amplitude factors and the station amplitude factors are given in Table IV. The radiation patterns

determined are shown in Figures 34 and 35 for A_{ij} corrected for instrumental response and in Figures 36 and 37 for A_{ij} not corrected for instrumental response. These patterns show some scatter which is less in the case of no instrumental correction to A_{ij}. The points in brackets indicate a poor signal-to-noise ratio for the PT-OR HARDHAT signal.

The Rayleigh amplitudes considered by themselves do not seem to require a large tectonic component of energy. However, the Rayleigh signals from HARDHAT received at stations to the north (e.g. HL-ID and PT-OR) and to the southwest of NTS may be 180° out of phase with respect to Rayleigh signals recorded at the same stations from other explosions (Toksöz, et al, 1964). The HARDHAT Rayleigh signal recorded at HL-ID (Figure 33) when compared to the HL-ID recording shown in Figure 2 seems to be out of phase. The only reasons for adding a significant tectonic force to the explosive source are this phase reversal and the fact that Love waves were generated by the HARDHAT explosion. The Rayleigh amplitude pattern apparently was not greatly influenced by this tectonic component. This is in agreement with theory, which suggests that for a horizontal strike-slip fault, much more Love wave than Rayleigh wave energy will be generated in most directions from the source (S.S. Alexander, personal communication).

As a further investigation of the amplitude patterns for collapses, the following set of events was chosen: CORDUROY collapse, DUMONT collapse, HALF BEAK collapse and DUMONT explosion. These events were analyzed using the same techniques previously described. Since DR-CO was not one of the stations recording these events, the station amplitude factor for TFO was scaled to be the same as given in Table II in order to make the station amplitude factors for this set of events

compatible with the station amplitude factors previously determined for other sets of events (i.e., with the factors given in Tables II, III and IV). The stations used in the analysis are shown in Figures 38 through 41. The event amplitude factors and the station amplitude factors determined are listed in Table V. Radiation patterns computed with A_{ij} corrected for instrumental response are shown in Figures 42 through 45 and with A_{ij} not corrected for instrumental response in Figures 46 through 49.

Figures 42 through 45 show the CORDUROY collapse, HALF BEAK collapse and DUMONT explosion to have the same amplitude radiation pattern, and the DUMONT collapse to have some deviation from a unit circle in the northeast direction. The amplitude radiation patterns computed with no instrumental correction to the A_{ij} values (shown in Figures 46 through 49) differ less from a unit circle than the radiation patterns given in Figures 42 through 45. The deviation of the DUMONT collapse amplitude pattern (Figure 47) from a unit circle is also less. Therefore, with the possible exception of the DUMONT collapse, no significant difference between the explosion and the collapse amplitude radiation patterns for Rayleigh waves in the 9 to 20 second period range was found.

Since the station amplitude factors determined represent primarily the effect of the crustal and upper mantle structure on the amplitudes of Rayleigh waves propagating from southern Nevada, contours of these amplitude factors should indicate the actual amplitude "attenuation" to be expected for a Rayleigh wave propagating from the southern Nevada area. The Rayleigh wave amplitudes seem to be very dependent on the crust and upper mantle structure, and so the term attenuation is employed here to mean the actual decay in the amplitude of a Rayleigh signal

due to all the effects of earth structure along the path from southern Nevada to the recording station. Station amplitude factors for measured signals with periods of 12-13 seconds (within the range of 11.5 to 14.0 seconds) were contoured and are shown in Figure 50. These contours show a lower attenuation in the northeast direction between the Northern and Southern Rocky Mountain Ranges and in the southeast direction across the Colorado Plateau and through northern New Mexico and Texas. A region of high attenuation exists in central Arizona. For Rayleigh waves propagating across this region, the earth would appear to have a negative Q because of the amplitudes recorded at stations beyond this region being larger than the amplitudes recorded within the region. The contours in the northeast direction are not as certain as those in the southeast because of the smaller amplitude differences between the northeast station factors. If the density of stations were greater, more detailed structural variations would probably be evident. The strong influence of the structure on the amplitudes of surface waves has been noted previously by Pasechnik (1962) in a study of body and surface wave amplitudes measured at Russian stations. He found that the nature of the geological structure in the district of the recording station affected the magnitude determined from the surface waves.

The velocity of S waves in the crust and upper mantle can be expected in general to be low where there is high Rayleigh wave attenuation and high were there is low attenuation. Contours of S wave time anomalies (adapted from Hales and Roberts, 1970) are shown in Figure 51 together with the Rayleigh wave station amplitude factor contours. There is a strong agreement in the low attenuation-high velocity region in the northeast direction from NTS and in the high attenuation -- low velocity region in central Arizona. Both LRSM and WWSSN stations were used in the

Hales and Roberts study. Although Hales and Roberts used a greater number of stations, they did not find much more complexity in earth structure than is shown in our station amplitude factor contours. The more significant seismic features of the Western United States are probably revealed by Figures 50 and 51 (e.g. the high and the low attenuation regions discussed above).

RAYLEIGH RADIATION PATTERNS FOR SOME SOUTH NEVADA EARTHQUAKES

Rayleigh wave amplitudes were used to investigate the radiation patterns of four southern Nevada earthquakes. The locations of these events are shown in Figure 1, and their coordinates (from the USC&GS) are given in Table VI. The earthquake amplitudes were scaled by $(\sin\Delta)^{1/2}$ and adjusted amplitudes were then computed using equation (3) with the event scale factors E_i set equal to one and the station amplitude factors S_j taken from Tables II and V. In this way the effect on the Rayleigh amplitudes of the path from southern Nevada to each of the stations was removed. The stations recording Rayleigh signals for each of the four earthquakes are shown in Figure 52. Figure 53 shows the Rayleigh signal recorded at CR-NB for each of the earthquakes with the time of measurement indicated. The adjusted amplitude patterns are given in Figures 54 through 57. Except for the earthquake of 18 August 1966 (09:15Z), the Rayleigh signals measured at each station had approximately the same period as signals from NTS explosions measured at these stations (see the period values given in the Appendix). For the 18 August 1966 (09:15Z) earthquake, longer periods were measured for the Rayleigh signals recorded at TFO, WN-SD and RK-ON.

The amplitude patterns given in Figures 54 through 57 are similar to each other, indicating that the source mechanisms of the earthquakes are also similar. The radiation pattern for each earthquake has a pronounced lobe in the northeast and in the southeast direction. Except for the 18 August 1966 (09:15Z) earthquake, the radiation patterns using amplitudes corrected for the instrumental response show the same patterns as obtained using amplitudes not corrected for instrumental response. The

source radiation pattern of each of the earthquakes is obvious from the Figures 54 through 57 with the superimposed "structural" radiation pattern having been removed. The ratio of the largest to smallest amplitude for each source radiation pattern is much greater for the earthquakes than for any of the explosions investigated. Therefore, the true source radiation pattern for Rayleigh amplitudes appears to be a good discriminant between explosions and earthquakes occurring in southern Nevada.

SURFACE WAVE MAGNITUDE

A better estimate of the magnitude of an earthquake or an explosion can be attained if the variations in the measured seismic wave amplitudes due to lateral differences in physical properties of the crust and upper mantle can be removed. Using the station amplitude factors (Tables II, III, IV, and V) and equation (3), the effect on surface wave amplitudes of earth structure can be eliminated for any southern Nevada event. The same technique is of course applicable to any region which has been "calibrated" by nuclear explosions.

As seen from the explosion and collapse amplitude patterns, the average deviation from a unit circle in the adjusted amplitudes is less than $\pm$ 30 per cent. We may assume this to be the 2σ level. Therefore with 95% confidence the logarithm of an event amplitude factor for an explosion or collapse will be within the range.

$$\log \left(E_i - \frac{0.33}{\sqrt{N}} E_i\right) \text{ to } \log \left(E_i + \frac{0.33}{\sqrt{N}} E_i\right) \qquad (4)$$

where N is the number of stations used.

In Figure 58, all event amplitude factors for explosions computed using measured amplitudes corrected for instrumental response are presented, and the best fit straight line is:

$$\log E_i = 1.46\, m_b - 6.37 \qquad (5)$$

where the m_b values have been obtained from the shot reports (Air Force Technical Applications Center, 1962; Clark, 1963a,b; 1965a,b,c; 1966a,b,c). The same event amplitude factors are plotted against Evernden's adjusted body wave magnitudes m_b^e (Evernden, 1967) in

Figure 59, with the best fit straight line:

$$\log E_i = 1.24\ m_b^e - 4.90 \tag{6}$$

Equation (6) is therefore a relation between magnitudes computed using body wave amplitudes corrected for local changes in earth structure and event amplitude factors calculated using Rayleigh amplitudes corrected for the effect of structure along the travel path. A relationship may be similarly attained (Figure 60) between the event amplitude factors and adjusted surface wave magnitudes M_s (Von Seggern, 1969):

$$\log E_i = 1.17\ M_s - 3.86 \tag{7}$$

Using Equations (6) and (7), a relationship between the magnitudes M_s and m_b can be derived with both magnitudes being adjusted for distances less than 15°:

$$M_s = 1.06\ m_b^e - 0.89 \tag{8}$$

This relationship may be compared with that found by Lambert and Alexander (1970b):

$$M_s = 1.04\ m_b^e - 0.74 \tag{9}$$

Marshall (1970) derived from theoretical considerations, using a homogeneous semi-infinite solid with the properties of granite as an Earth model, the relation:

$$M = 1.0\ m_b - 1.6 \tag{10}$$

where M is the surface wave magnitude determined for distances greater than 15°.

From the range of values given in equation (4), it can be seen that the m_b^e and M_s values for all explosions obtained from equations (6) and (7) (assuming the slopes and intercepts to be correct) will be (with probability 95%) within -0.08 to + 0.07 of the true value for N equal to 4. This is better by a factor of five than many of the m_b determinations given in the shot reports. Analysis of a large number of NTS explosions using a greater number of stations should, of course, result in a more accurate slope and intercept values for equations (6) and (7) and a smaller range of values for the event amplitude factors.

The source radiation pattern of an earthquake along with the seismic station distribution about the source can strongly affect the magnitude assigned to the earthquake (Von Seggern, 1970). Perhaps the best method of attaining the magnitude of an earthquake is by first determining the source radiation pattern. Again, this can best be accomplished if the effect of the earth structure along the travel path has been eliminated from the amplitude values.

CONCLUSIONS

For all the southern Nevada explosions and collapses investigated, it was found that the Rayleigh wave amplitude recorded at any given station could be represented by the product of an event amplitude factor and a station amplitude factor. The station amplitude factors were determined to represent primarily the effect of earth structure along the travel path on the observed amplitudes, with any non-circular source radiation pattern having a minor influence. The Rayleigh wave amplitude radiation patterns for all the explosions and collapses were found therefore to be similar within the expected variation of 30% due to calibration and measurement errors. Contours of the station amplitude factors reveal the actual Rayleigh wave attenuation across the western United States for seismic sources in southern Nevada. Amplitude radiation patterns (corrected for the effect of the earth structure along the travel paths) of four southern Nevada earthquakes reveal strong lobes in the northeast and southeast directions. Application of the station amplitude factors to all measured Rayleigh signals from events in the southern Nevada region should reduce the scatter of the amplitude values and allow a better estimate of event magnitude to be made. Determination of the true source radiation pattern (found by eliminating the superimposed "structural" radiation pattern) should serve as a discriminant between earthquakes and explosions. In future studies, in order to obtain as a function of frequency the station amplitude factors and also, therefore, the attenuation across a given region, spectral amplitudes should be computed for each Rayleigh signal.

ACKNOWLEDGEMENTS

We wish to thank S.S. Alexander, R.R. Blandford, J.N. Brune, D.G. Harkrider, D.G. Lambert and R.H. Shumway for valuable discussions. We are also grateful to J.E. Dunavant for assistance in obtaining the Rayleigh amplitude measurements.

REFERENCES

Aki, K., 1960a, Study of earthquake mechanism by a method of phase equalization applied to Rayleigh and Love waves, J. Geophys. Res., v. 65, p. 729-740.

Aki, K., 1960b, Interpretation of source functions of circum-Pacific earthquakes obtained from long-period Rayleigh waves, J. Geophys. Res., v. 65, p. 2405-2417.

Aki, K., 1960c, The use of long-period surface waves in the study of earthquake mechanism, Pub. of Dom. Obs. Ottawa, v. 24, p. 371-372.

Aki, K., 1964a, Study of Love and Rayleigh waves from earthquakes with fault plane solutions or with known faulting. Part 1. A phase difference method based on a new model of earthquake source, Bull. Seism. Soc. Am., v. 54, p. 511-527.

Aki, K., 1964b, A note on surface wave generated from the HARDHAT nuclear explosion, J. Geophys. Res., v. 69, p. 1131-1134.

Air Force Technical Applications Center, 1962, Long range seismic measurements - HARDHAT, HQ. USAF (AFTAC), Washington, D.C.

Ben-Menahem, A., and Toksöz, M.N., 1963, Source mechanism from spectrums of long-period surface waves. 2. Kamchatka earthquake of November 4, 1952, J. Geophys. Res., v. 68, p. 5207-5222.

Brune, J.N., and Pomeroy, P.W., 1963, Surface wave radiation patterns for underground nuclear explosions and small magnitude earthquakes, J. Geophys. Res., v. 68, p. 5005-5028.

Clark, D.M., 1963a, Long range seismic measurements - AARDVARK, UED Earth Sciences Division, Teledyne, Inc.

Clark, D.M., 1963b, Long range seismic measurements - BILBY, UED Earth Sciences Division, Teledyne, Inc.

Clark, D.M., 1965a, Long range seismic measurements - KLICKITAT, UED Earth Sciences Division, Teledyne, Inc., Seismic Data Laboratory Report No. 131.

Clark, D.M., 1965b, Long range seismic measurements - BRONZE, UED Earth Sciences Division, Teledyne, Inc.

Clark, D.M., 1965c, Long range seismic measurements - WAGTAIL, UED Earth Sciences Division, Teledyne, Inc., Seismic Data Laboratory Report No. 122.

Clark, D.M., 1966a, Long range seismic measurements - AUK, UED Earth Sciences Division, Teledyne, Inc., Seismic Data Laboratory Report No. 134.

Clark, D.M., 1966b, Long range seismic measurements - CUP, UED Earth Sciences Division, Teledyne, Inc., Seismic Data Laboratory Report No. 136.

Clark, D.M., 1966c, Long range seismic measurements - DUMONT, Earth Sciences Division, Teledyne, Inc., Seismic Data Laboratory Report No. 160.

Clark, D.M., 1966d, Long range seismic measurements - HALF BEAK, Earth Sciences Division, Teledyne, Inc., Seismic Data Laboratory Report No. 171.

Evernden, J.F., 1967, Magnitude determination at regional and near-regional distances in the United States, Bull. Seism. Soc. Am., v. 57, p. 591-639.

Hales, A.L., and Roberts, J.L, 1970, The travel times of S and SKS, Bull. Seism. Soc. Am., v. 60, p. 461-489.

Honda, H., 1962, Earthquake mechanism and seismic waves, J. of Phys. of the Earth, v. 10, p. 1-97.

Lambert, D.G., and Ahner, R.O., 1970a, Seismic analysis of the RULISON explosion (Appendix 8), Teledyne Geotech, Seismic Data Laboratory Report No. 255, Alexandria, Virginia.

Lambert, D.G. and Alexander, S.S., 1970b, Relationship of Rayleigh and body wave magnitudes for small earthquakes and explosions, Teledyne Geotech, Seismic Data Laboratory Report No. 245, Alexandria, Virginia.

Lambert, D.G., Flinn, E.A., and Archambeau, C.B., 1970c, Seismic radiation and source parameters for earthquakes and underground explosions, Teledyne Geotech, (in preparation), Alexandria, Virginia

Marshall, P.D., 1970, Aspects of the spectral differences between earthquakes and underground explosions, Geophys. J.R. Astr. Soc., v. 20, p. 397-416.

Pasechnik, I.P., 1962, The dependence of earthquake magnitude on the seismogeological features in the district of the observations, Izvestia, Geophys. Ser., p. 937-943, English edition.

Reakes, R.G., Simons, R.S., Frye, W.H., Craig, L.F., and Chiled, A.S., 1966, Long range seismic measurements - CORDUROY, Teledyne Geotech, Geotech Technical Report No. 66-43, Garland, Texas

Smith, S.W., 1963, Generation of seismic waves by underground explosions and the collapse of cavities, J. Geophys Res., v. 68, p. 1477-1483.

Toksöz, M.N., Ben-Menahem, A., and Harkrider, D.G., 1964, Determination of source parameters of explosions and earthquakes by amplitude equalization of seismic surface waves, 1. Underground nuclear explosions, J. Geophys. Res., v. 69, p. 4355-4366.

Toksöz, M.N., Harkrider, D.G., and Ben-Menahem, A., 1965, Determination of source parameters by amplitude equalization of seismic surface waves. 2. Release of tectonic strain by underground nuclear explosions and mechanisms of earthquakes, J. Geophys. Res., v. 70, p. 907-922.

Toksöz, M.N., and Clermont, K., 1967, Radiation of seismic waves from the BILBY explosion, Teledyne Geotech, Seismic Data Laboratory Report No. 183, Alexandria, Virginia.

Von Seggern, D.H., 1969, Surface-wave amplitude-versus-distance relation in the western United States, Teledyne Geotech, Seismic Data Laboratory Report No. 249, Alexandria, Virginia.

Von Seggern, D.H., 1970, The effects of radiation patterns on magnitude estimates, Bull. Seism. Soc. Am., v. 60, p. 503-516.

TABLE I

Source Parameters of Some South Nevada Nuclear Explosions

EVENT	NORTH LATITUDE	WEST LONGITUDE	DATE	TIME	GEOLOGIC MEDIUM	MAGNITUDE m_b
AARDVARK	37°03'55.0"	116°01'49.0"	12 May 62	19:00:00.1	TUFF	4.9
AUK	37°04'41.0"	116°00'31.0"	02 Oct 64	20:03:00.0	TUFF	4.89 ± 0.34
BILBY	37°03'38.0"	116°01'18.0"	13 Sep 63	17:00:00.1	TUFF	5.8
BILBY COLLAPSE	37°03'38.0"	116°01'18.0"	13 Sep 63	17:31:20.5	TUFF	4.5
BRONZE	37°05'52.0"	116°01'59.0"	23 Jul 65	17:00:00.0	TUFF	5.22 ± 0.32
CORDUROY COLLAPSE	37°09'53.0"	116°03'08.0"	03 Dec 65	15:19:08.1	TUFF	4.5
CUP	37°08'51.0"	116°02'34.0"	26 Mar 65	15:34:08.2	TUFF	5.25 ± 0.34
DUMONT	37°06'40.0"	116°03'29.0"	19 May 66	13:56:28.1	TUFF	5.48 ± 0.56
DUMONT COLLAPSE	37°06'40.0"	116°03'29.0"	19 May 66	15:37:28.0	TUFF	Not Given
HALF BEAK COLLAPSE	37°18'57.0"	116°17'56.0"	01 Jul 66	01:33:00.1	RHYOLITE	Not Given
HARDHAT	37°13'35.0"	116°03'34.0"	15 Feb 62	18:00:00.1	GRANITE	4.9
KLICKITAT	37°09'03.0"	116°02'24.0"	20 Feb 64	15:30:00.1	TUFF	4.95 ± 0.40
WAGTAIL	37°03'52.0"	116°02'14.0"	03 Mar 65	19:13:00.0	TUFF	5.33 ± 0.40

TABLE II

Station and Event Amplitude Factors for Rayleigh Waves Computed for Stations Recording the Nuclear Explosions AUK, BILBY, BRONZE, CUP, KLICKITAT and WAGTAIL

Station	Station Amplitude Factor (Instrumental Correction made to A_{ij})	Station Amplitude Factor (Instrumental Correction not made to A_{ij})
BX-UT	69.1	70.8
CP-CL	164.5	65.6
DR-CO	50.0	50.0
FR-MA	45.2	29.1
GE-AZ	133.5	58.7
GV-TX	96.4	62.0
HL-ID	59.0	41.4
HR-AZ	216.0	67.9
JR-AZ	79.7	75.9
LC-NM	193.8	73.4
LG-AZ	89.6	75.7
NL-AZ	171.2	87.6
RK-ON	28.7	15.2
RT-NM	49.1	42.2
SG-AZ	204.7	62.3
SK-TX	29.9	36.5
SN-AZ	155.0	58.6
TFO	49.1	48.7
WO-AZ	165.2	78.2

Event	Event Amplitude Factor (Instrumental Correction made to A_{ij})	Event Amplitude Factor (Instrumental Correction not made to A_{ij})
AUK	4.83	2.74
BILBY	142.19	76.89
BRONZE	20.97	12.05
CUP	16.14	8.51
KLICKITAT	9.63	4.60
WAGTAIL	14.46	7.60

TABLE III

Station and Event Amplitude Factors for Rayleigh Waves Computed for Stations Recording the Nuclear Explosion BILBY and the BILBY Collapse

Station	Station Amplitude Factor (Instrumental Correction made to A_{ij})	Station Amplitude Factor (Instrumental Correction not made to A_{ij})
CP-CL	131.4	56.6
MV-CL	133.5	57.6
BX-UT	61.8	64.3
DR-CO	50.0	50.0
HL-ID	75.1	43.3
RT-NM	50.3	45.9
FR-MA	49.2	37.9
TK-WA	35.2	35.0
SK-TX	36.0	37.6
DU-OK	23.9	28.8

Event	Event Amplitude Factor (Instrumental Correction made to A_{ij})	Event Amplitude Factor (Instrumental Correction not made to A_{ij})
BILBY	141.52	77.15
BILBY COLLAPSE	8.96	6.31

TABLE IV

Station and Event Amplitude Factors for Rayleigh Waves Computed for Stations Recording the Nuclear Explosions AARDVARD and HARDHAT

Station	Station Amplitude Factor (Instrumental Correction made to A_{ij})	Station Amplitude Factor (Instrumental Correction not made to A_{ij})
DR-CO	50.0	50.0
HL-ID	46.7	43.2
PT-OR	70.6	62.7
LC-NM	218.1	98.2
LP-TX	78.9	78.9

Event	Event Amplitude Factor (Instrumental Correction made to A_{ij})	Event Amplitude Factor (Instrumental Correction not made to A_{ij})
AARDVARK	11.19	4.49
HARDHAT	3.12	1.64

TABLE V

Station and Event Amplitude Factors for Rayleigh Waves Computed For Stations Recording the Collapse of the Nuclear Explosions CORDUROY, DUMONT, and HALF BEAK and the DUMONT Explosion

Station	Station Amplitude Factor (Instrumental Correction made to A_{ij})	Station Amplitude Factor (Instrumental Correction not made to A_{ij})
CR-NB	105.8	71.3
JP-AT	76.2	49.7
KC-MO	57.1	55.4
RG-SD	63.4	48.0
SW-MA	52.1	36.5
TFO	49.1	48.7
WN-SD	32.2	42.2

Event	Event Amplitude Factor (Instrumental Correction made to A_{ij}	Event Amplitude Factor (Instrumental Correction not made to A_{ij}
CORDUROY COLLAPSE	13.24	6.46
DUMONT COLLAPSE	9.35	5.81
HALF BEAK COLLAPSE	12.93	8.44
DUMONT	42.67	19.39

TABLE VI

Source Parameters of Some South Nevada Earthquakes

North Latitude	West Longitude	Date	Time	Magnitude m_b	Depth km
37°18'	114°06'	18 Aug 66	09:15:34.9	5.1	9
37°24'	114°12'	18 Aug 66	17:35:06.4	5.2	33
37°24'	114°06'	19 Aug 66	10:51:38.5	4.5	11
37°18'	114°12'	22 Aug 66	08:27:30.2	4.8	33

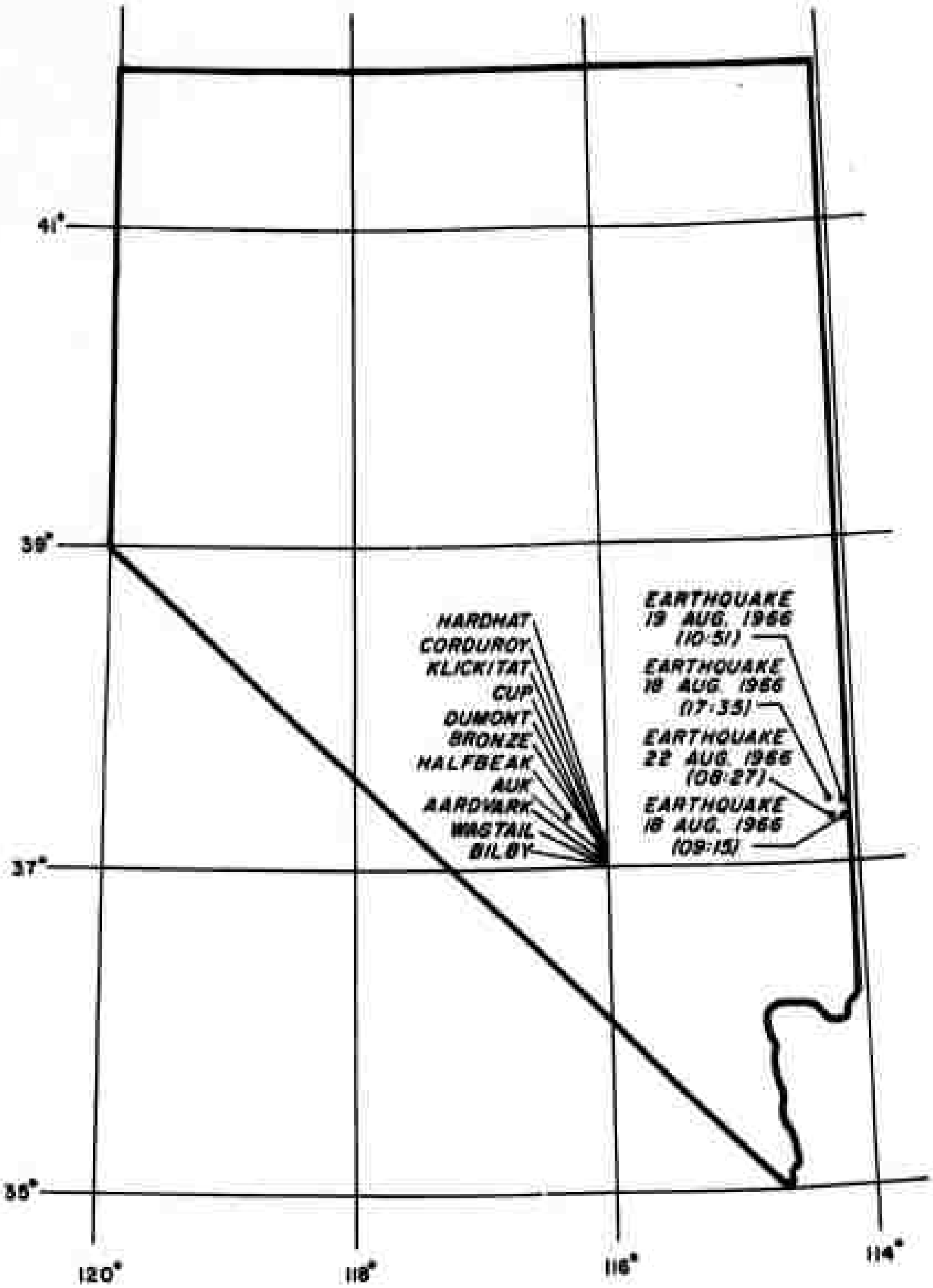

Figure 1. Epicenters of some south Nevada nuclear explosions and earthquakes.

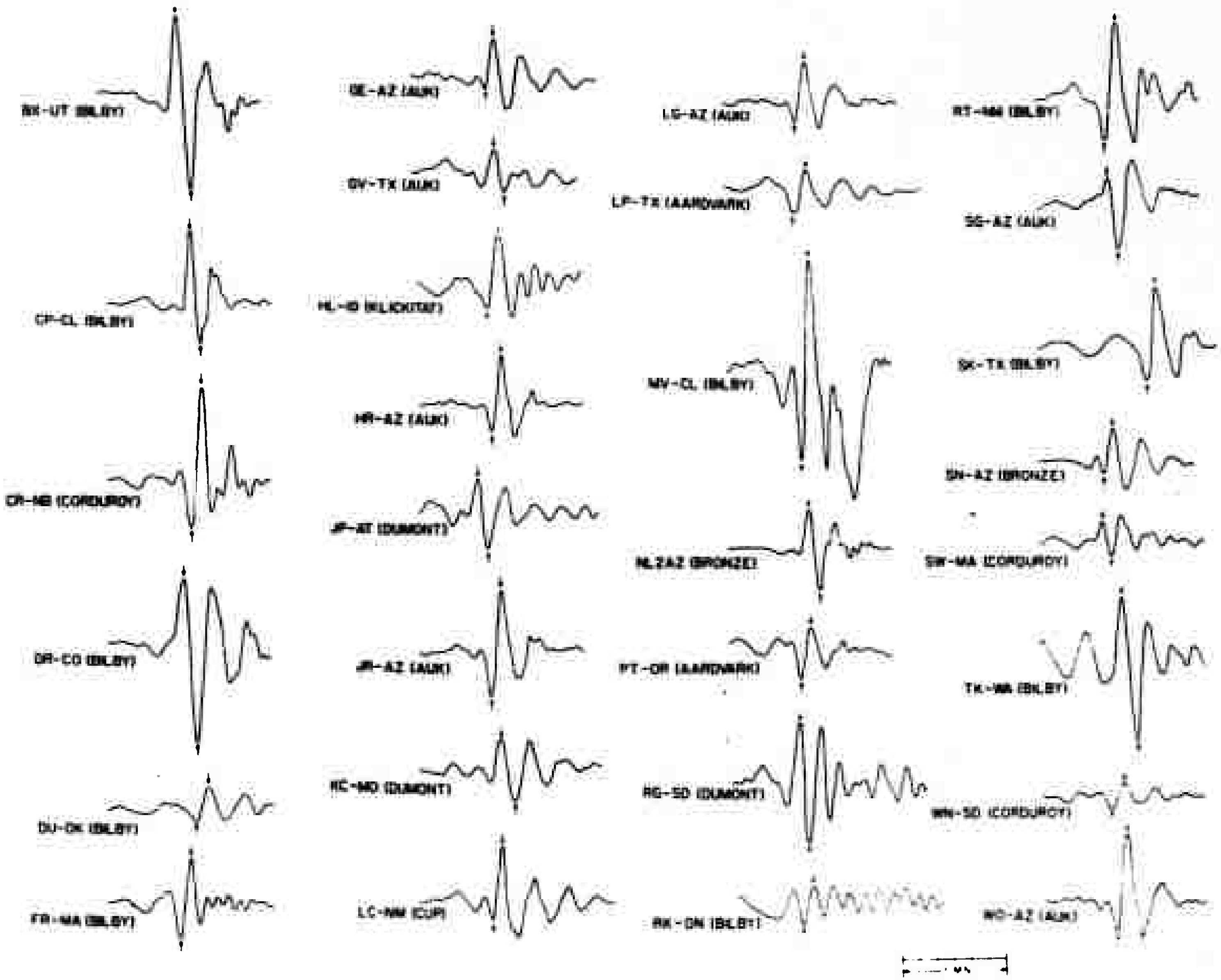

Figure 2. Rayleigh signals generated by NTS explosions recorded by LRSM stations.

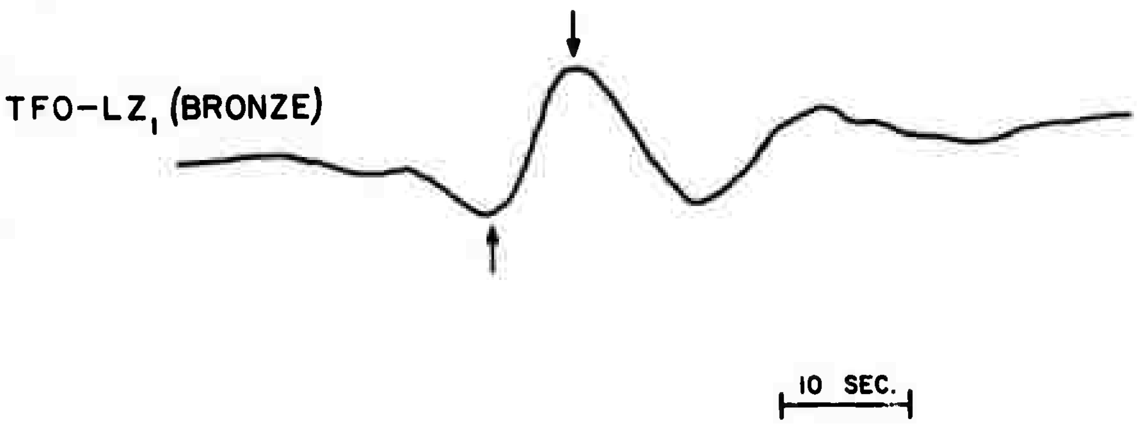

Figure 3. Rayleigh signal generated by the NTS explosion BRONZE as recorded at the TFO array (LZ1).

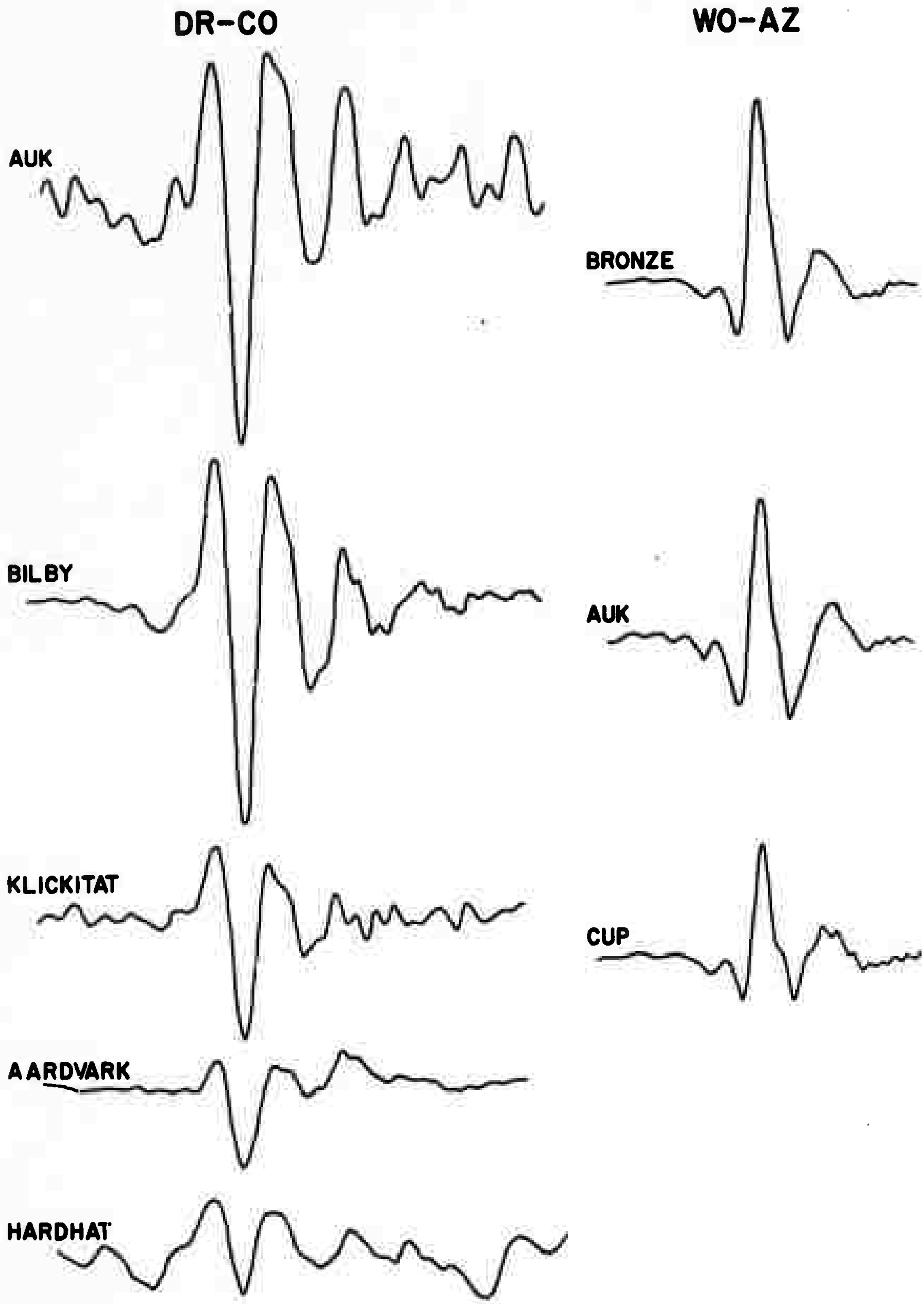

Figure 4. Rayleigh signals recorded at the seismic stations DR-CO and WO-AZ from several NTS explosions.

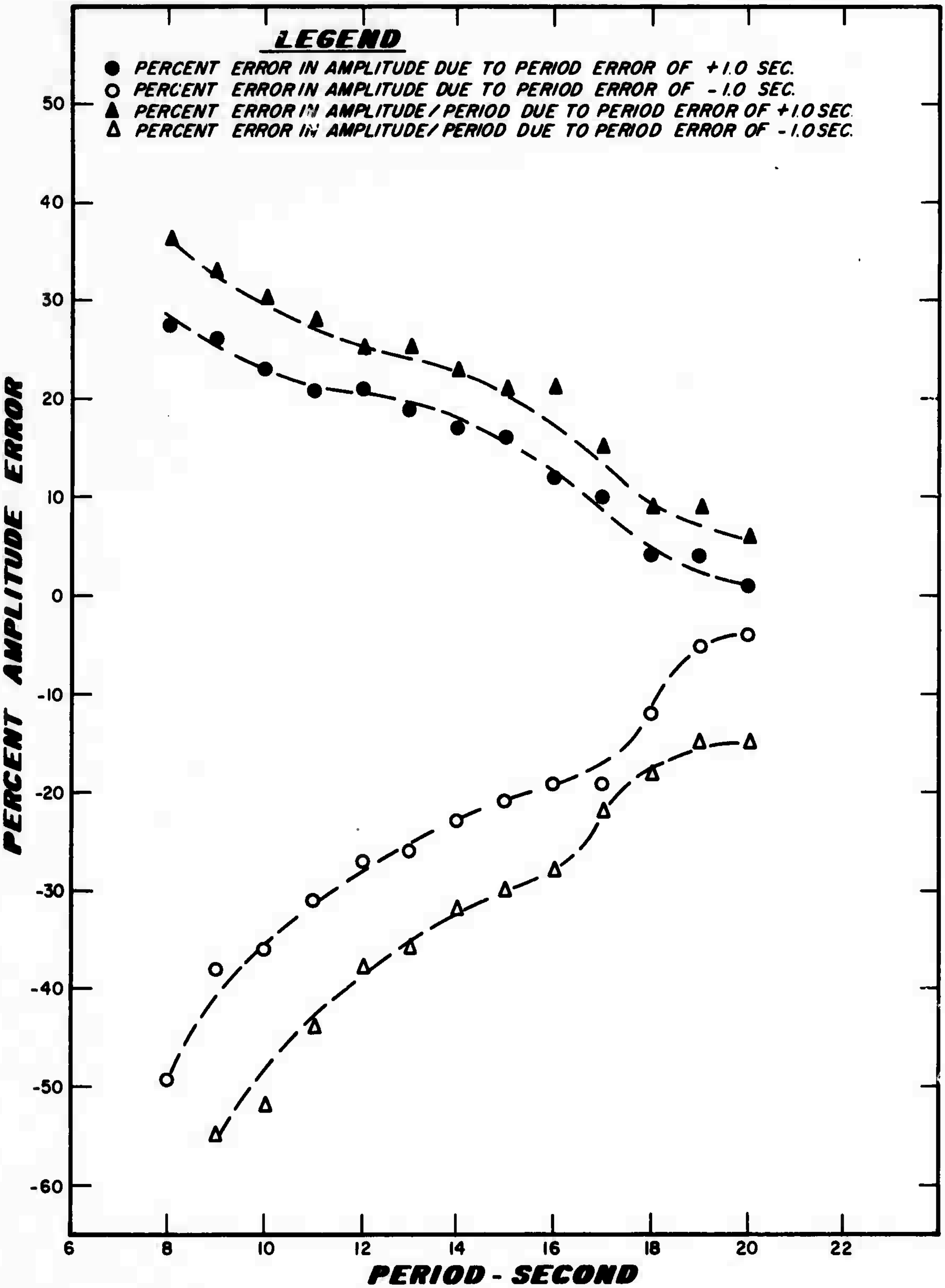

Figure 5. Per cent error in the calculated amplitude resulting from a measurement error of ± 1.0 second in the period which has been used to determine the amplitude correction factor for the LRSM long period seismograph response.

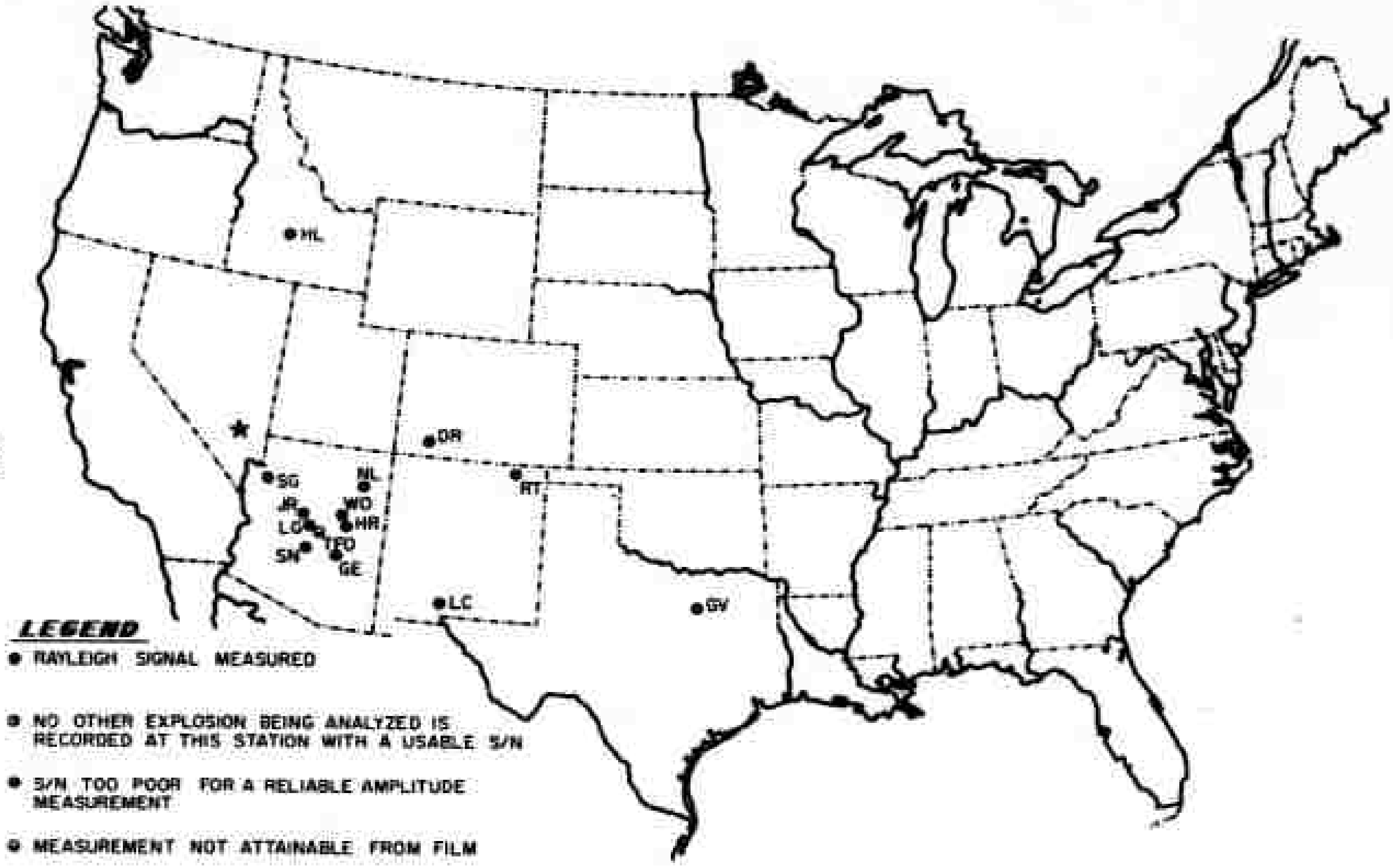

Figure 6. Location of stations recording long period seismic energy from the nuclear explosion AUK.

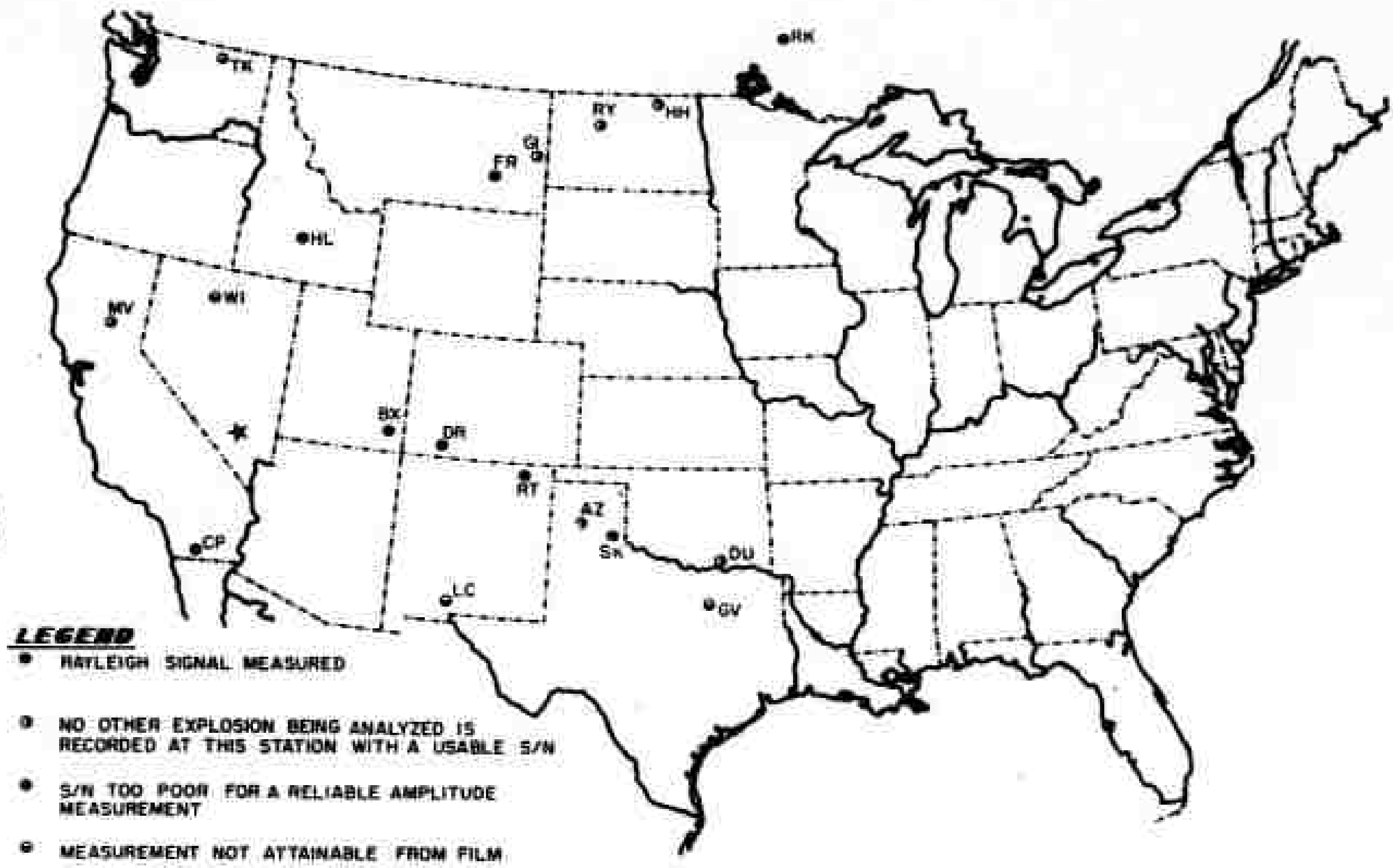

Figure 7. Location of stations recording long period seismic energy from the nuclear explosion BILBY.

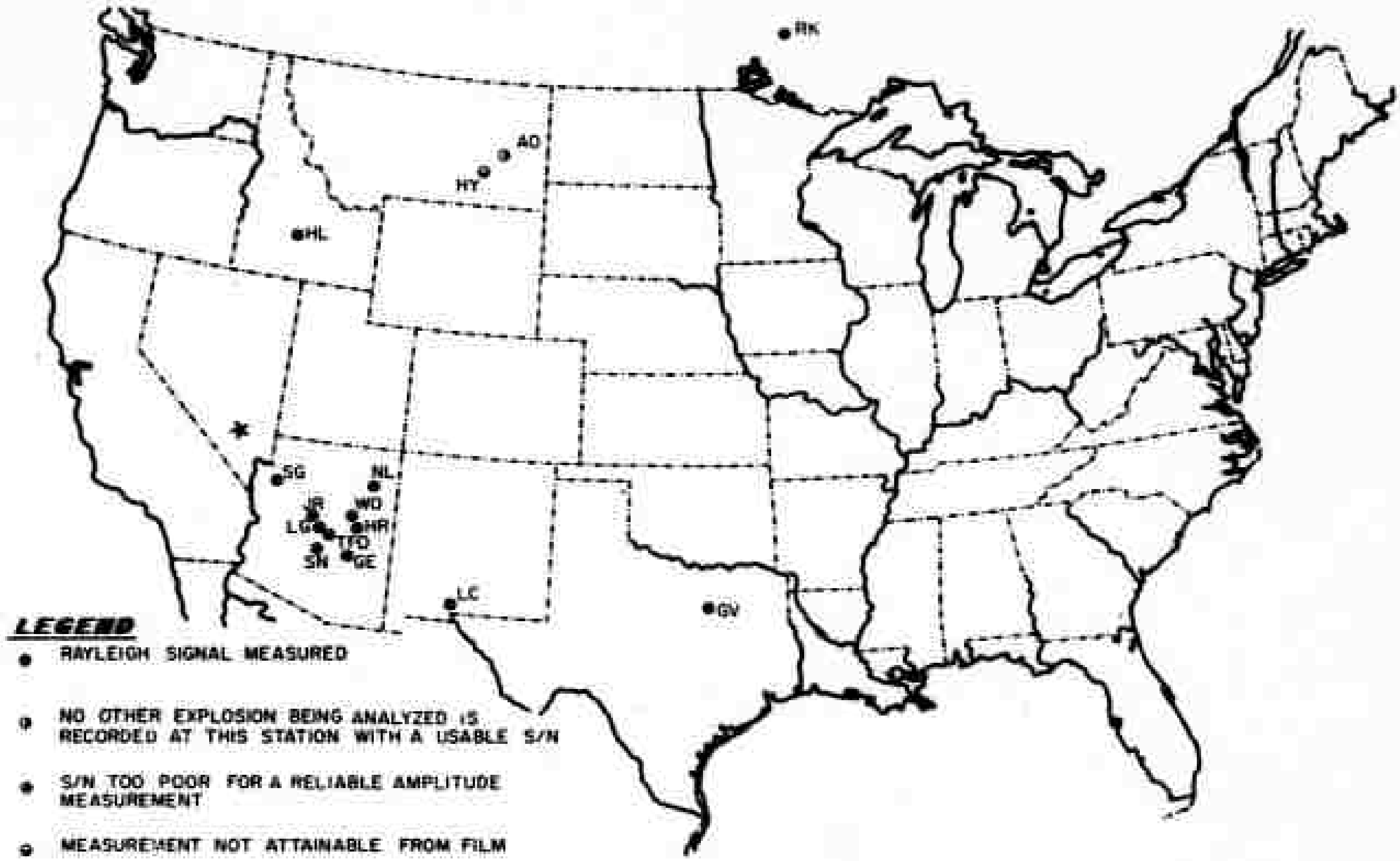

Figure 8. Location of stations recording long period seismic energy from the nuclear explosion BRONZE.

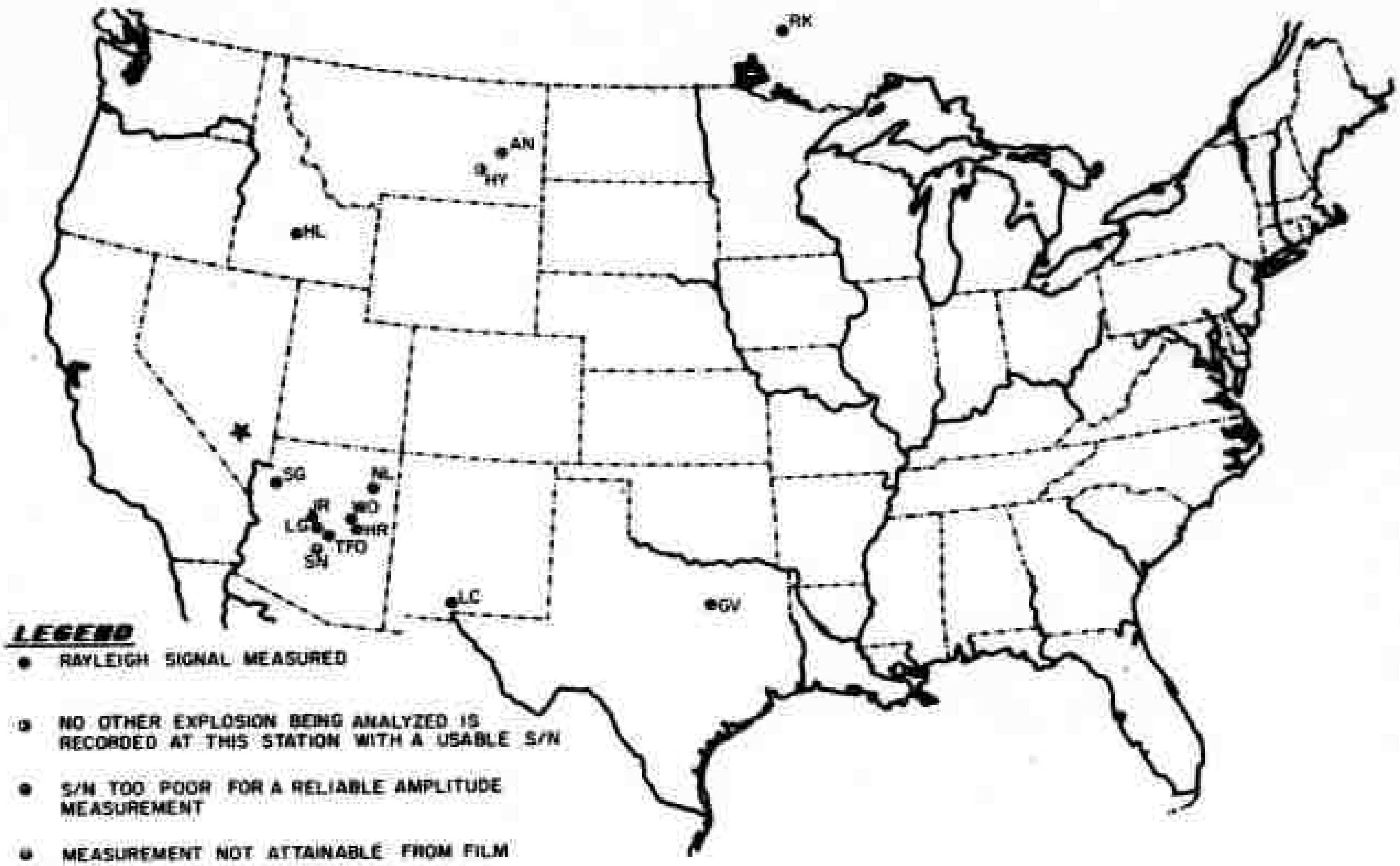

Figure 9. Location of stations recording long period seismic energy from the nuclear explosion CUP.

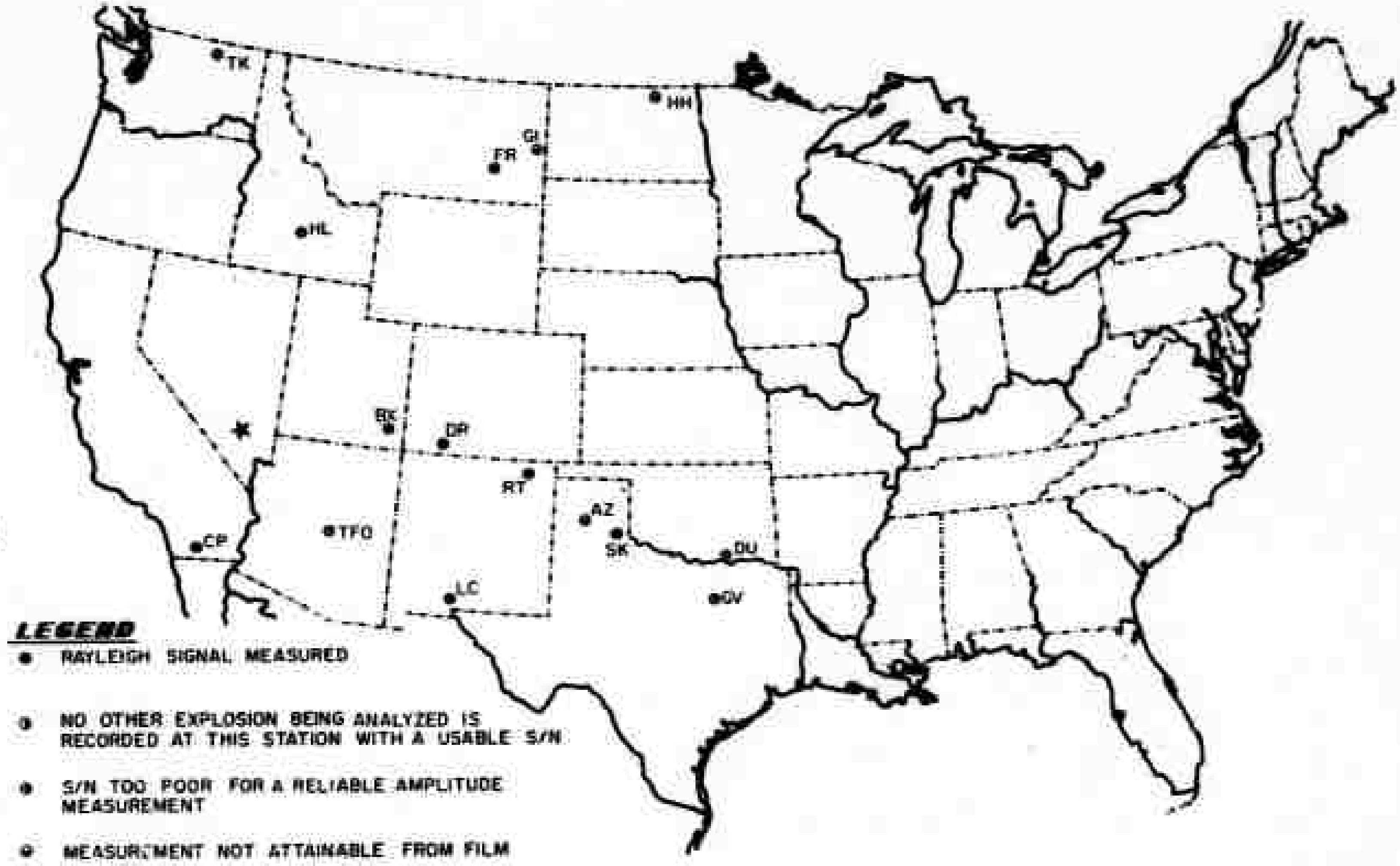

Figure 10. Location of stations recording long period seismic energy from the nuclear explosion KLICKITAT.

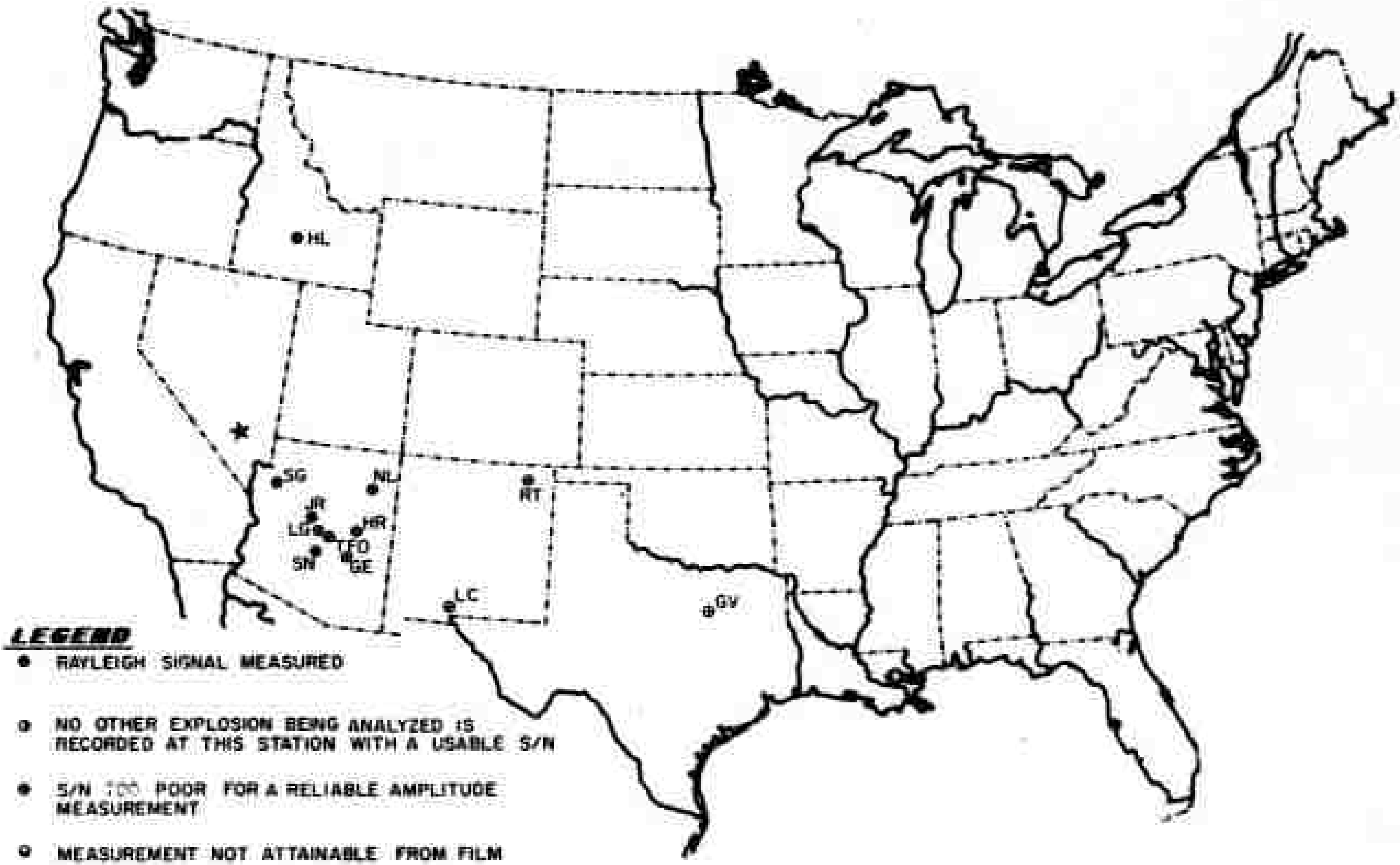

Figure 11. Location of stations recording long period seismic energy from the nuclear explosion WAGTAIL.

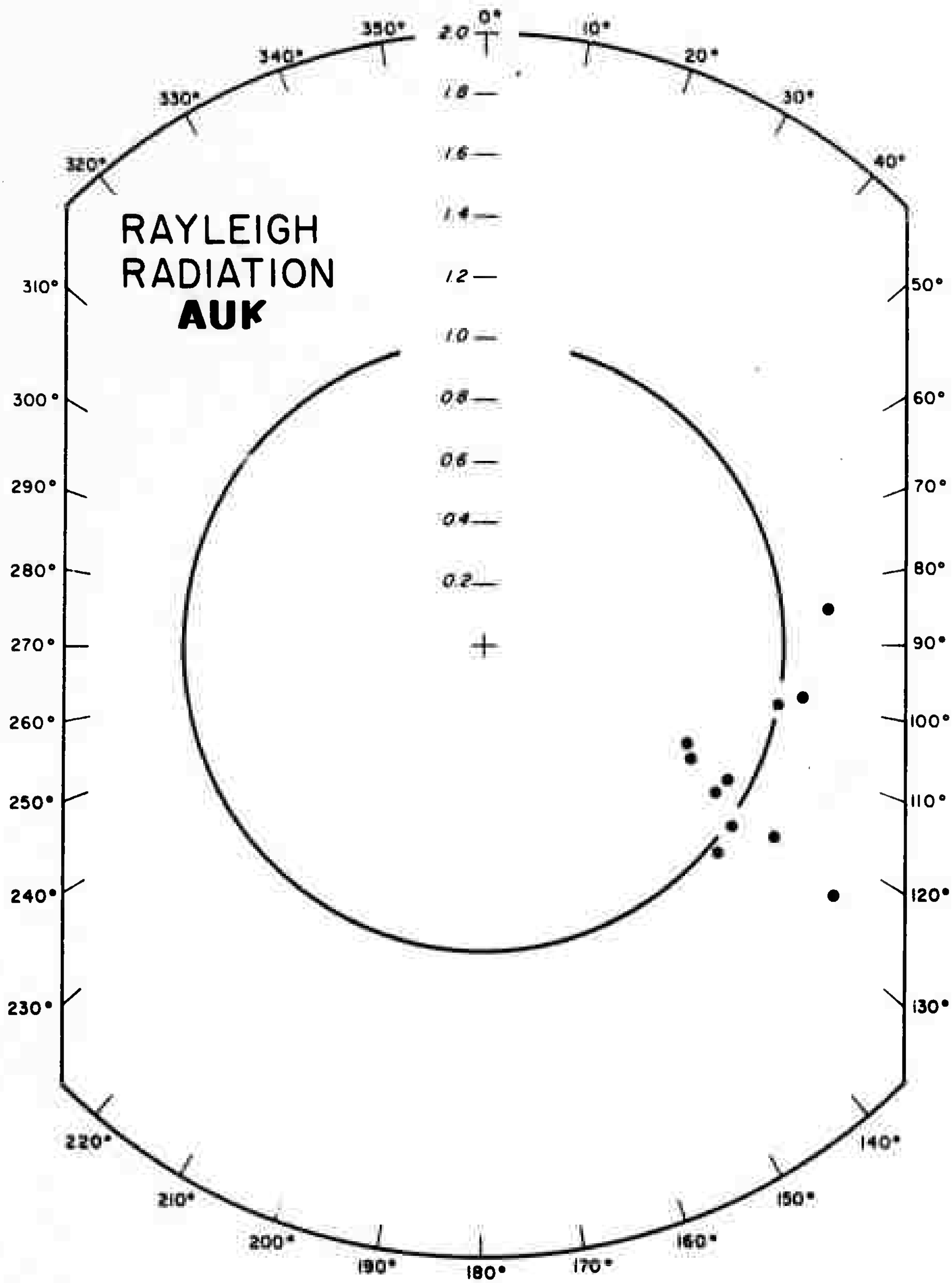

Figure 12. Rayleigh radiation pattern for the nuclear explosion AUK using amplitudes which were corrected for the instrumental response.

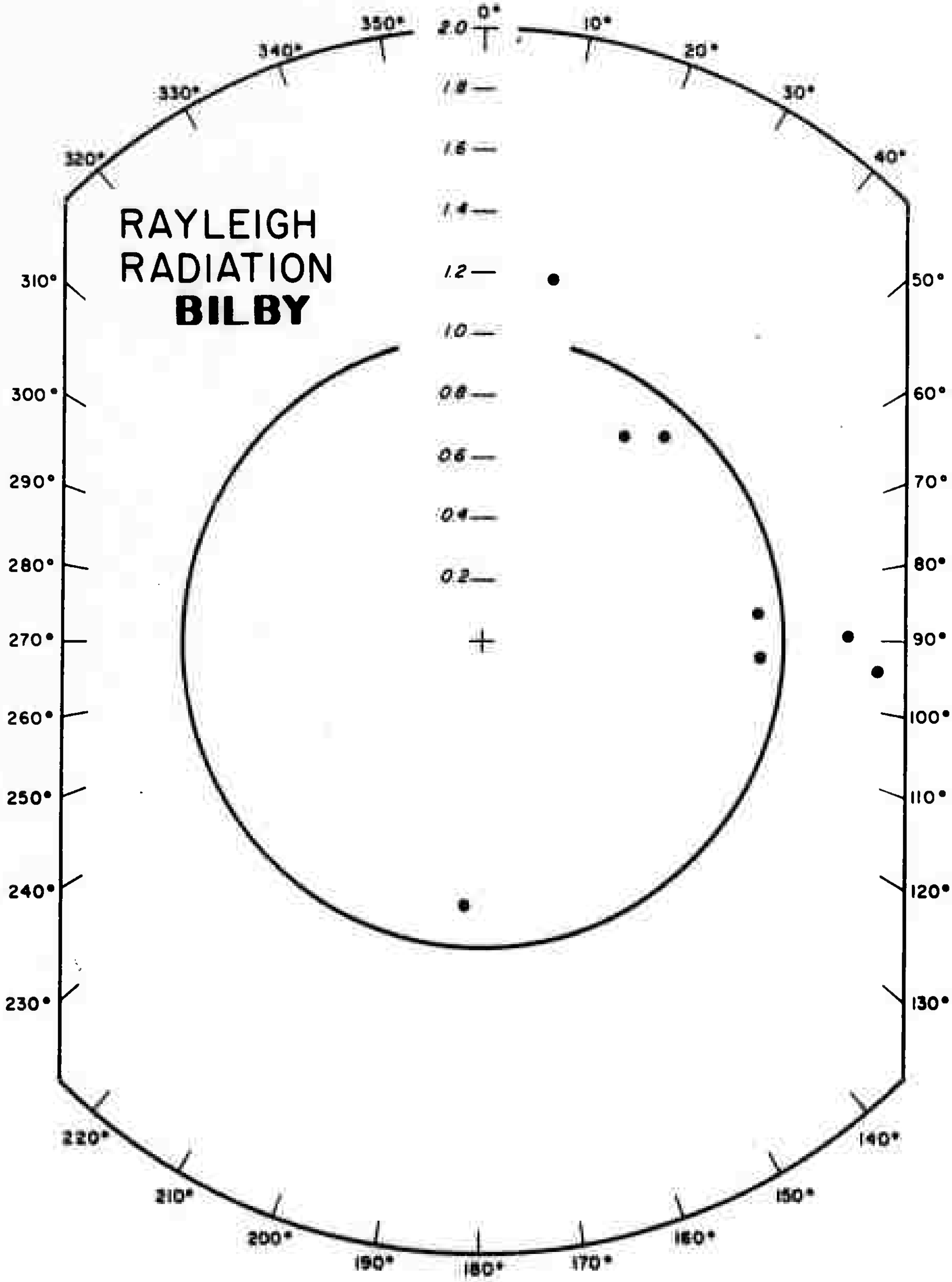

Figure 13. Rayleigh radiation pattern for the nuclear explosion BILBY using amplitudes which were corrected for the instrumental response.

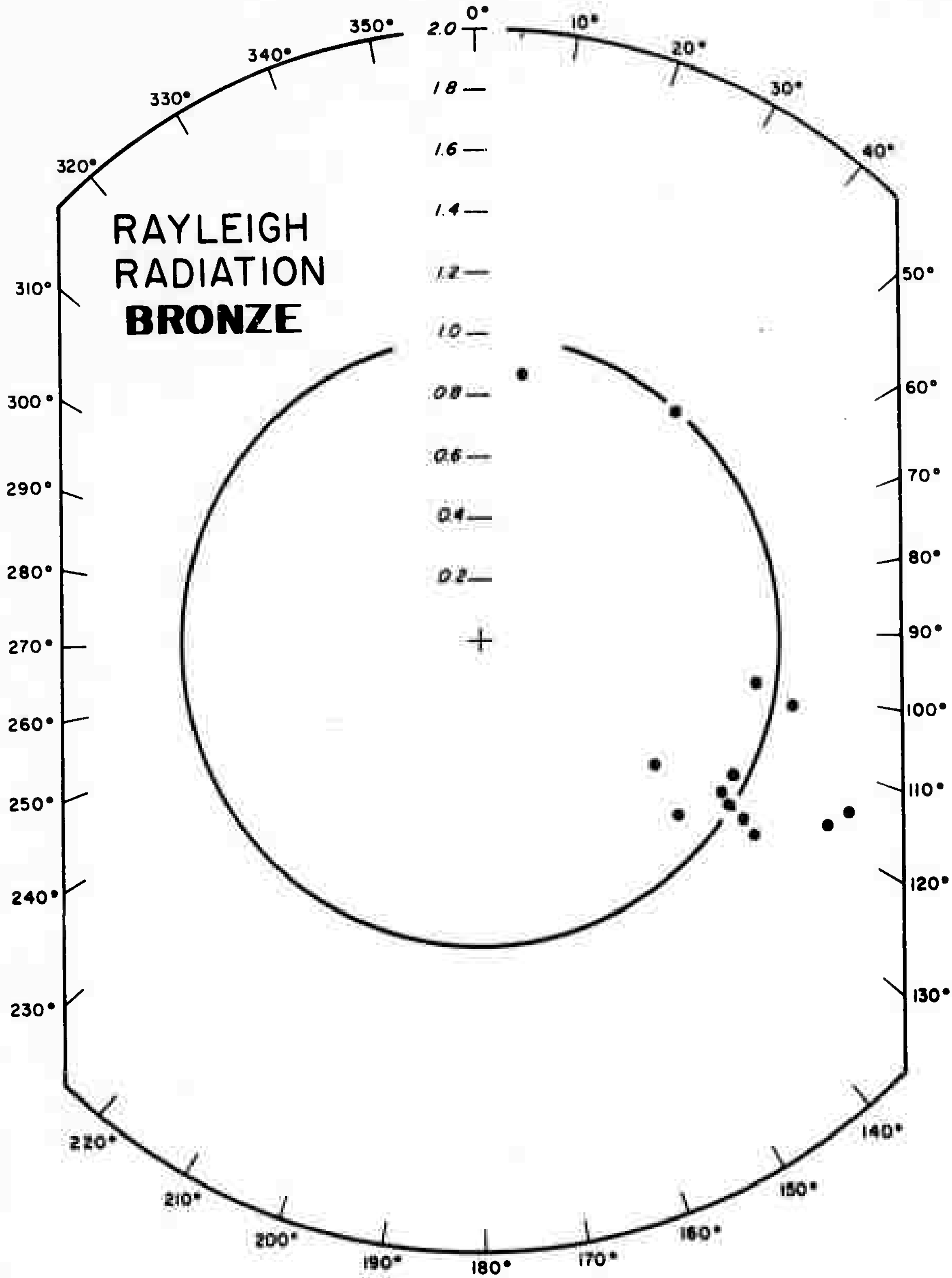

Figure 14. Rayleigh radiation pattern for the nuclear explosion BRONZE using amplitudes which were corrected for the instrumental response.

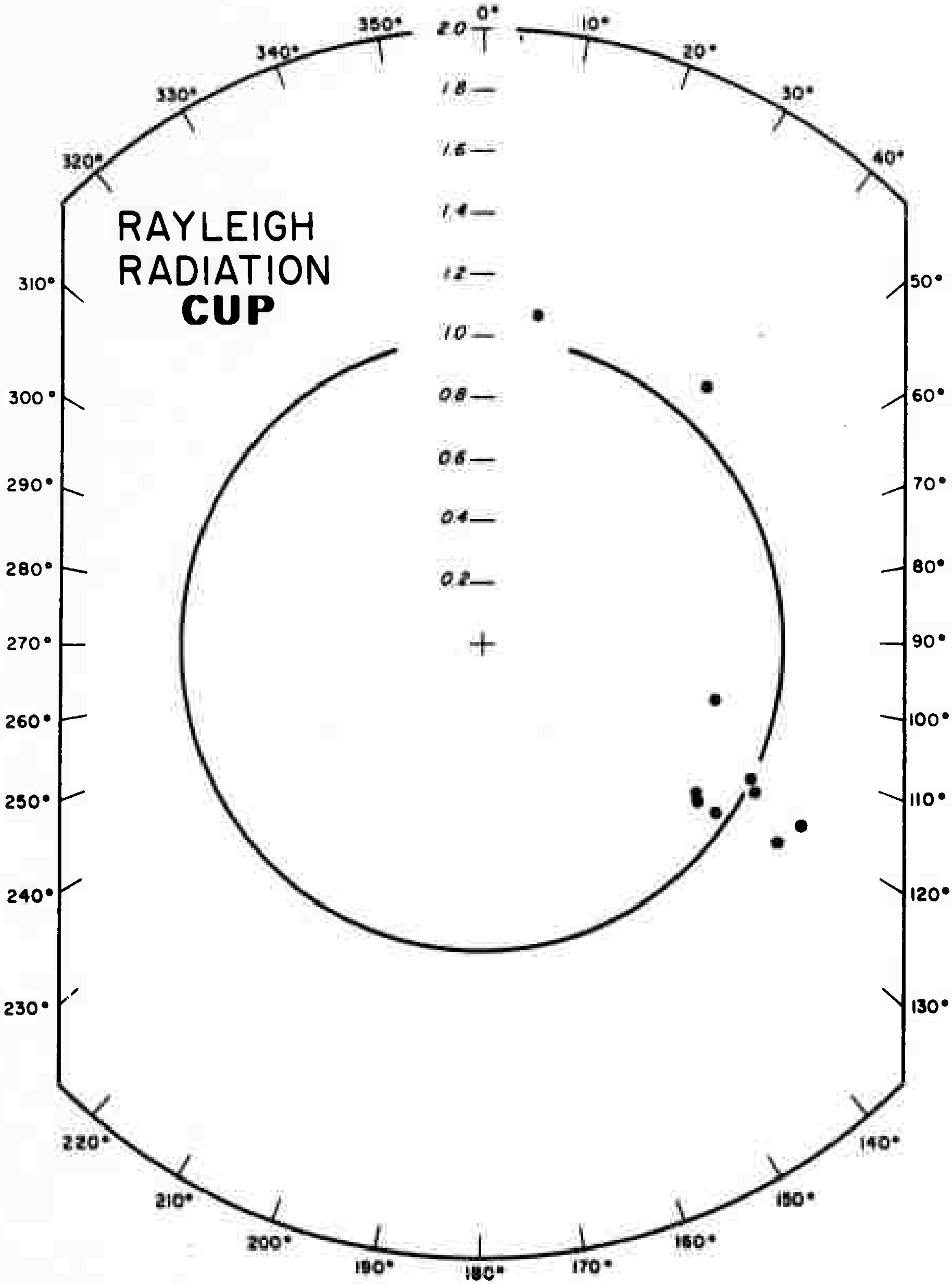

Figure 15. Rayleigh radiation pattern for the nuclear explosion CUP using amplitudes which were corrected for the instrumental response.

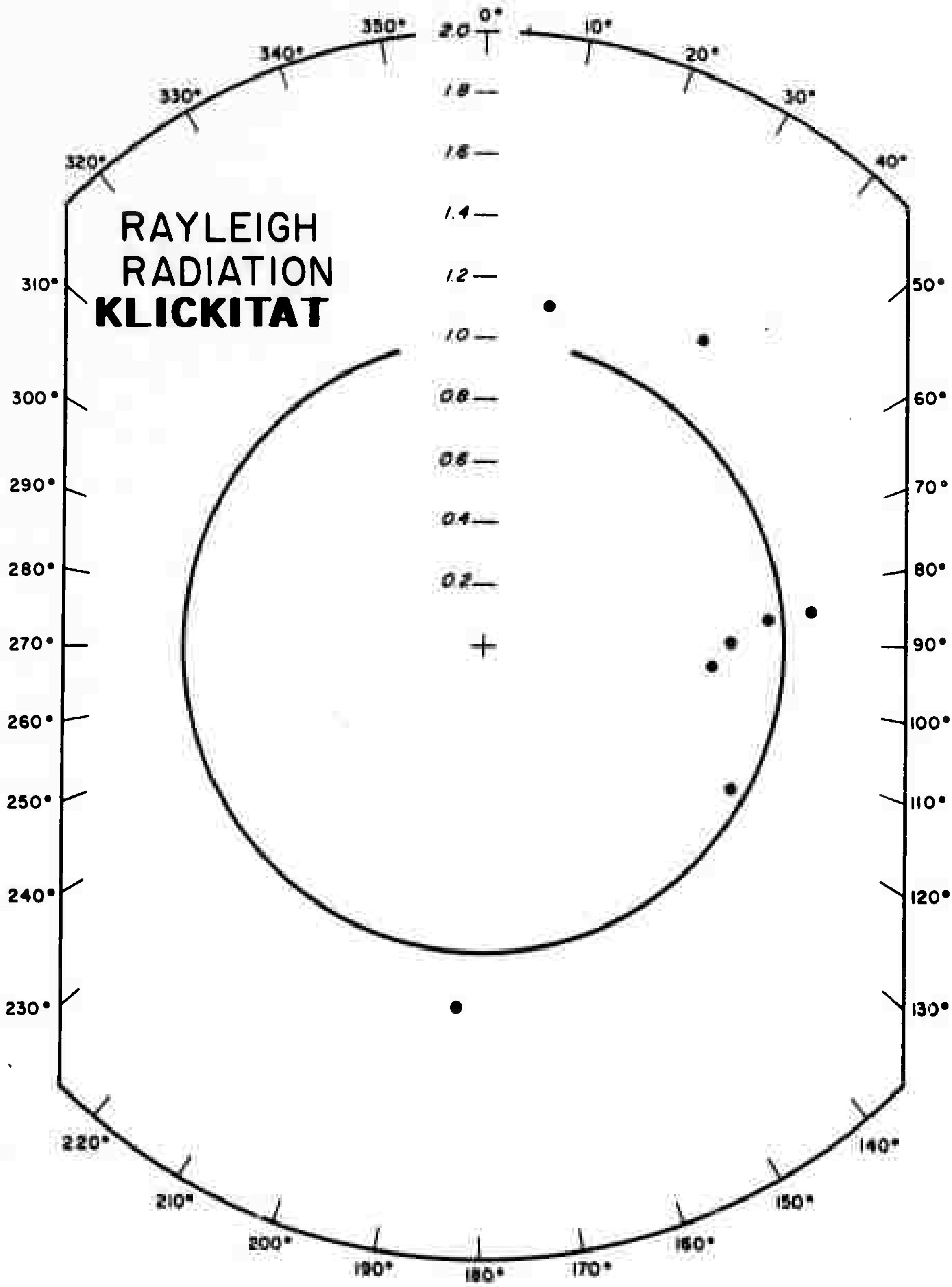

Figure 16. Rayleigh radiation pattern for the nuclear explosion KLICKITAT using amplitudes which were corrected for the instrumental response.

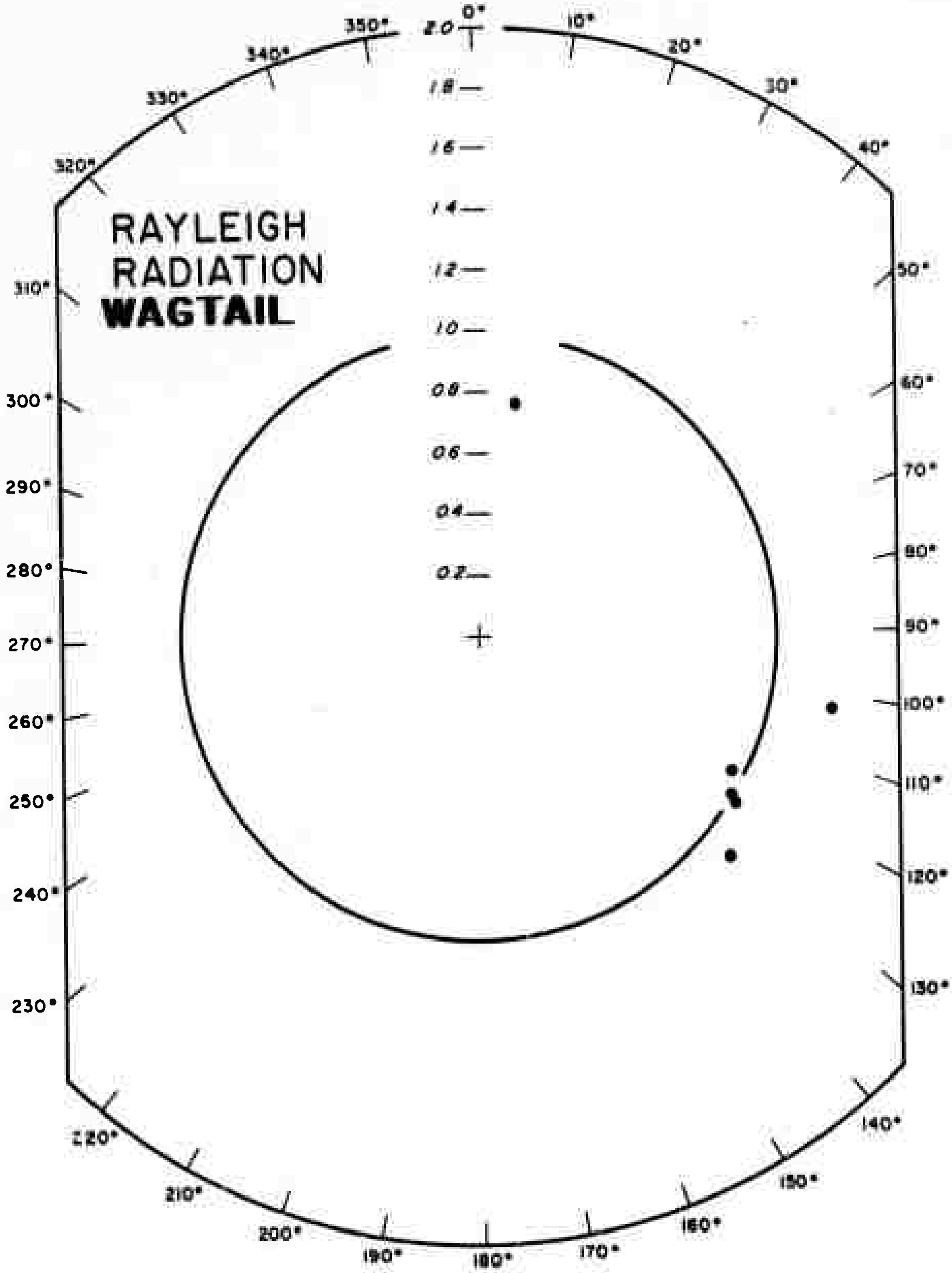

Figure 17. Rayleigh radiation pattern for the nuclear explosion WAGTAIL using amplitudes which were corrected for the instrumental response.

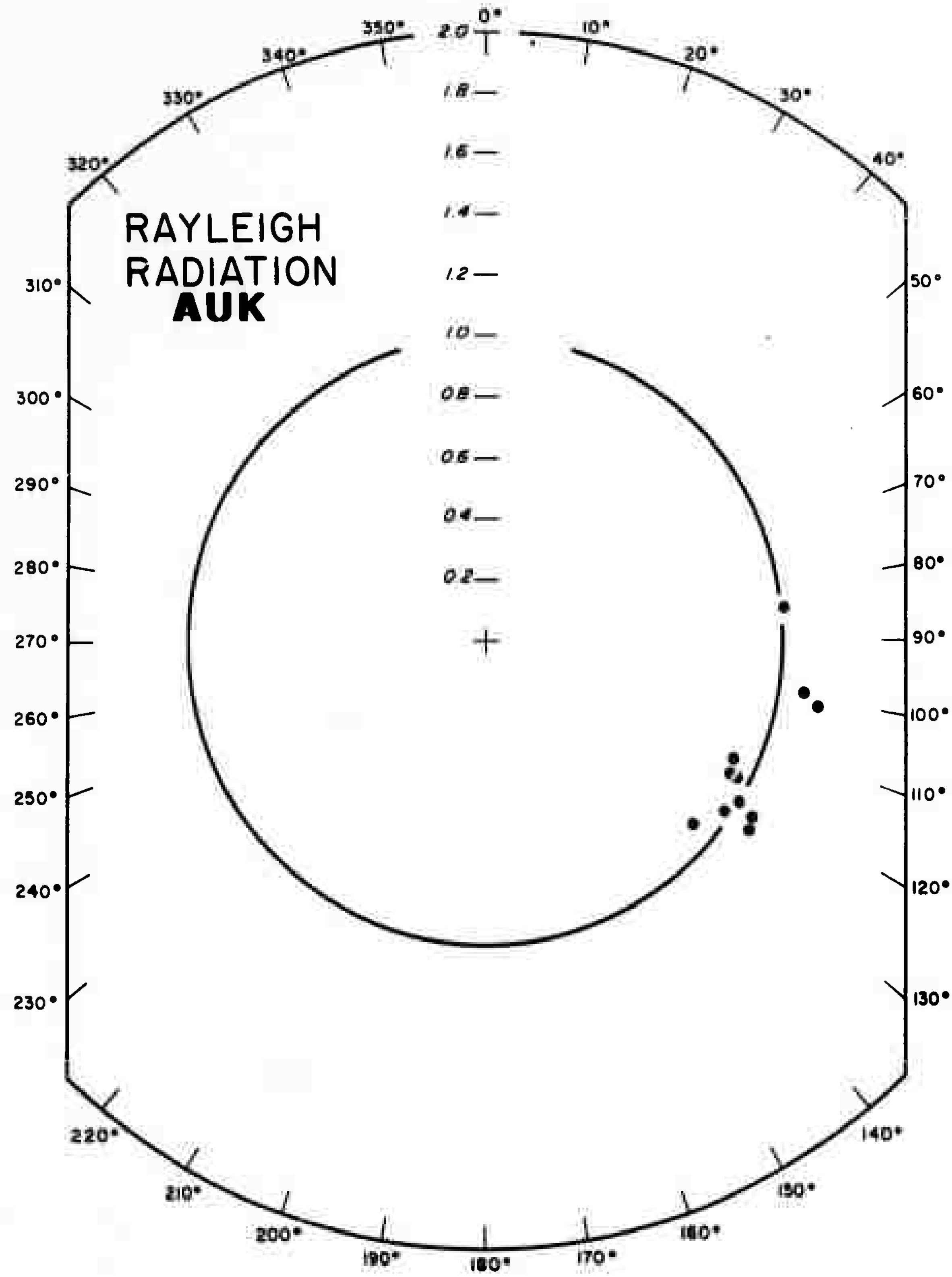

Figure 18. Rayleigh radiation pattern for the nuclear explosion AUK using amplitudes which were not corrected for the instrumental response.

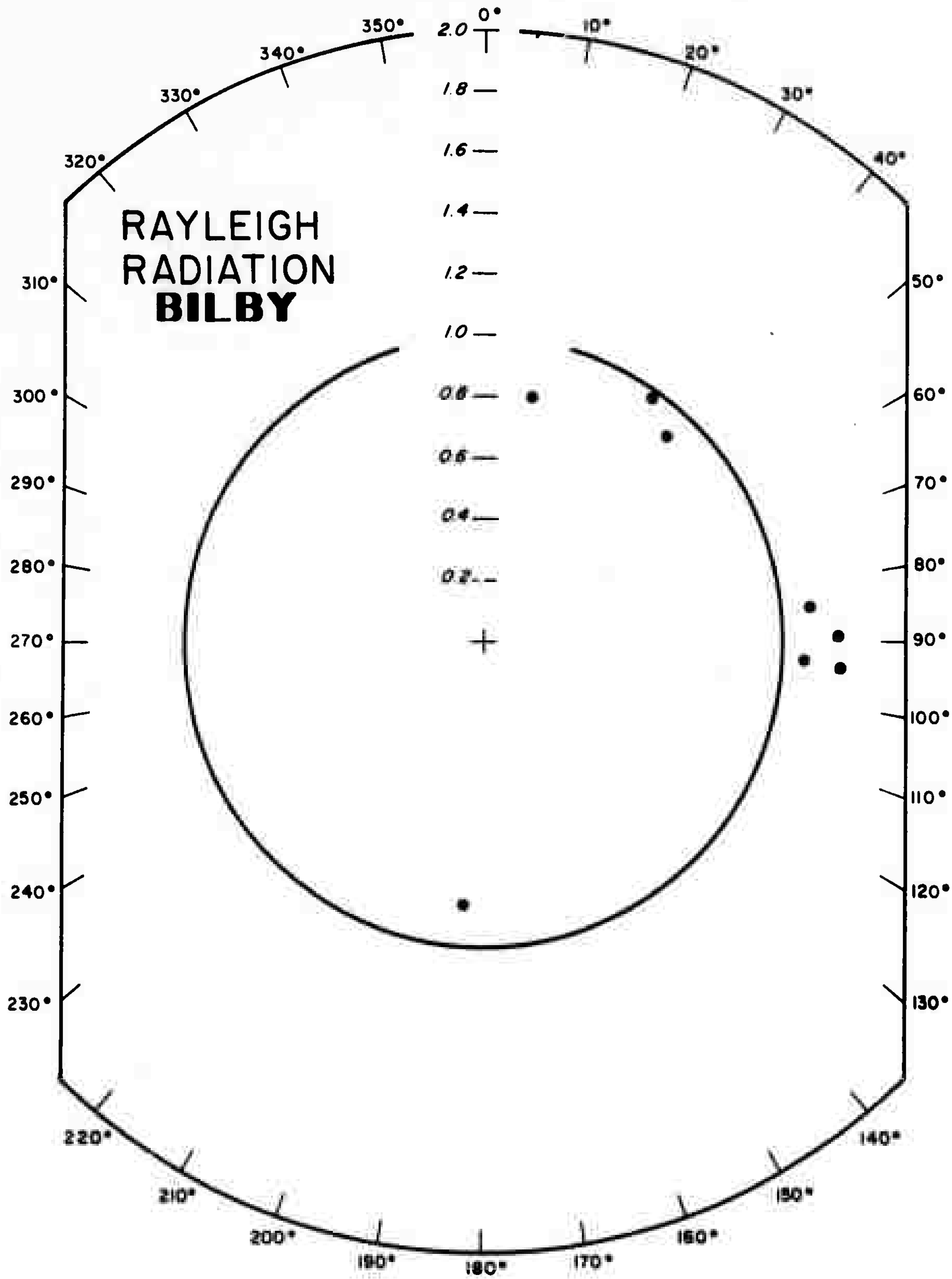

Figure 19. Rayleigh radiation pattern for the nuclear explosion BILBY using amplitudes which were not corrected for the instrumental response.

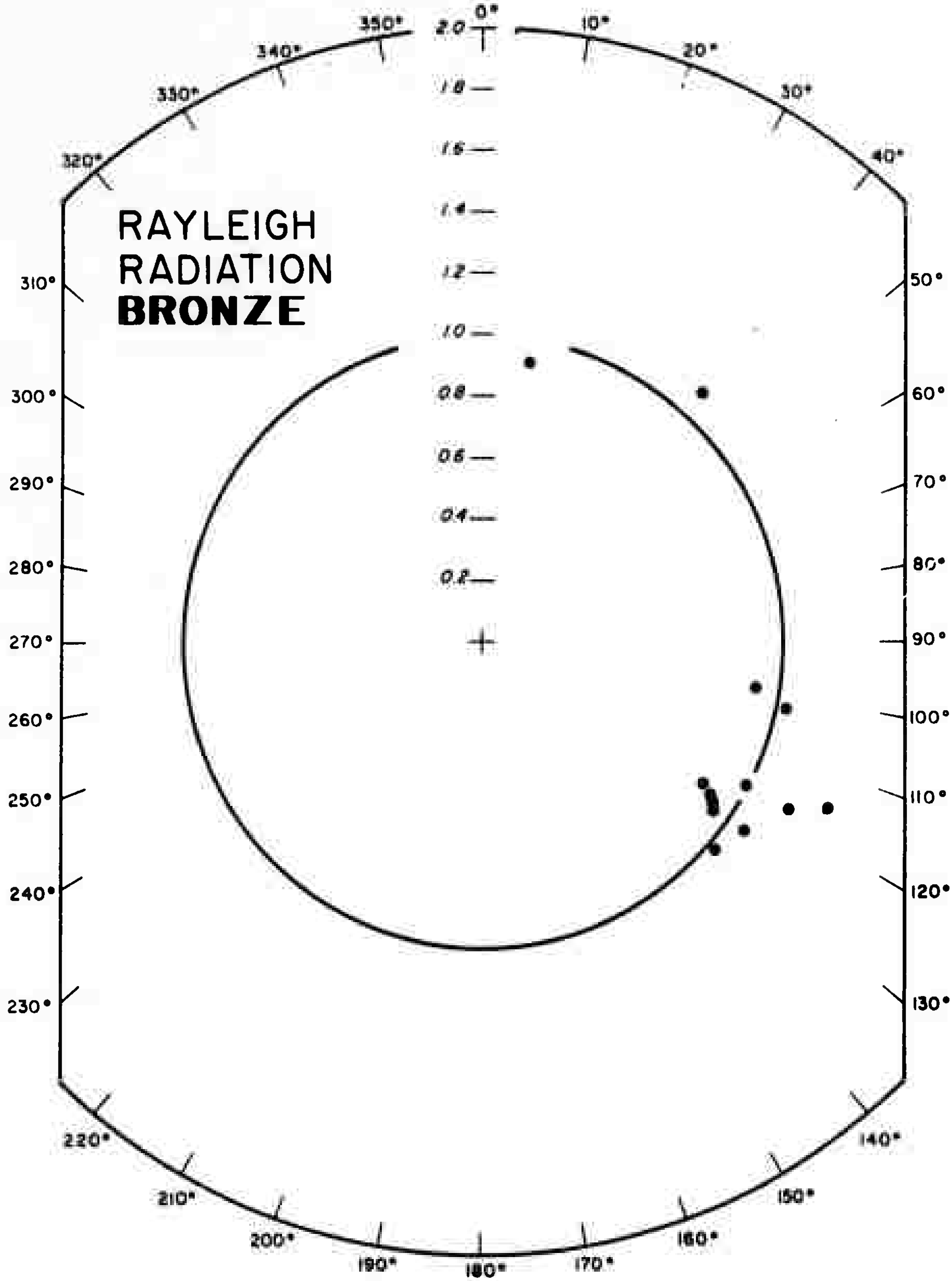

Figure 20. Rayleigh radiation pattern for the nuclear explosion BRONZE using amplitudes which were not corrected for the instrumental response.

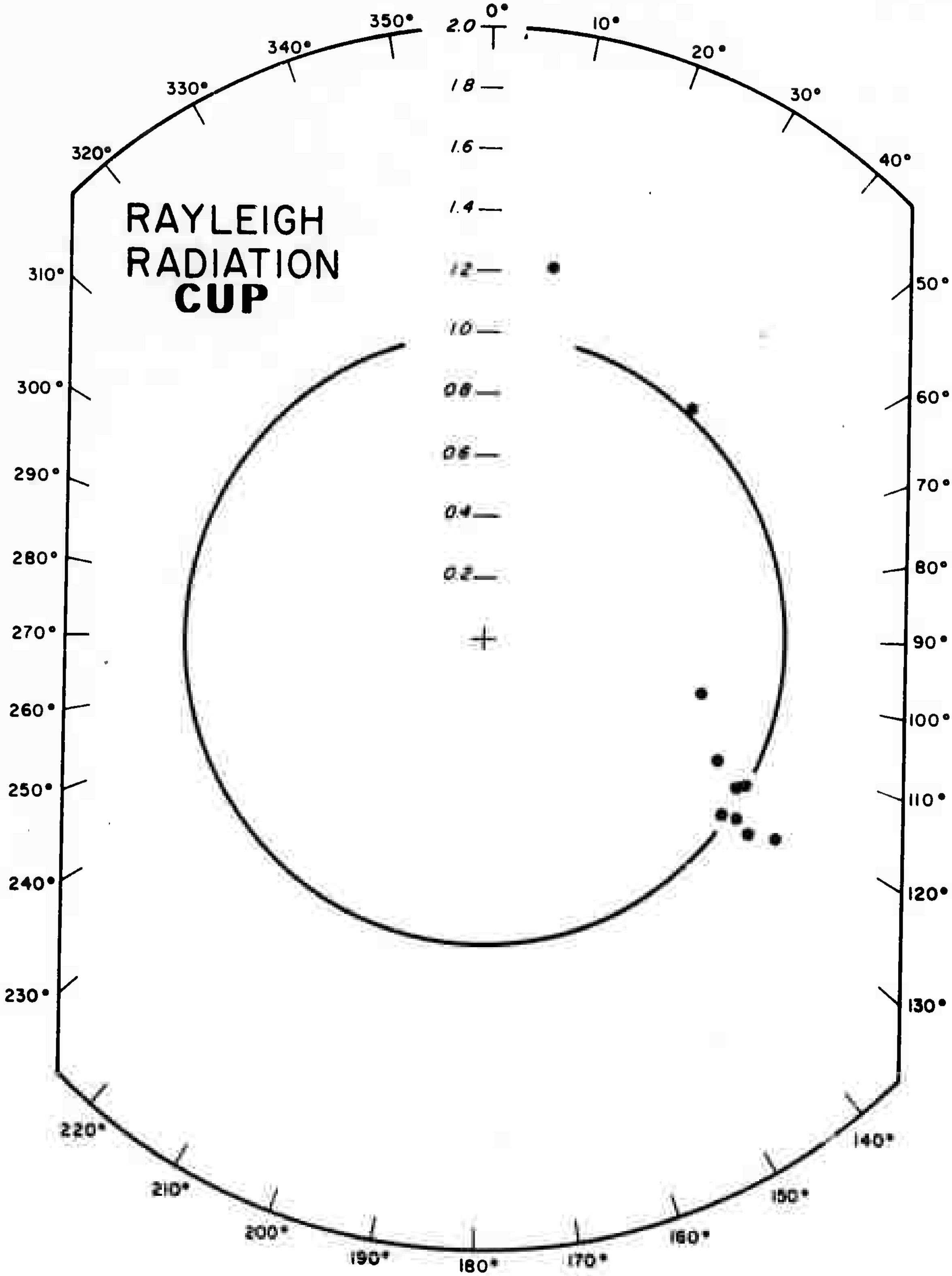

Figure 21. Rayleigh radiation pattern for the nuclear explosion CUP using amplitudes which were not corrected for the instrumental response.

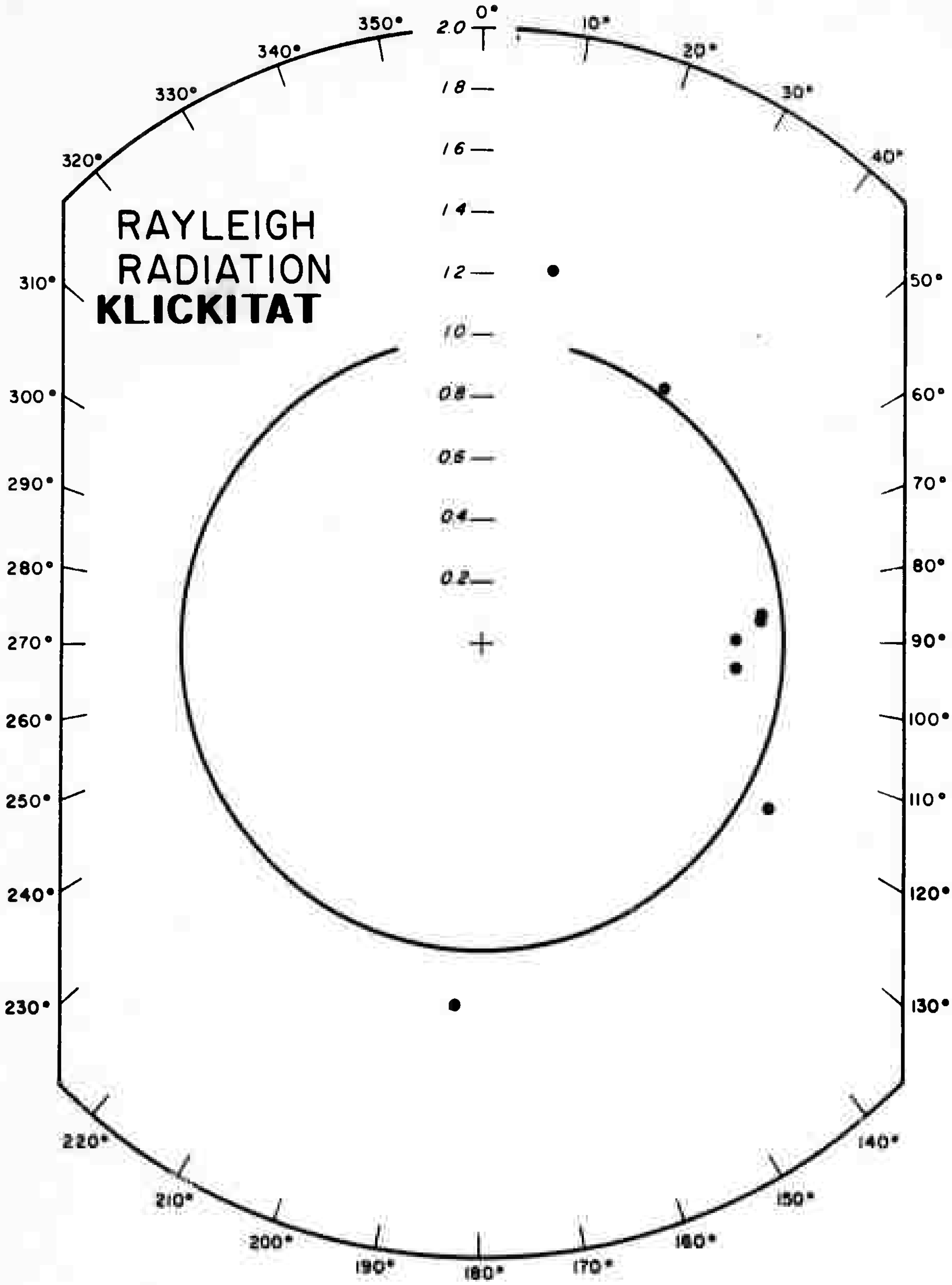

Figure 22. Rayleigh radiation pattern for the nuclear explosion KLICKITAT using amplitudes which were not corrected for the instrumental response.

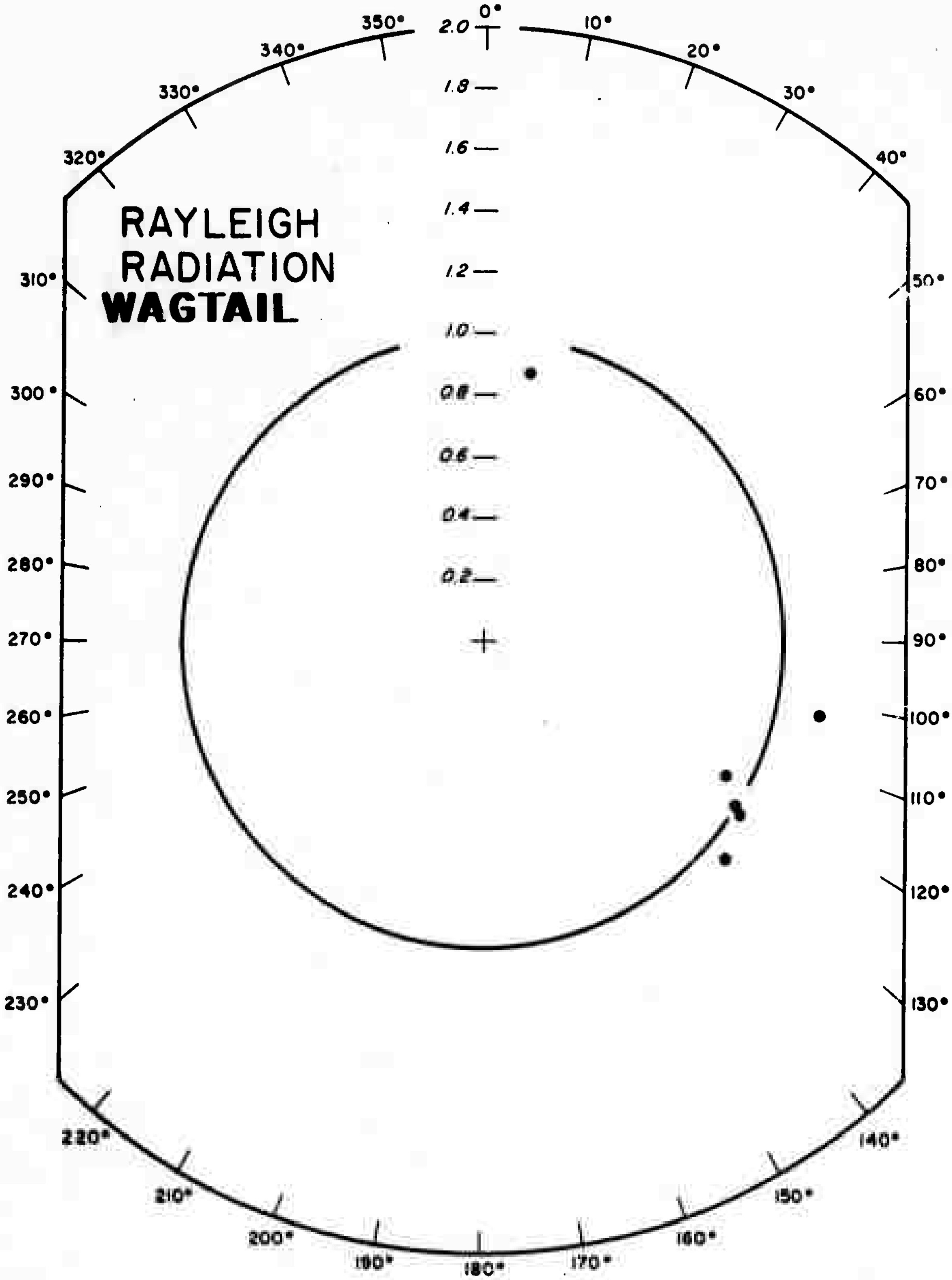

Figure 23. Rayleigh radiation pattern for the nuclear explosion WAGTAIL using amplitudes which were not corrected for the instrumental response.

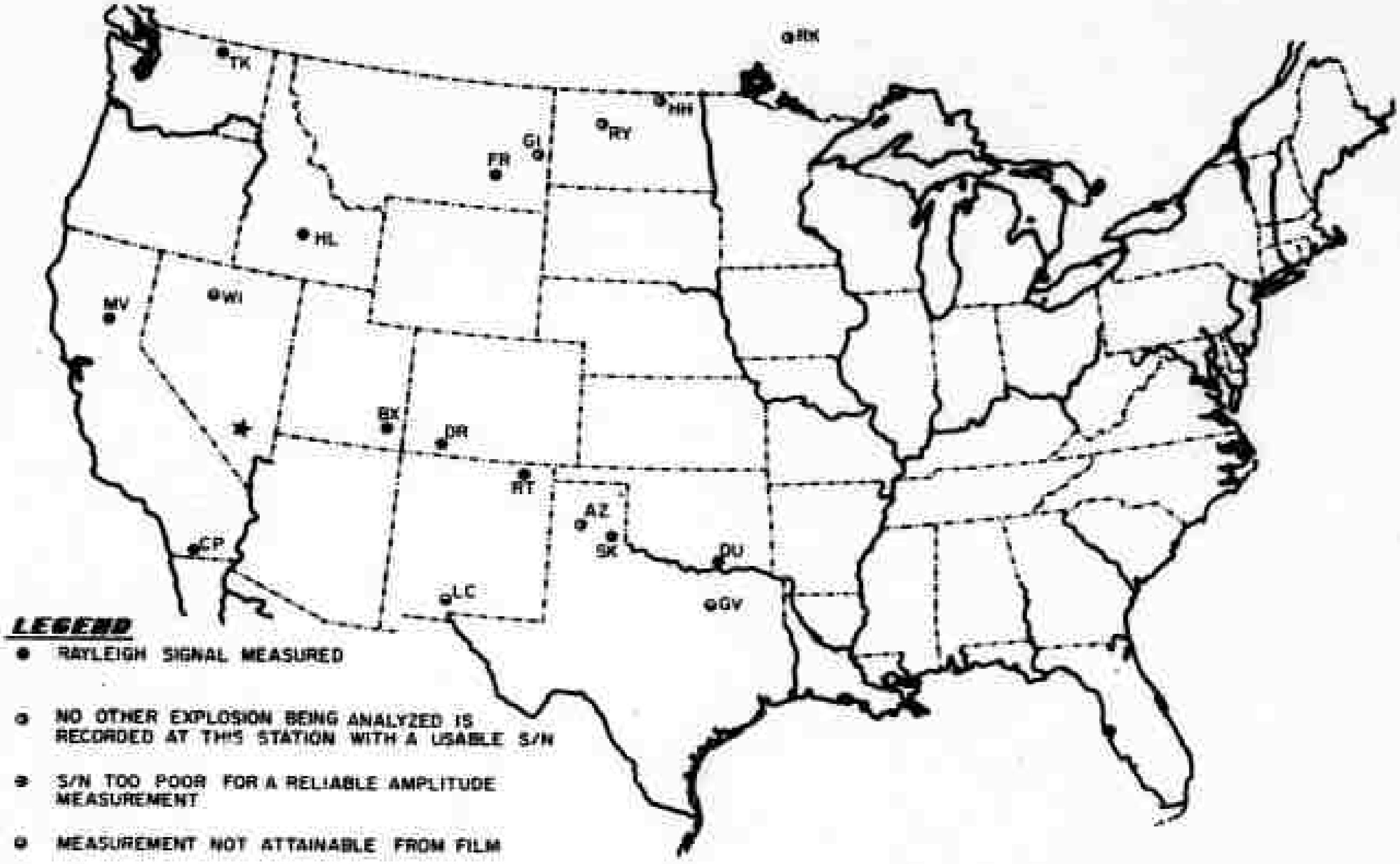

Figure 24. Location of stations recording long period seismic energy from the nuclear explosion BILBY.

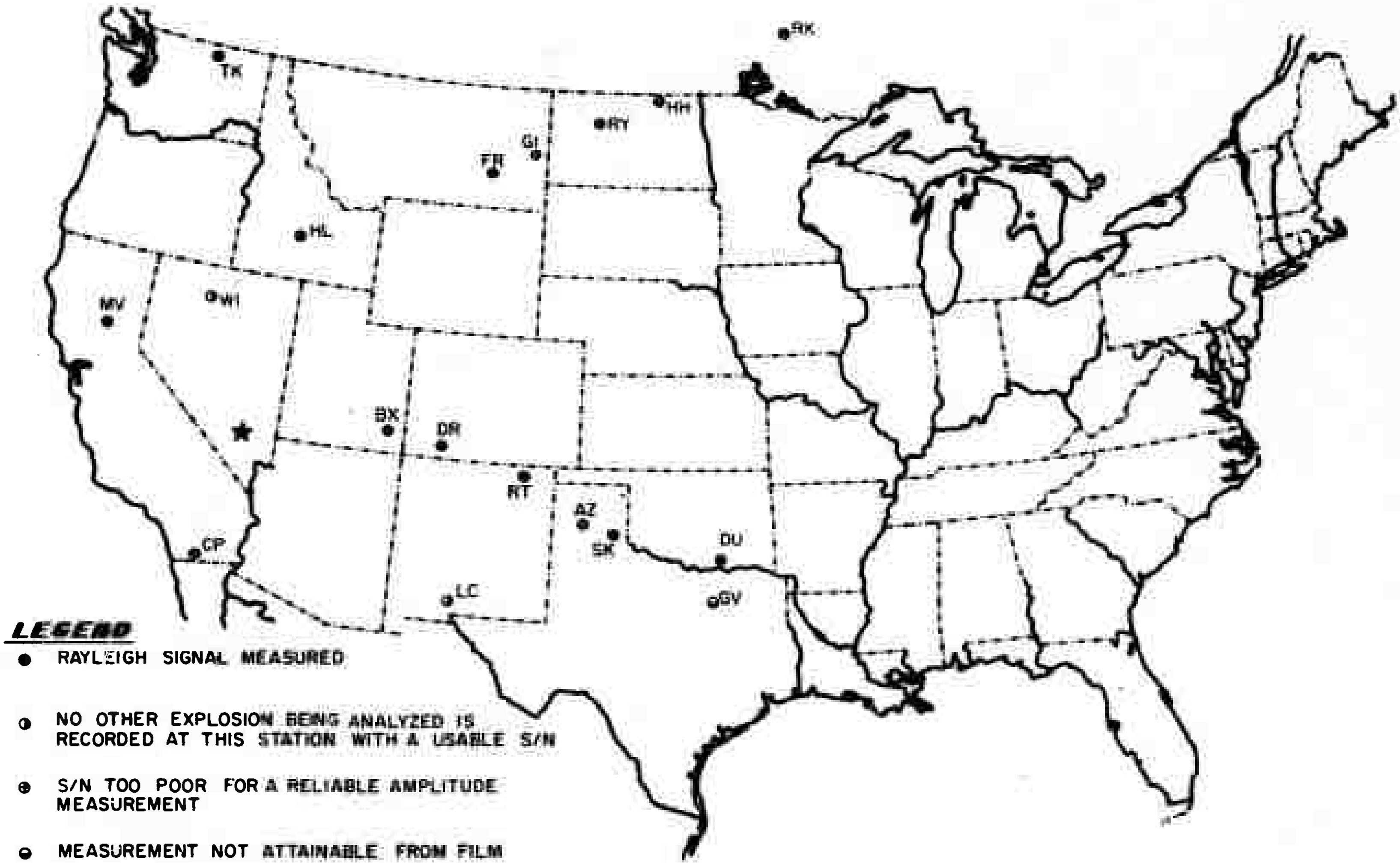

Figure 25. Location of stations recording long period seismic energy from the collapse of the nuclear explosion BILBY.

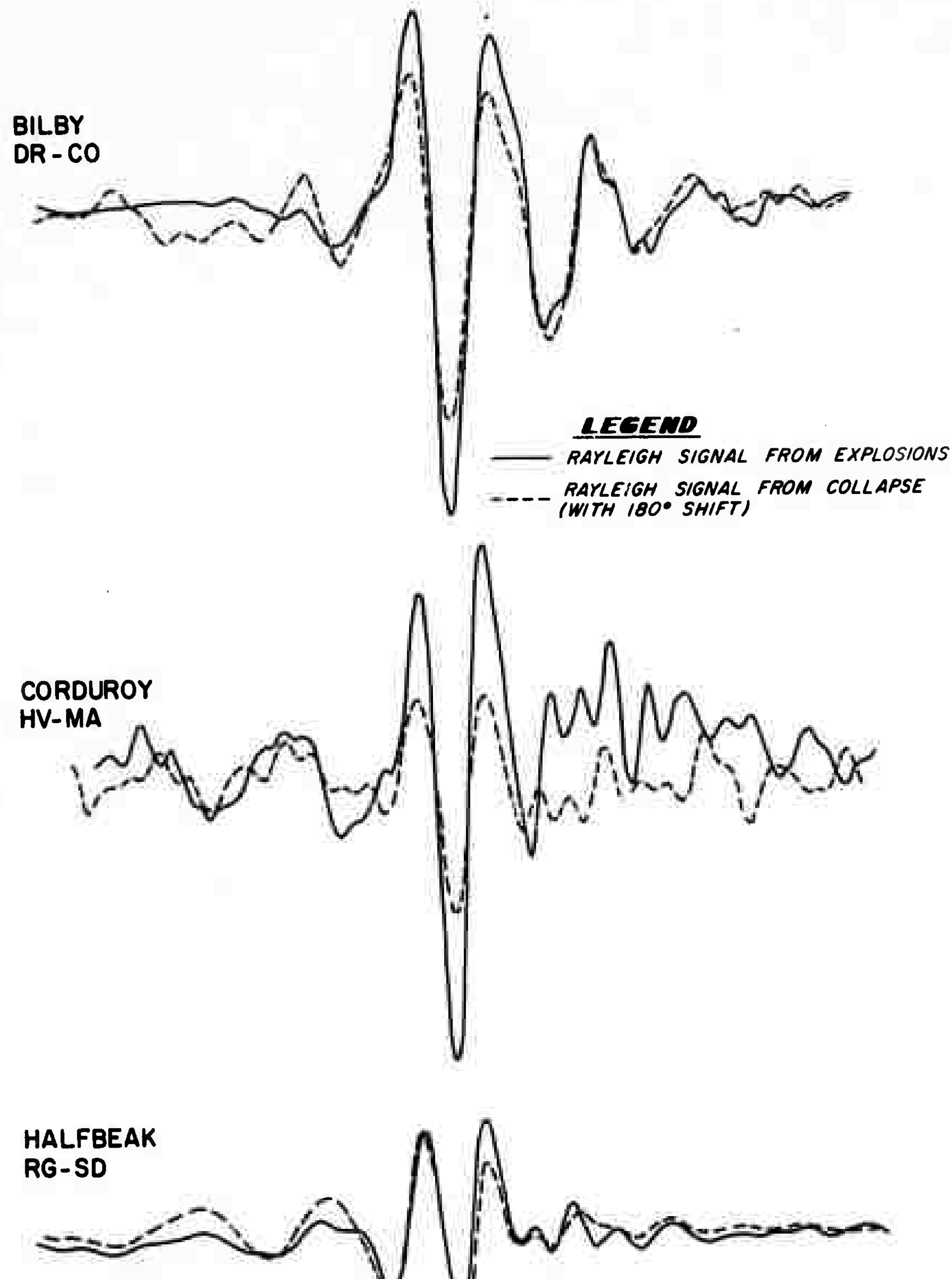

Figure 26. Rayleigh signals from NTS nuclear explosions and collapses.

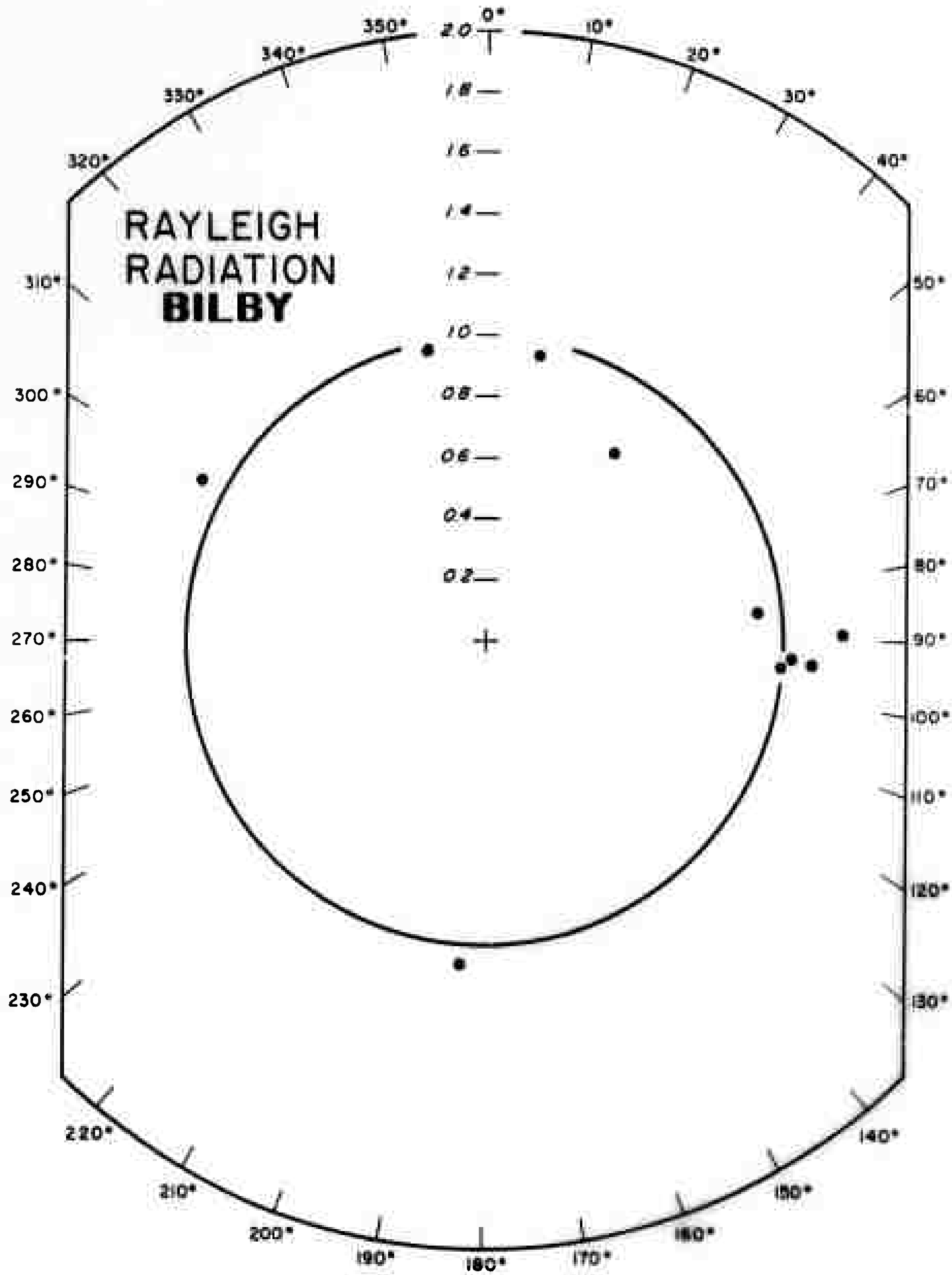

Figure 27. Rayleigh radiation pattern for the nuclear explosion BILBY using amplitudes which were corrected for the instrumental response.

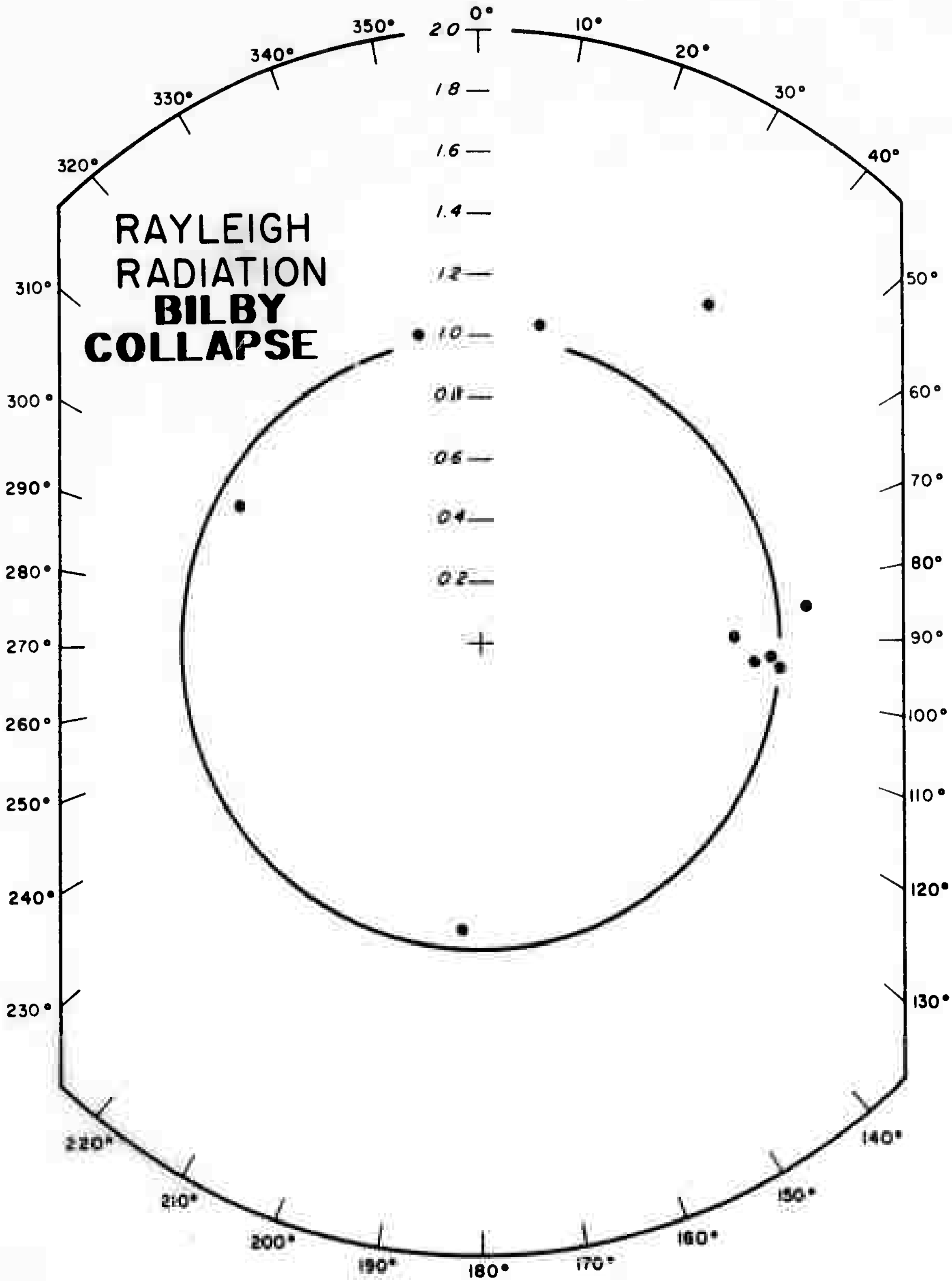

Figure 28. Rayleigh radiation pattern for the collapse of the nuclear explosion BILBY using amplitudes which were corrected for the instrumental response.

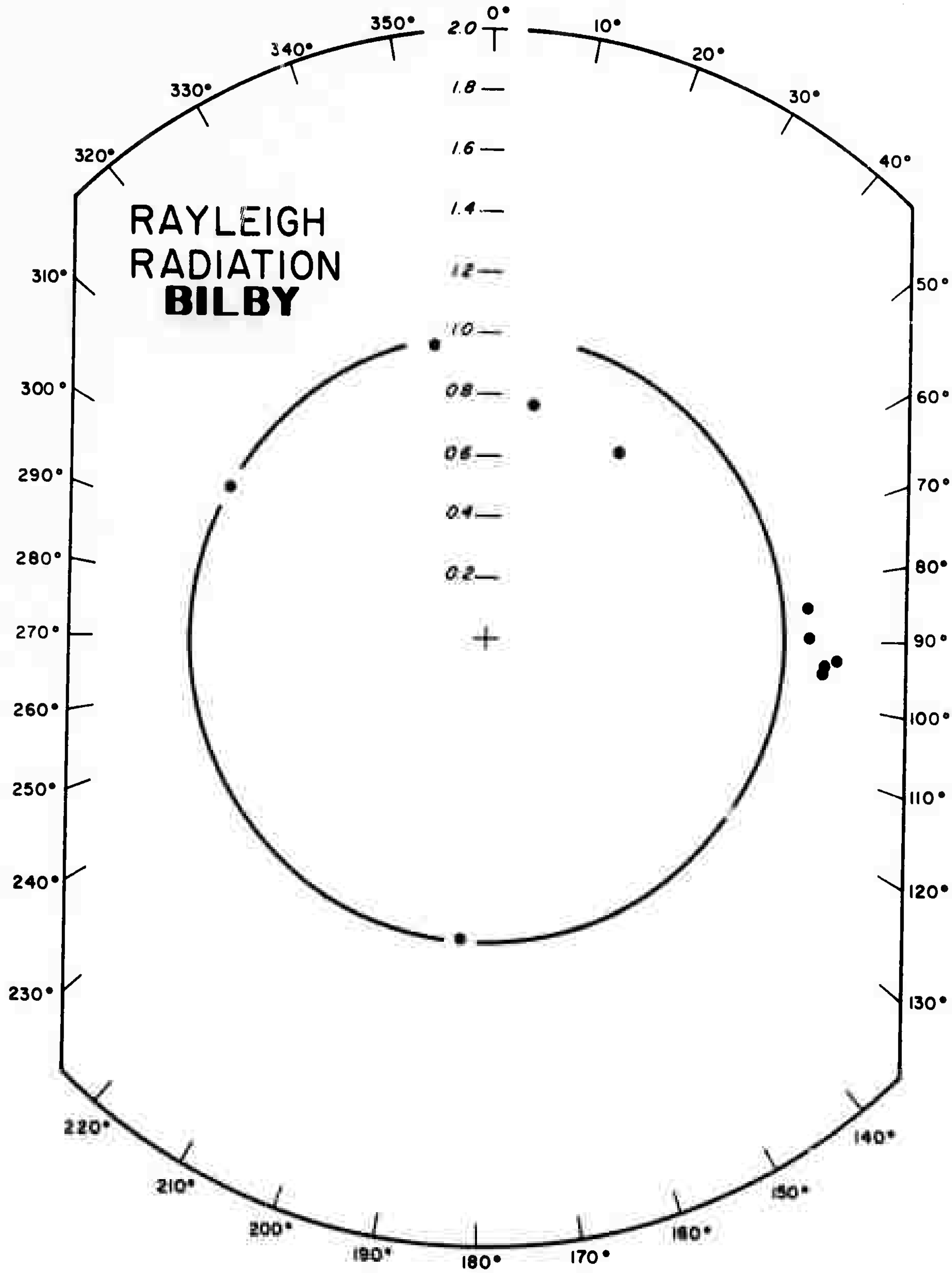

Figure 29. Rayleigh radiation pattern for the nuclear explosion BILBY using amplitudes which were not corrected for the instrumental response.

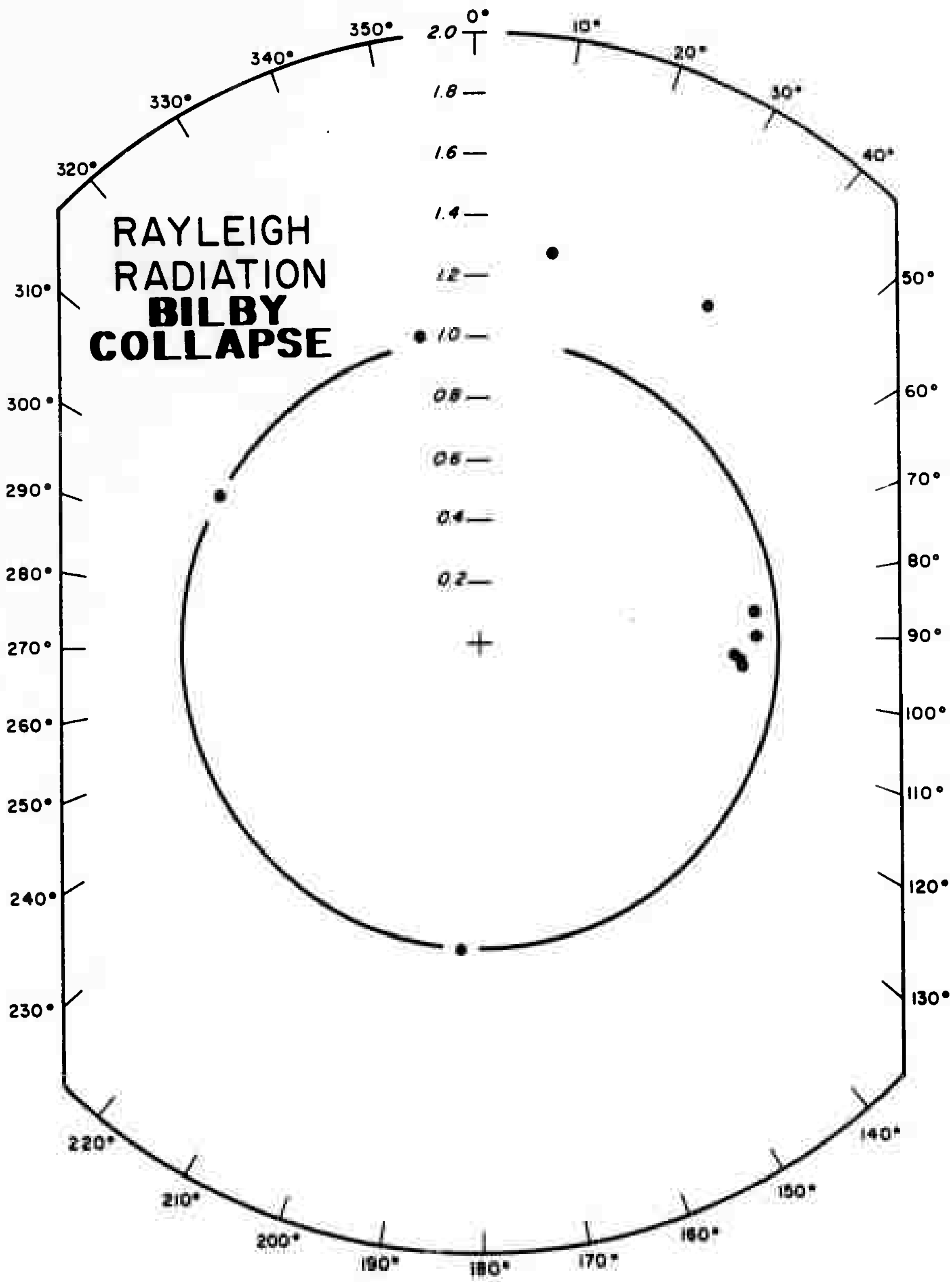

Figure 30. Rayleigh radiation pattern for the collapse of the nuclear explosion BILBY using amplitudes which were not corrected for the instrumental response.

Figure 31. Location of stations recording long period seismic energy from the nuclear explosion AARDVARK.

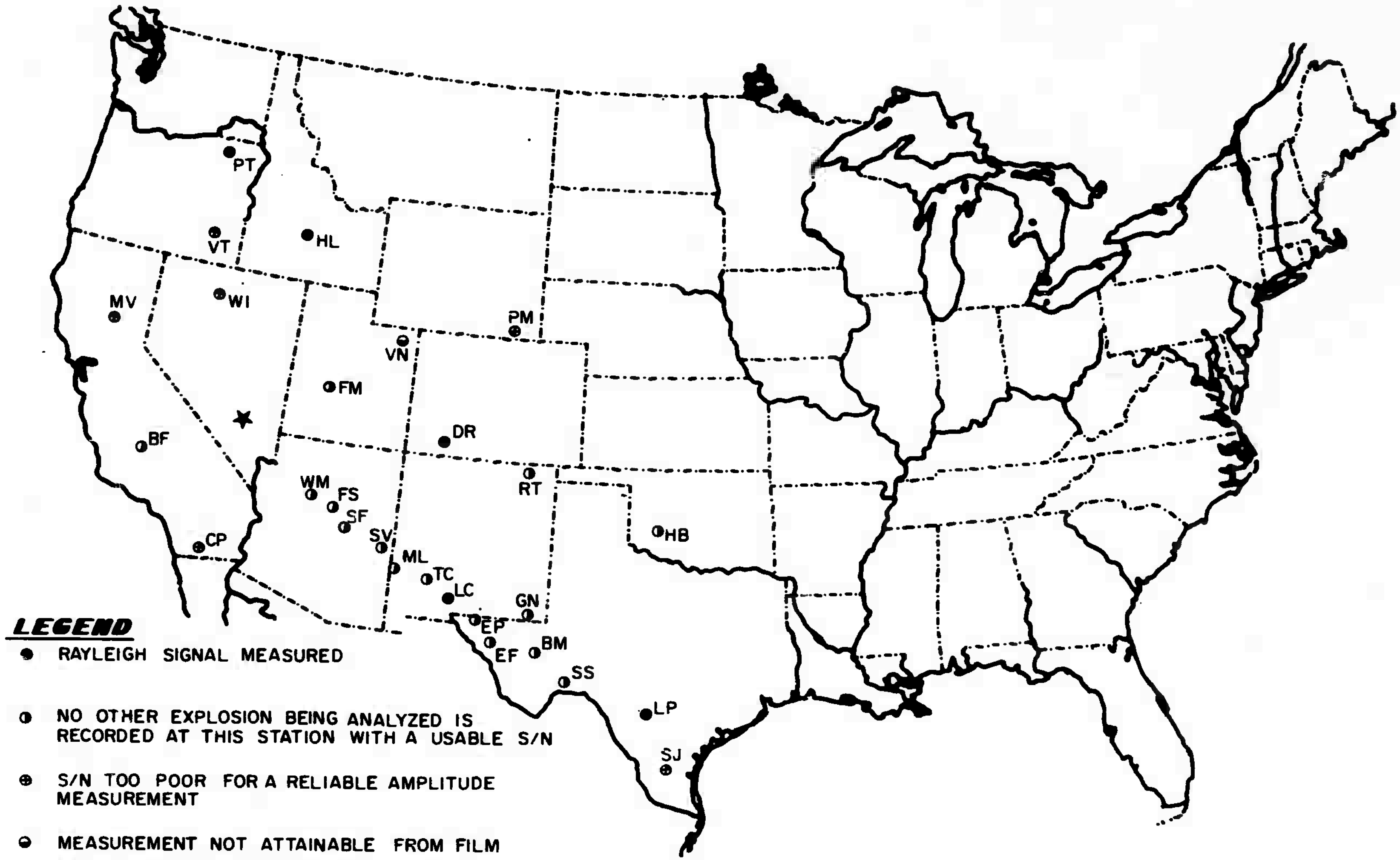

Figure 32. Location of stations recording long period seismic energy from the nuclear explosion HARDHAT.

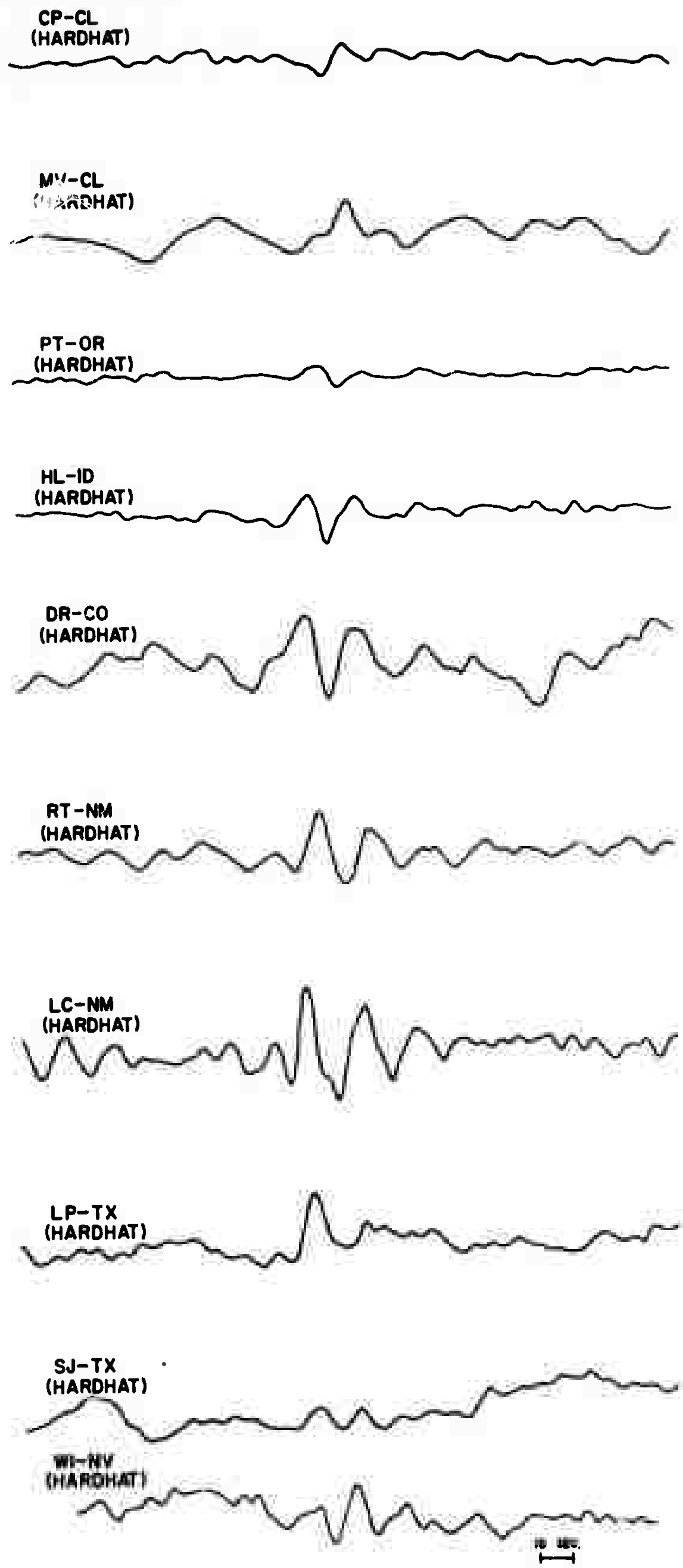

Figure 33. Rayleigh signals generated by the NTS explosion HARDHAT recorded at some LRSM stations.

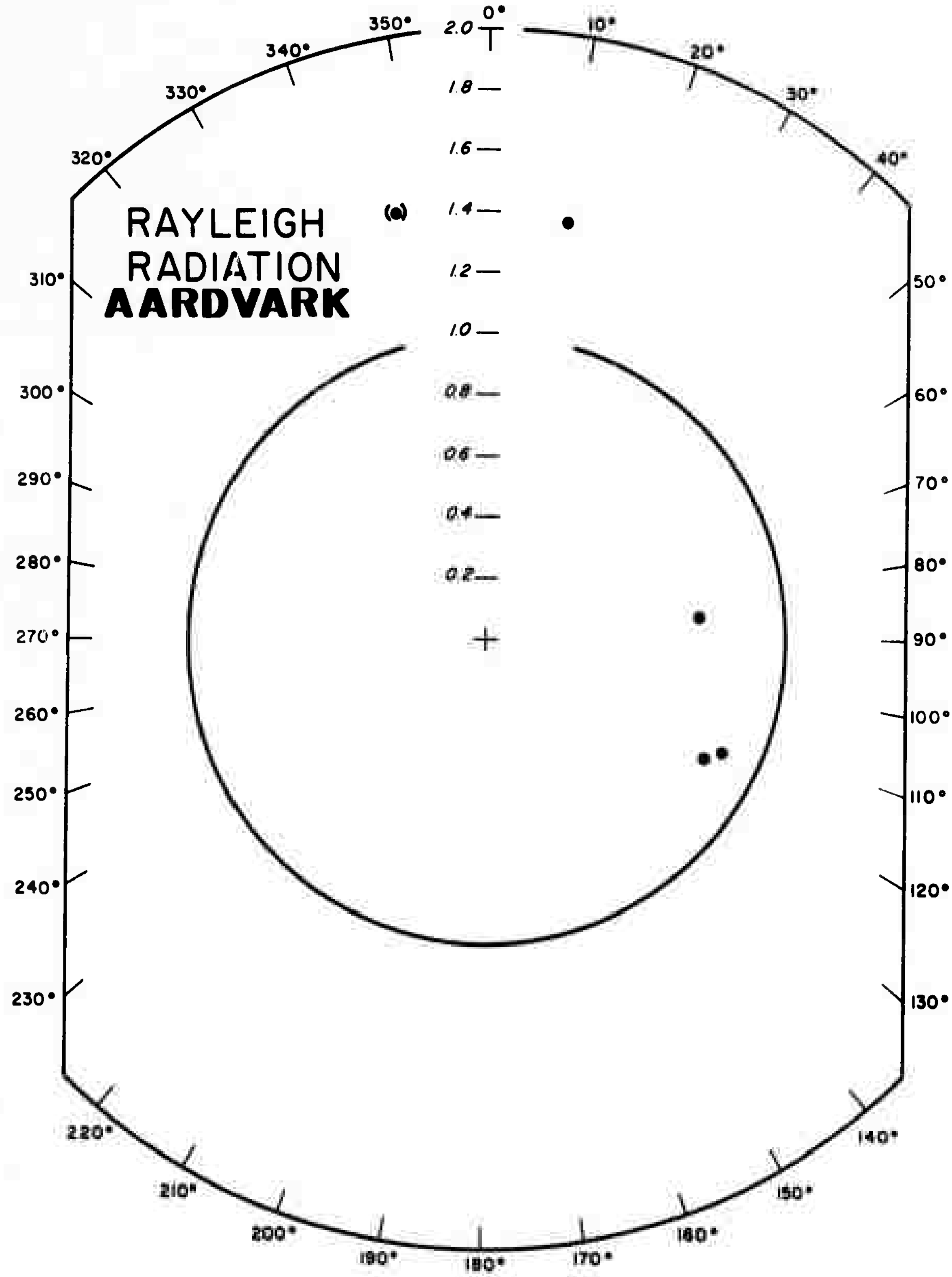

Figure 34. Rayleigh radiation pattern for the nuclear explosion AARDVARK using amplitudes which were corrected for the instrumental response.

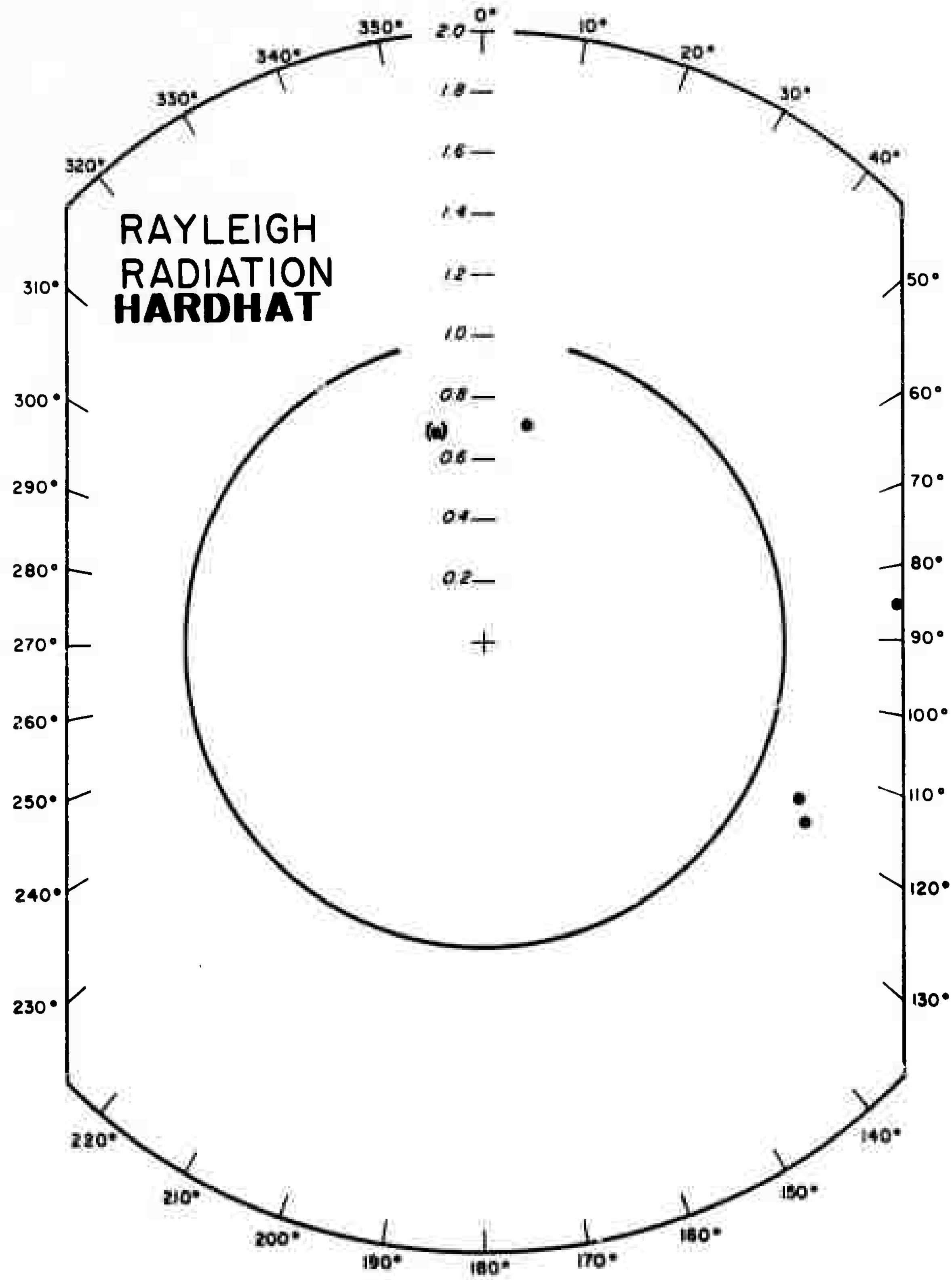

Figure 35. Rayleigh radiation pattern for the nuclear explosion HARDHAT using amplitudes which were corrected for the instrumental response.

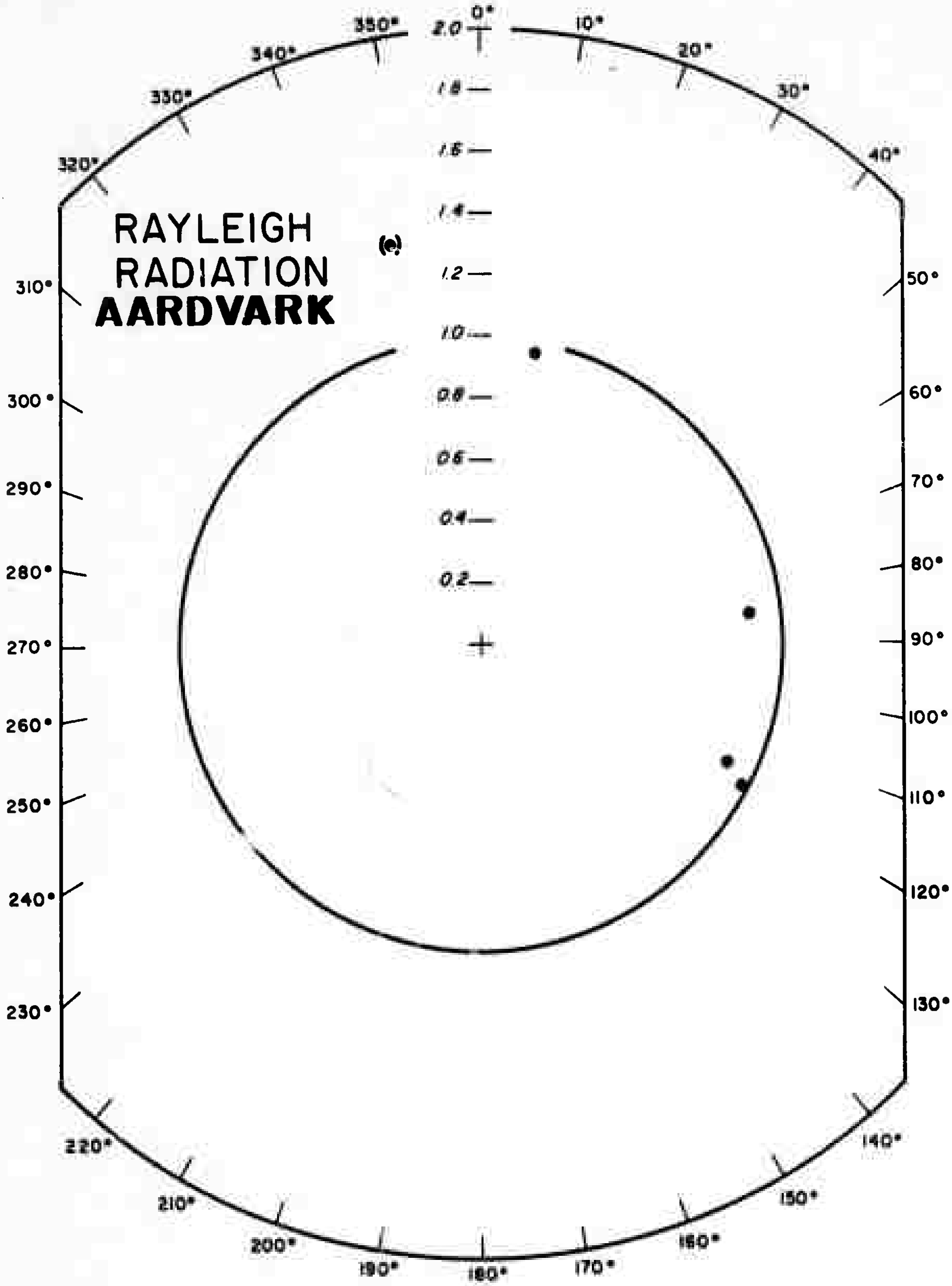

Figure 36. Rayleigh radiation pattern for the nuclear explosion AARDVARK using amplitudes which were not corrected for the instrumental response.

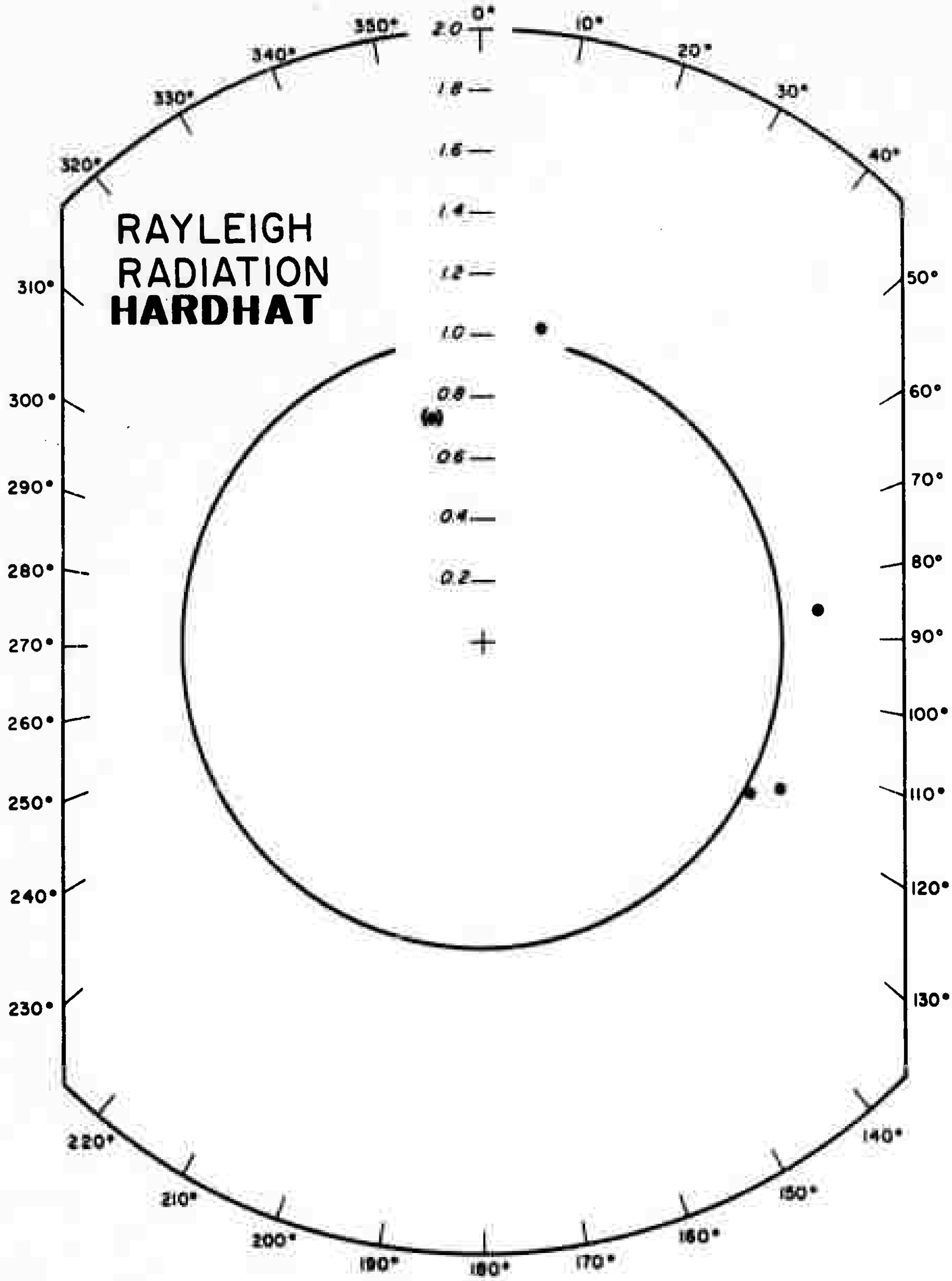

Figure 37. Rayleigh radiation pattern for the nuclear explosion HARDHAT using amplitudes which were not corrected for the instrumental response.

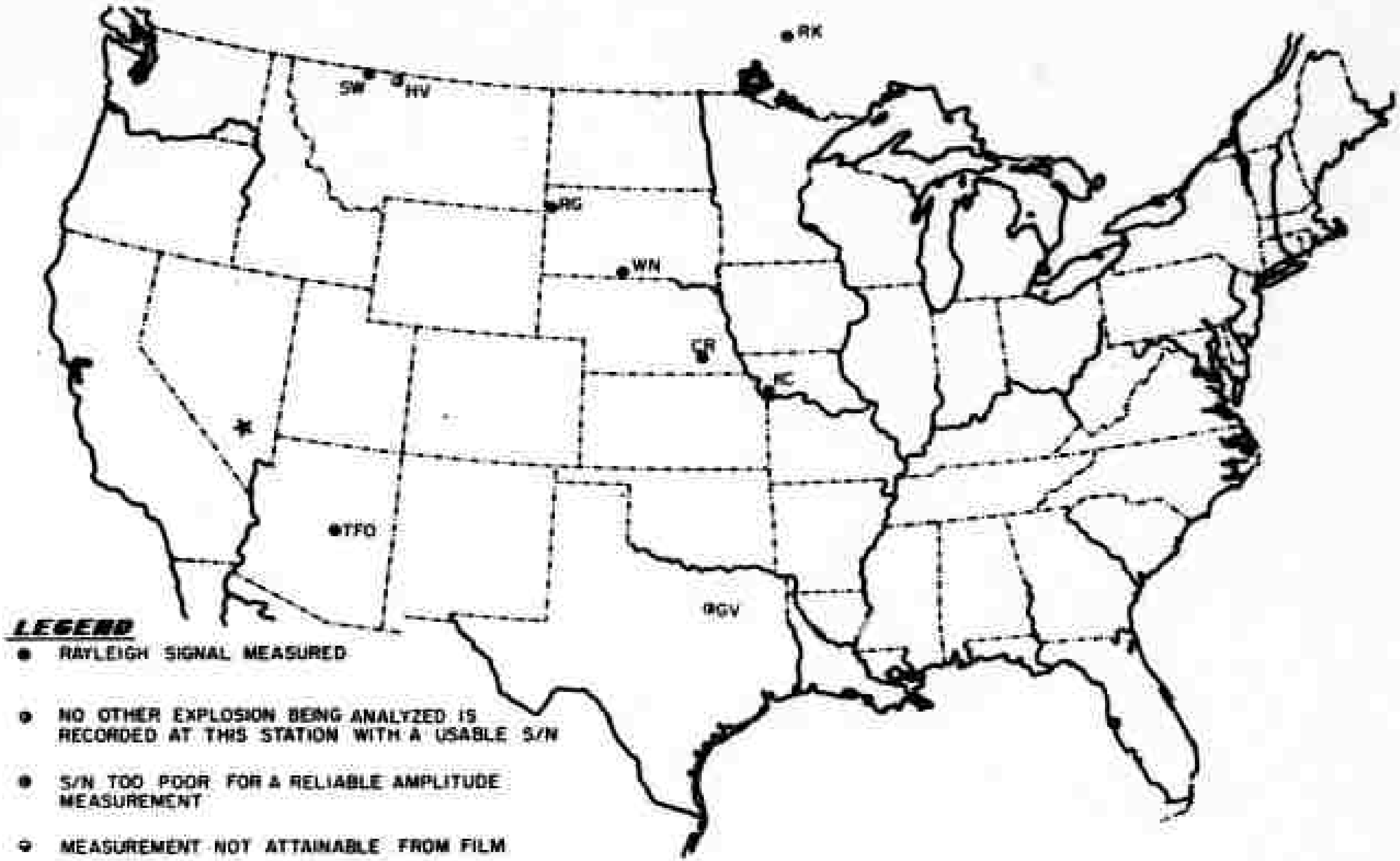

Figure 38. Location of stations recording long period seismic energy from the collapse of the nuclear explosion CORDUROY.

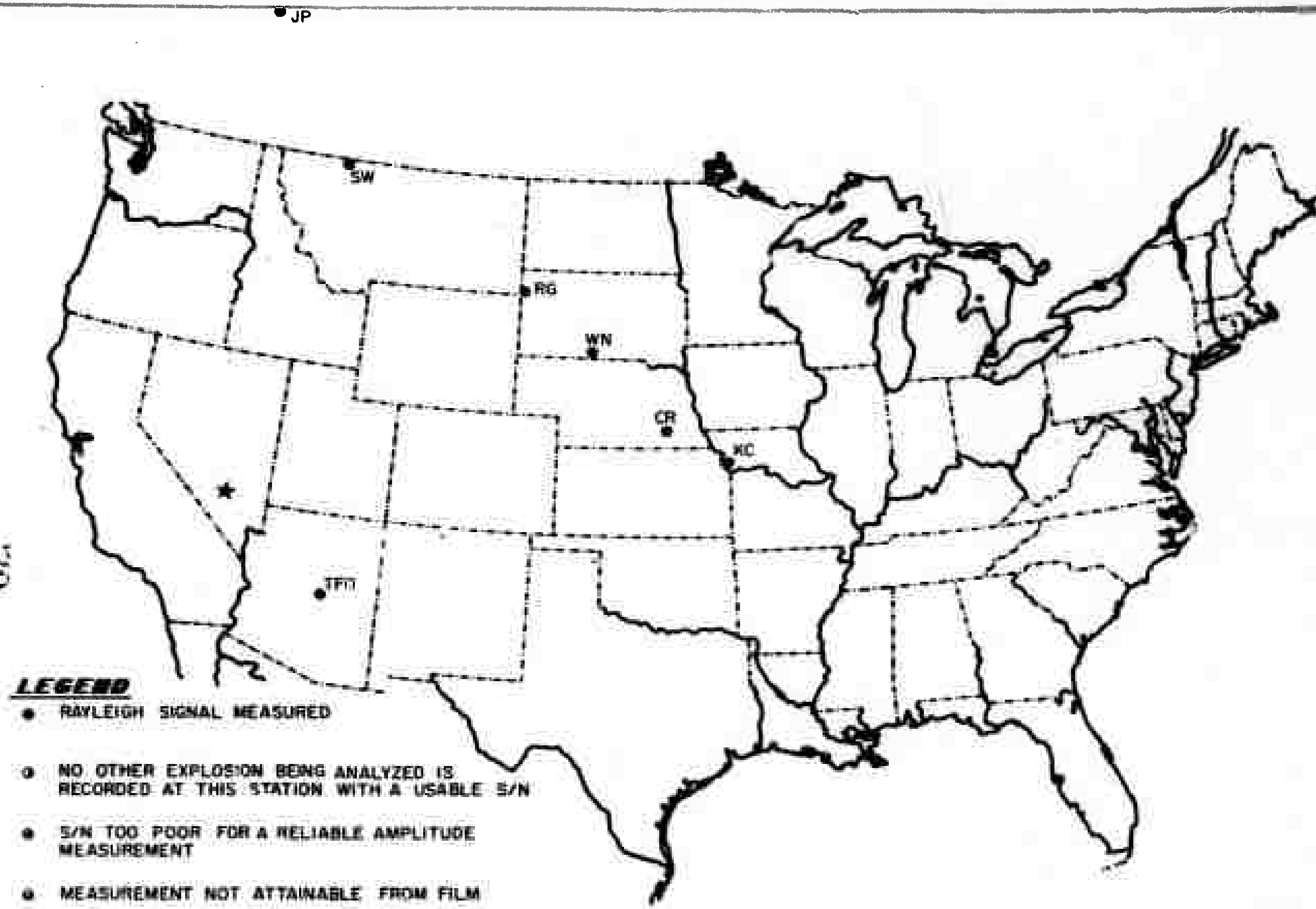

Figure 39. Location of stations recording long period seismic energy from the collapse of the nuclear explosion DUMONT.

Figure 40. Location of stations recording long period seismic energy from the collapse of the nuclear explosion HALF BEAK.

Figure 41. Location of stations recording long period seismic energy from the nuclear explosion DUMONT.

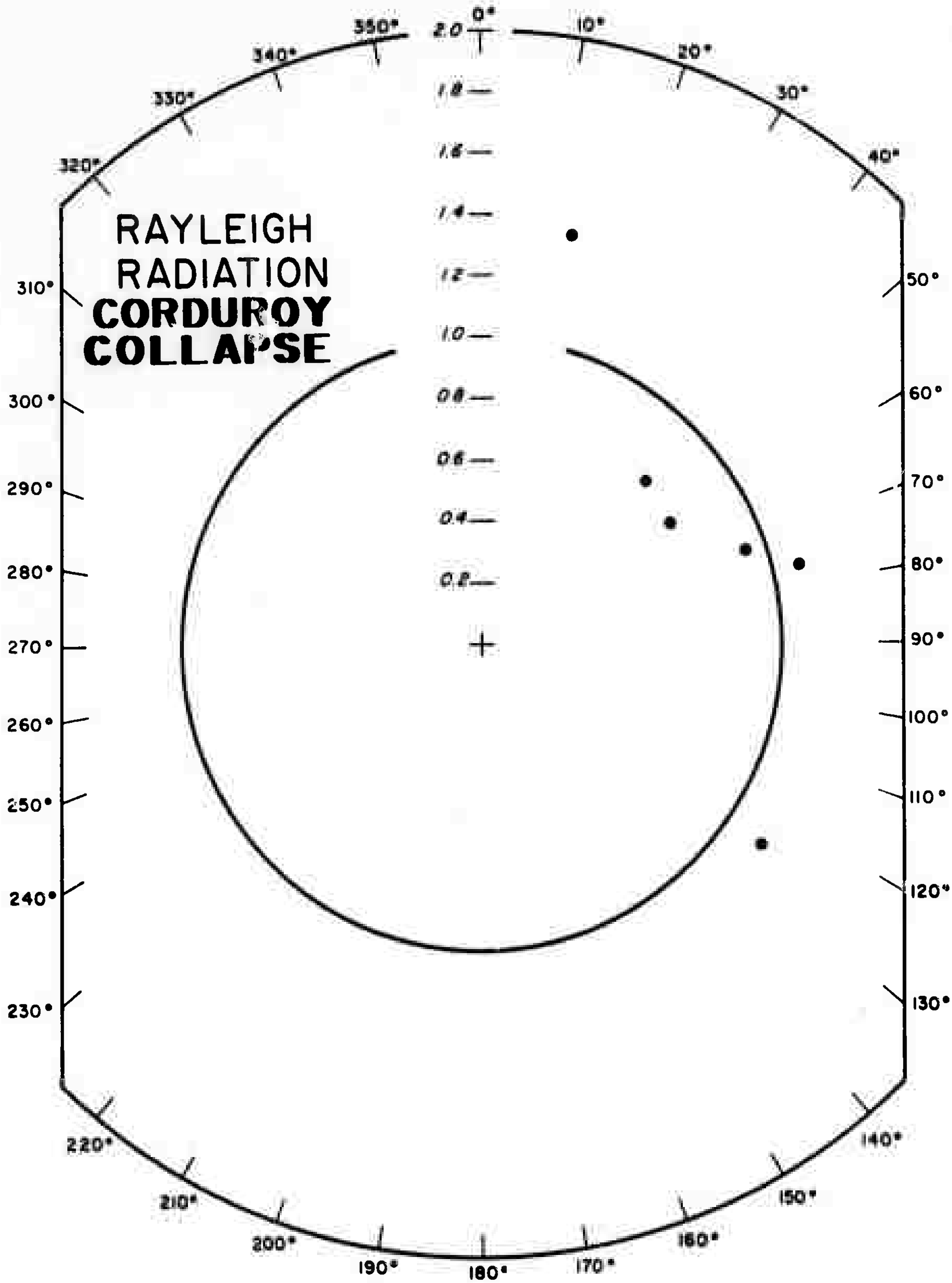

Figure 42. Rayleigh radiation pattern for the collapse of the nuclear explosion CORDUROY using amplitudes which were corrected for the instrumental response.

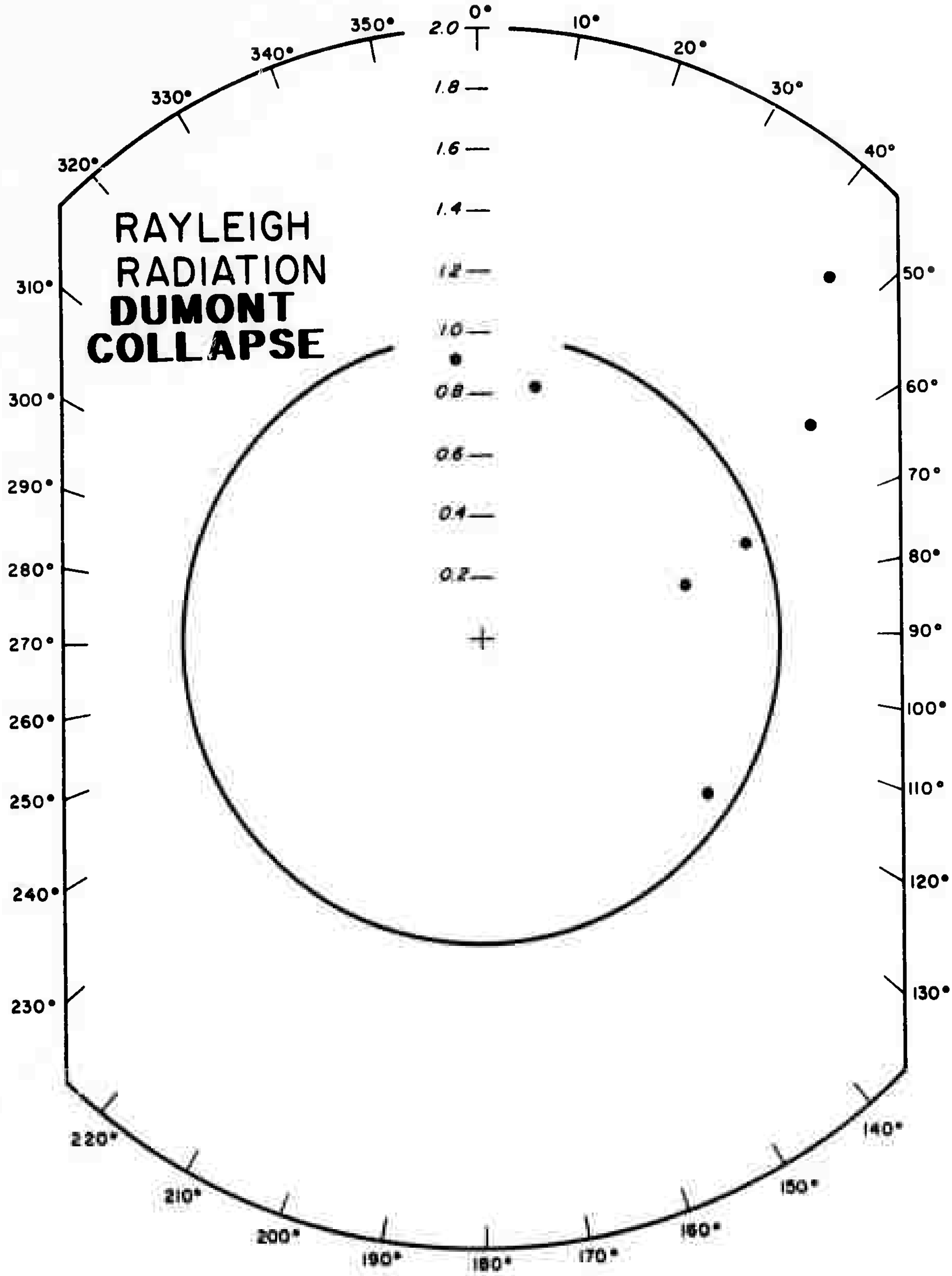

Figure 43. Rayleigh radiation pattern for the collapse of the nuclear explosion DUMONT using amplitudes which were corrected for the instrumental response.

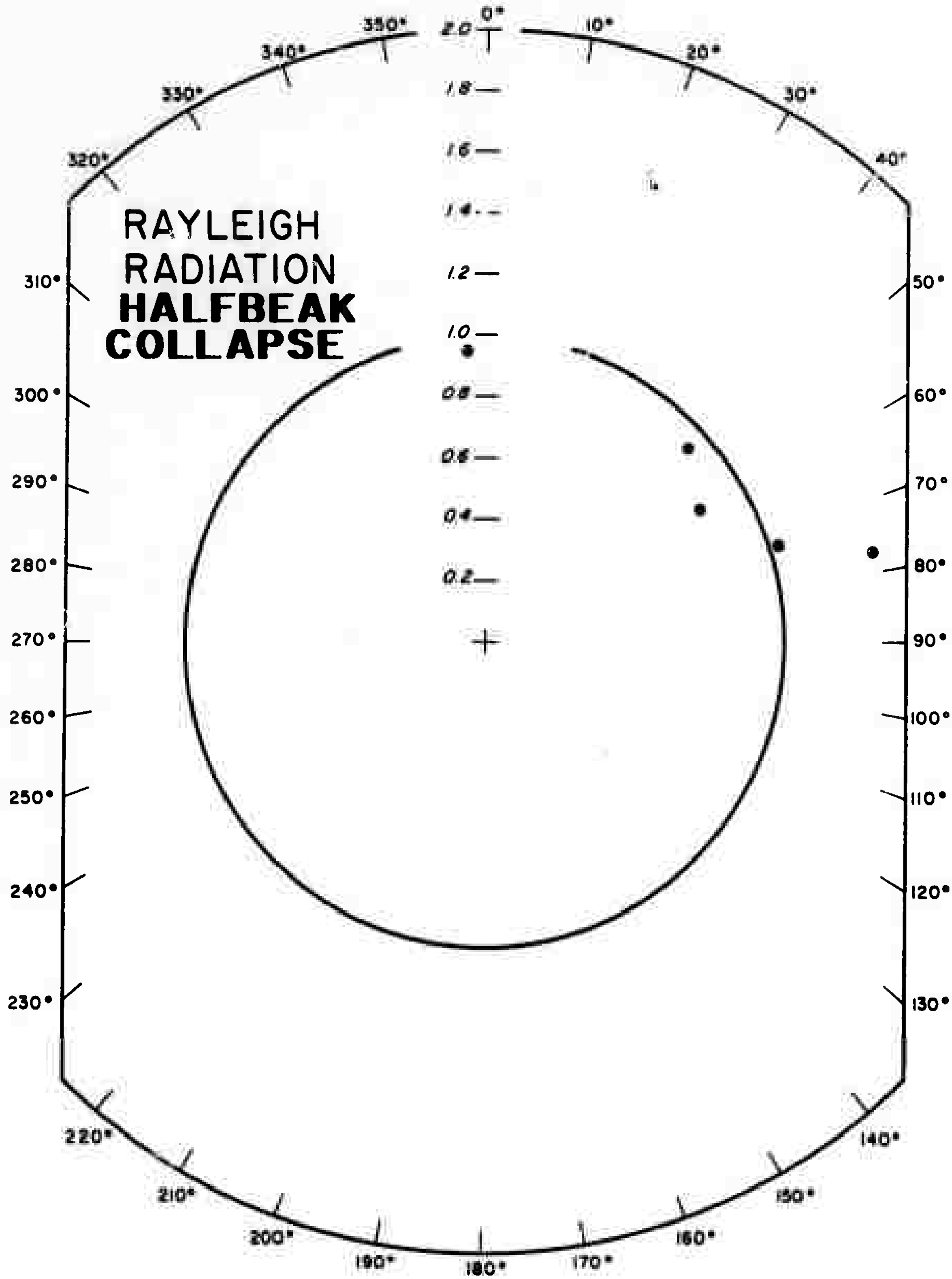

Figure 44. Rayleigh radiation pattern for the collapse of the nuclear explosion HALF BEAK using amplitudes which were corrected for the instrumental response.

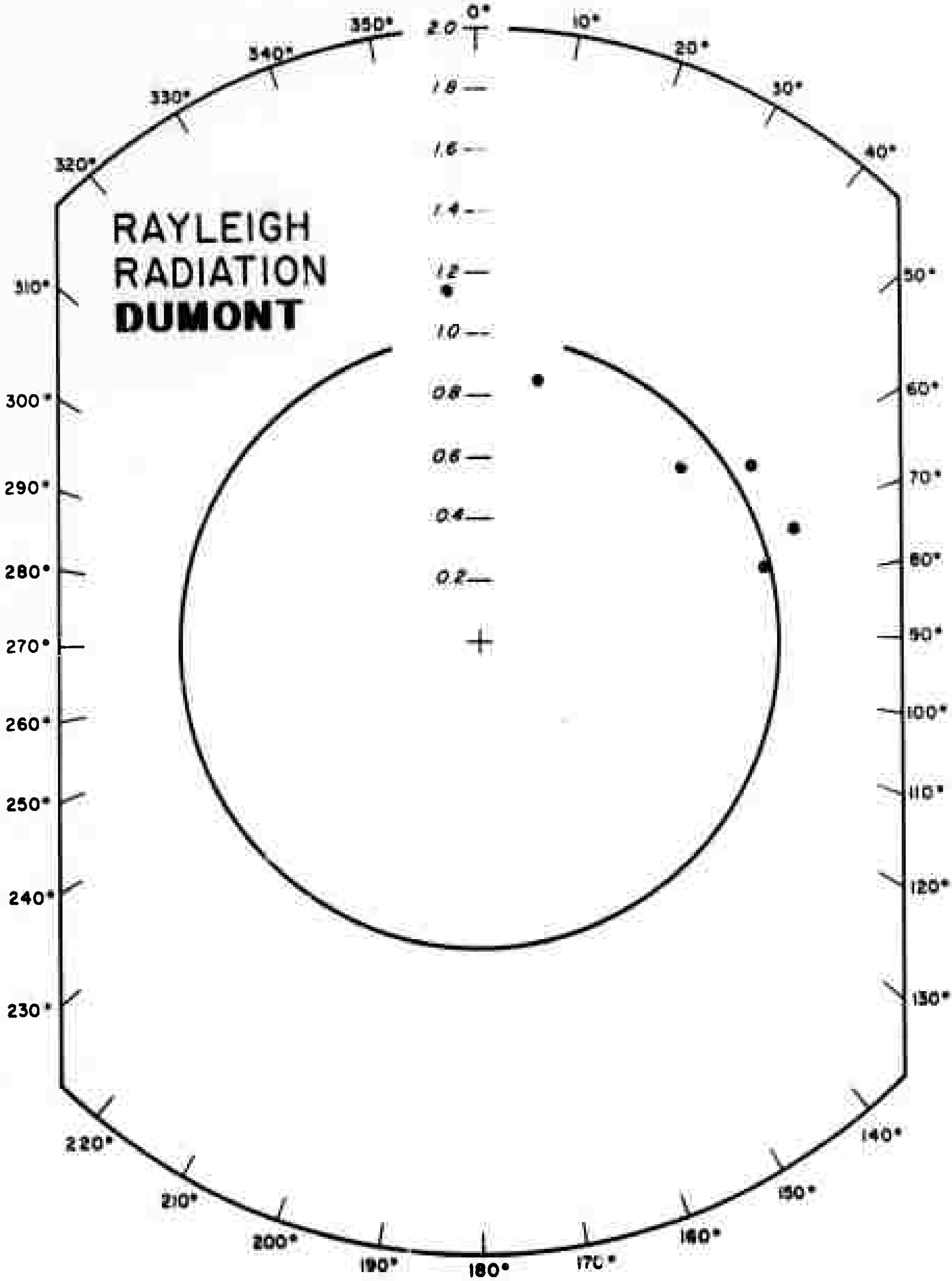

Figure 45. Rayleigh radiation pattern for the nuclear explosion DUMONT using amplitudes which were corrected for the instrumental response.

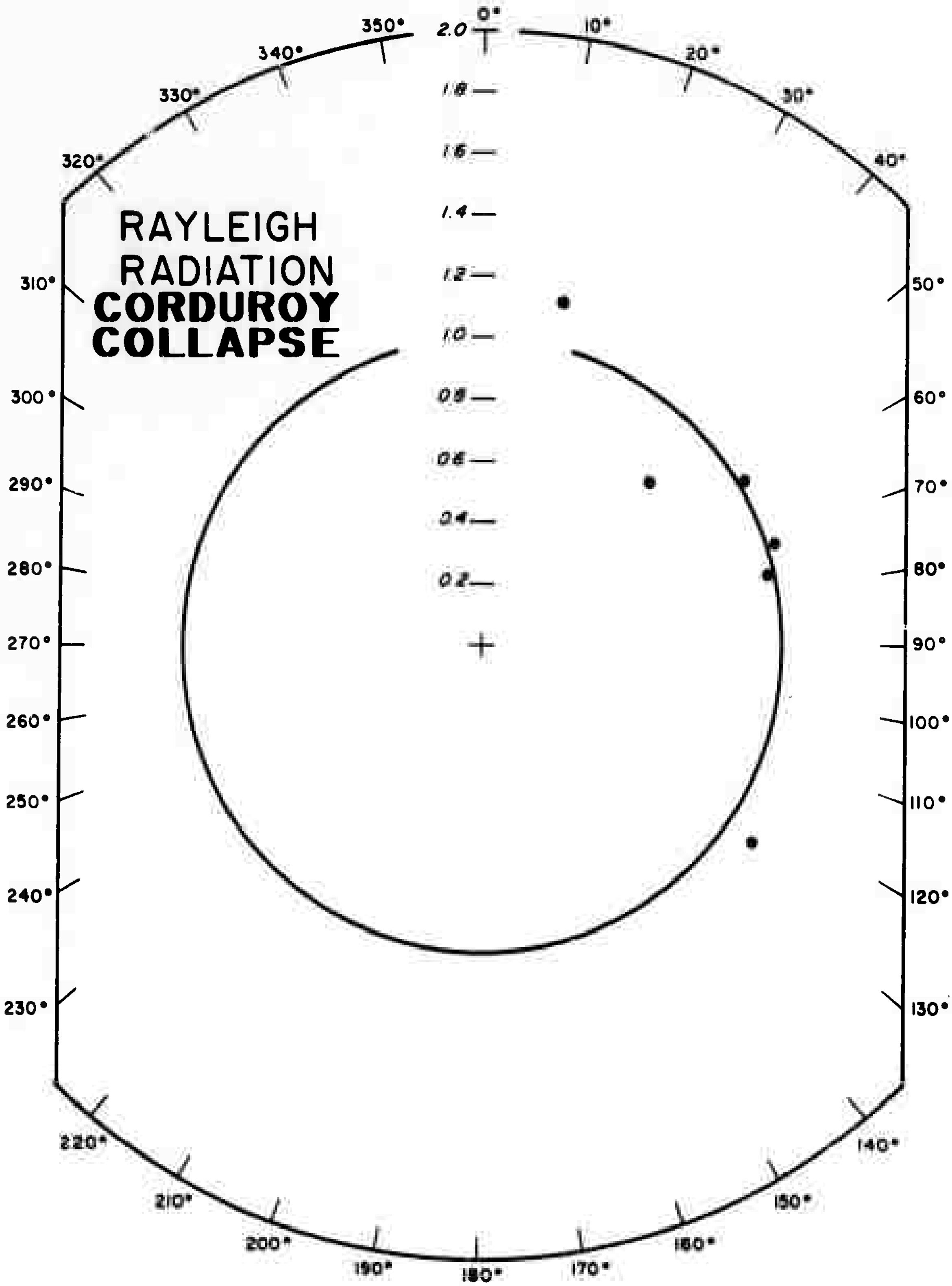

Figure 46. Rayleigh radiation pattern for the collapse of the nuclear explosion CORDUROY using amplitudes which were not corrected for the instrumental response.

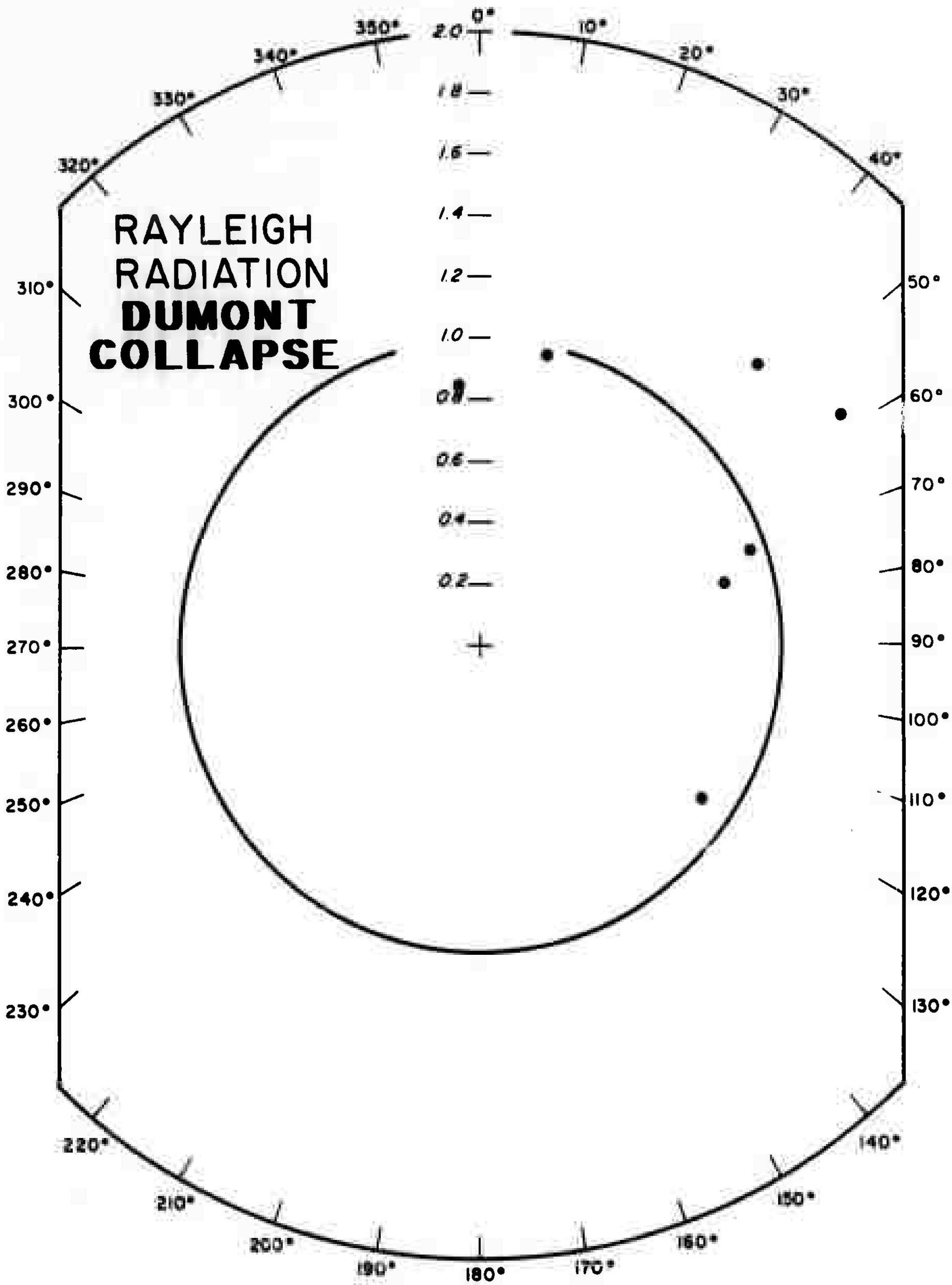

Figure 47. Rayleigh radiation pattern for the collapse of the nuclear explosion DUMONT using amplitudes which were not corrected for the instrumental response.

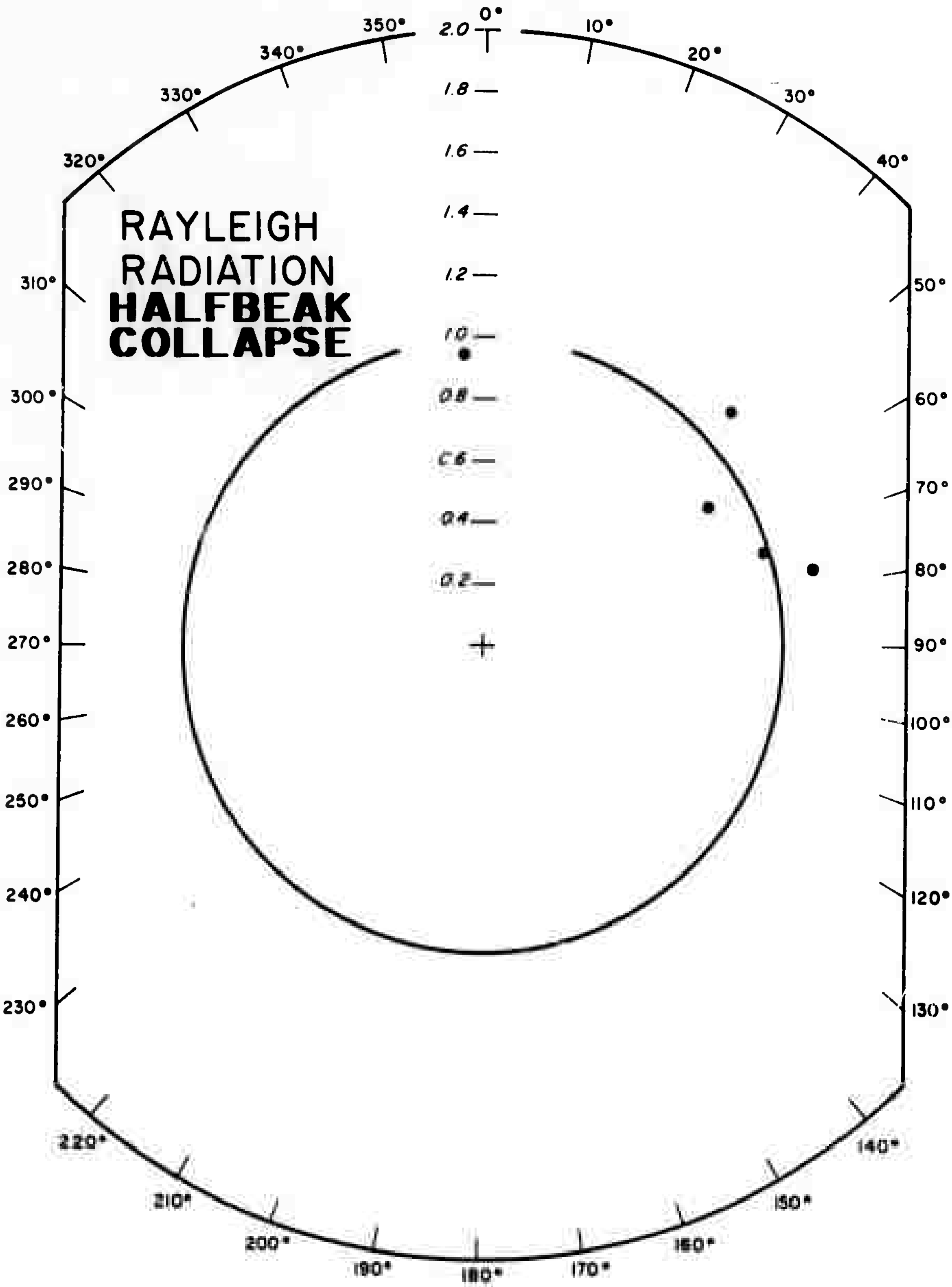

Figure 48. Rayleigh radiation pattern for the collapse of the nuclear explosion HALF BEAK using amplitudes which were not corrected for the instrumental response.

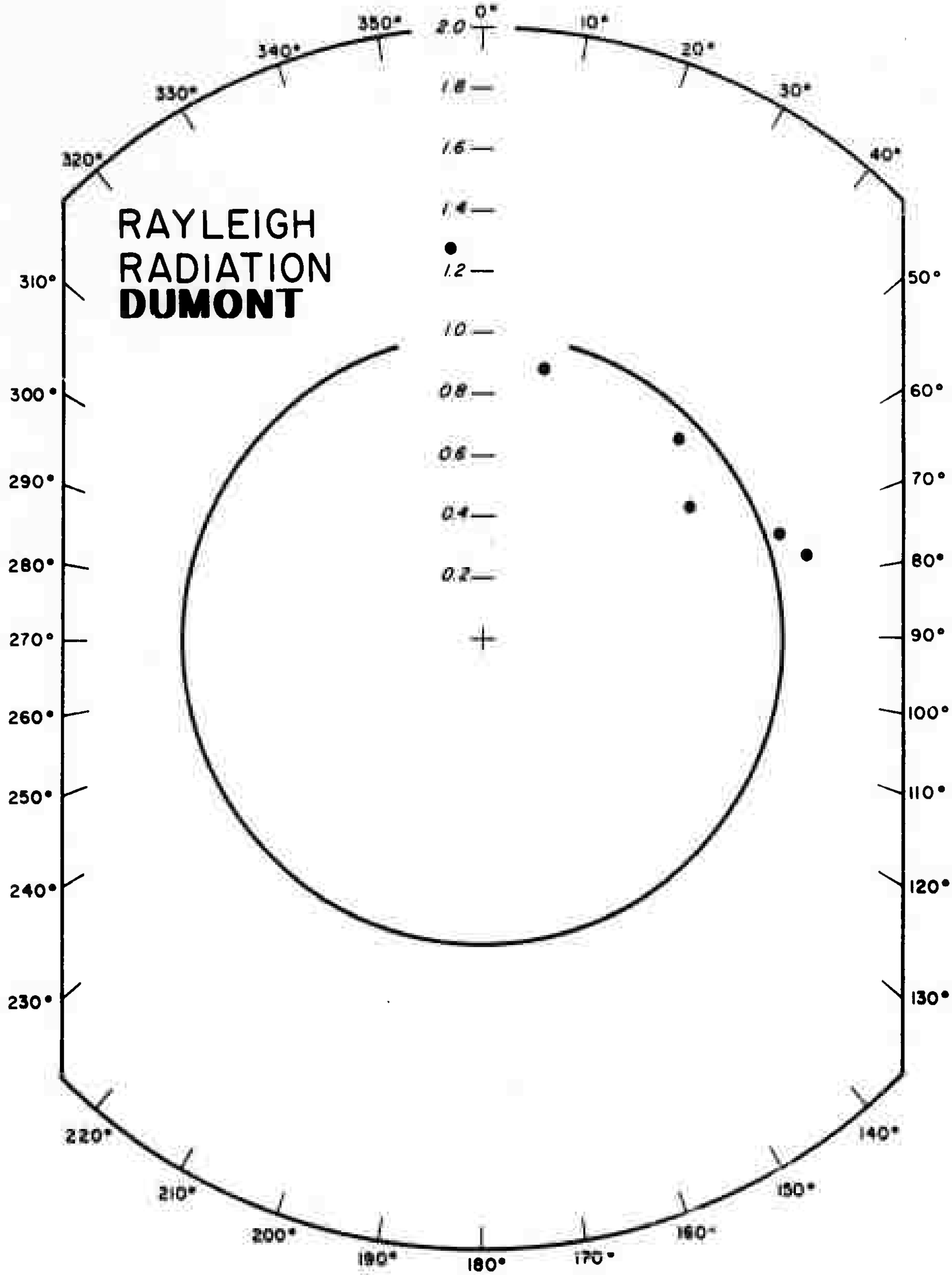

Figure 49. Rayleigh radiation pattern for the nuclear explosion DUMONT using amplitudes which were not corrected for the instrumental.response.

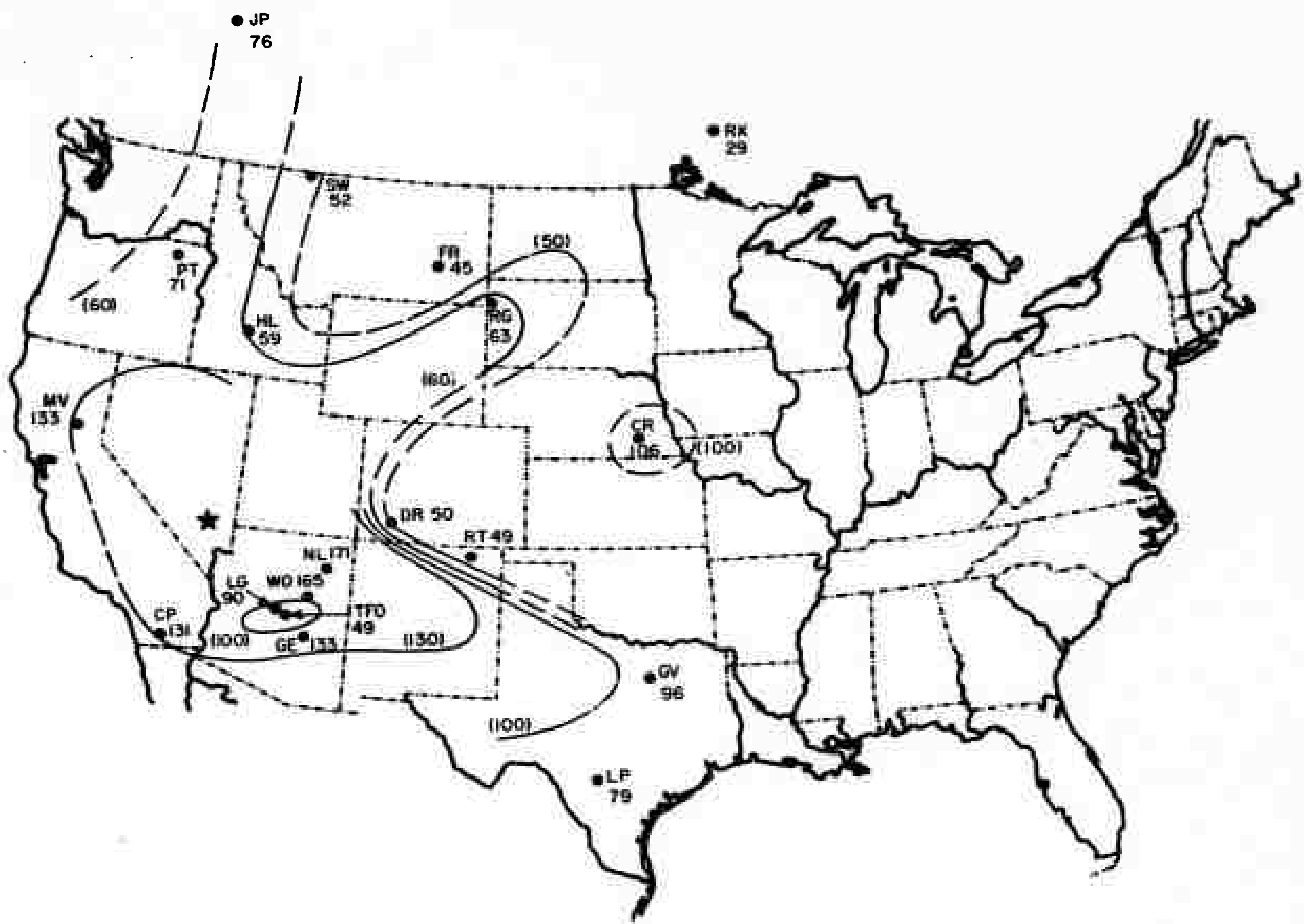

Figure 50. Station amplitude factor contours for Rayleigh waves.

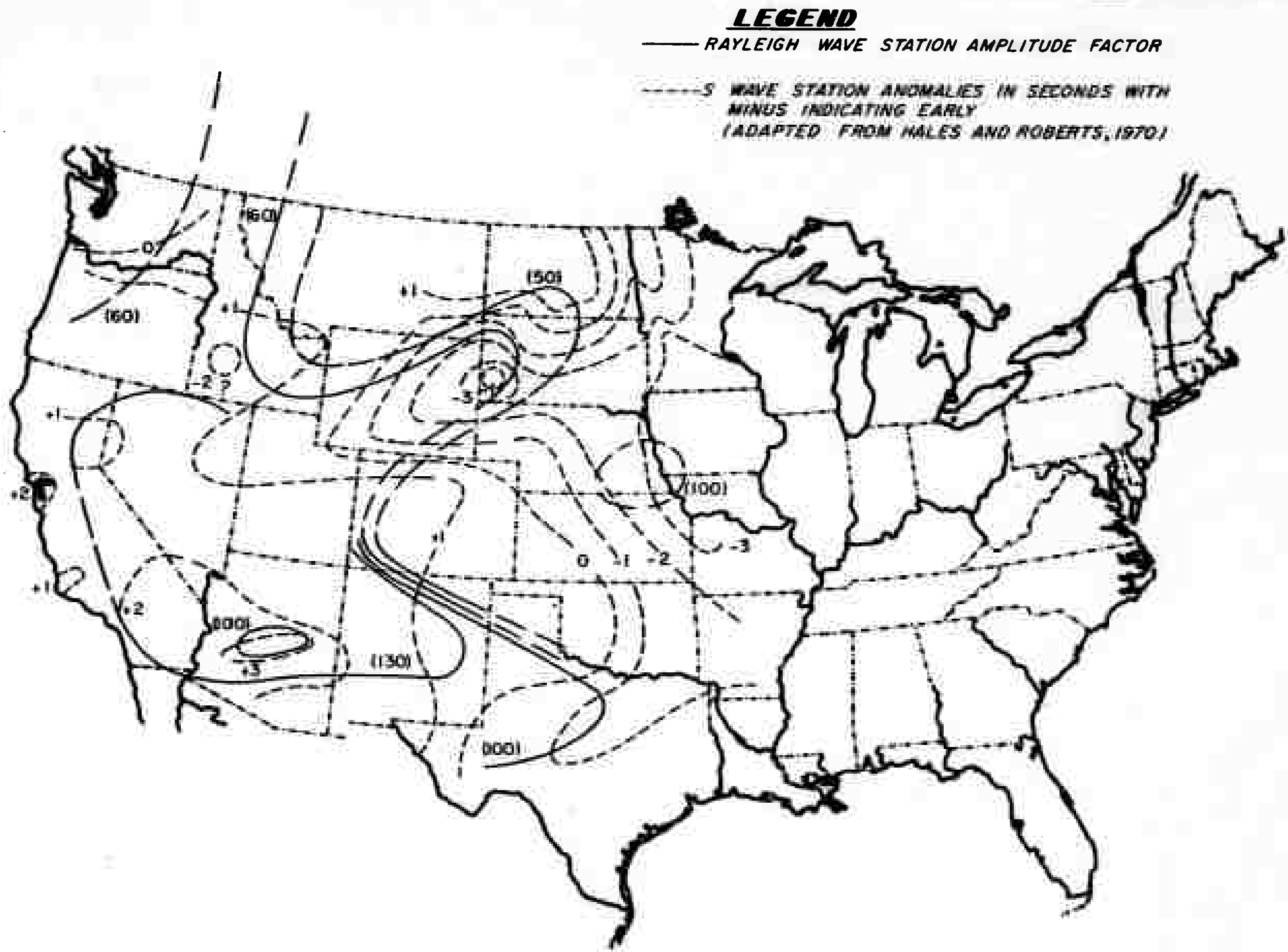

Figure 51. Station amplitude factor contours for Rayleigh waves and S wave travel time anomaly contours.

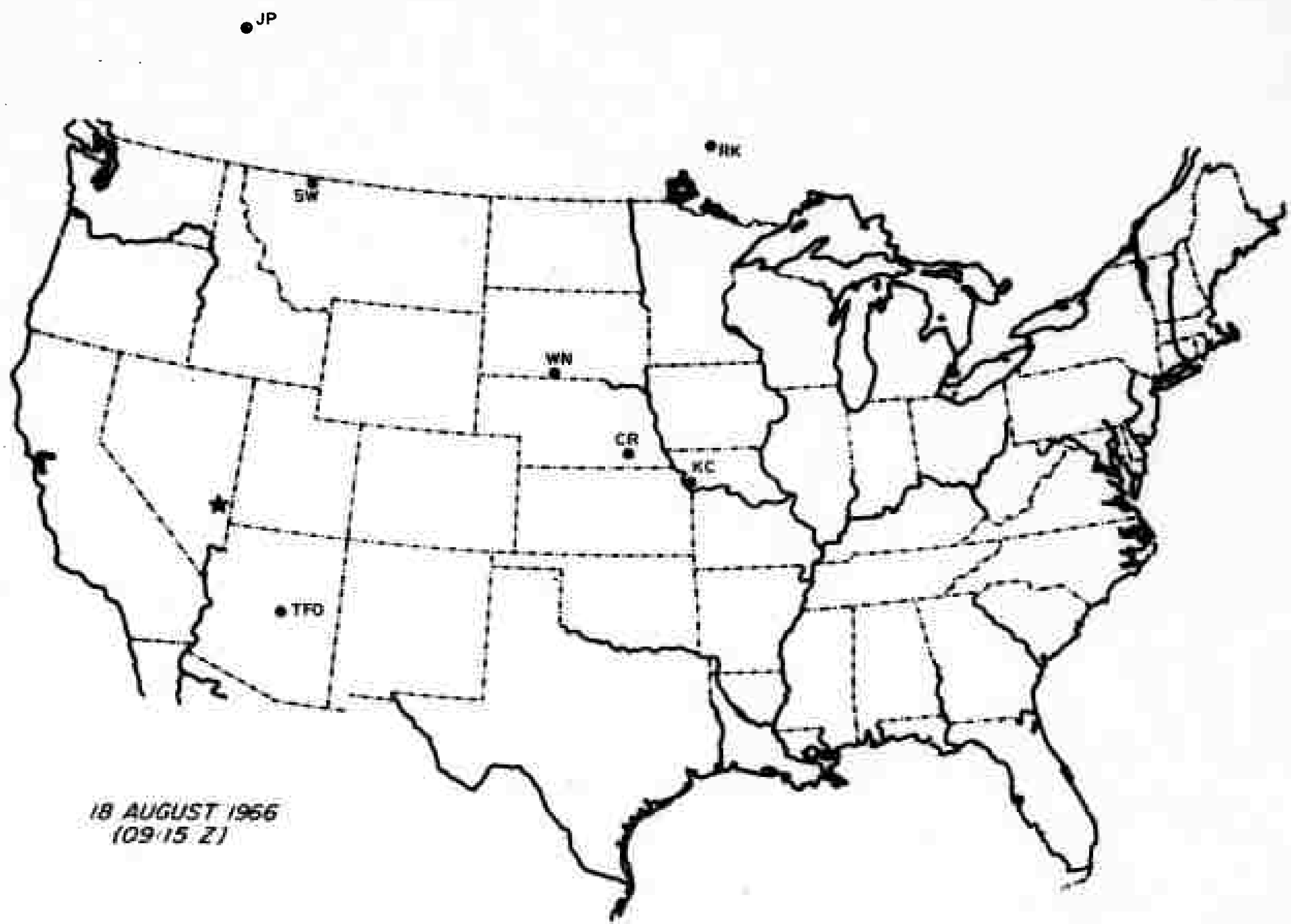

Figure 52a. Location of stations recording long period seismic energy from the southern Nevada earthquake of 18 August 1966 (09:15Z).

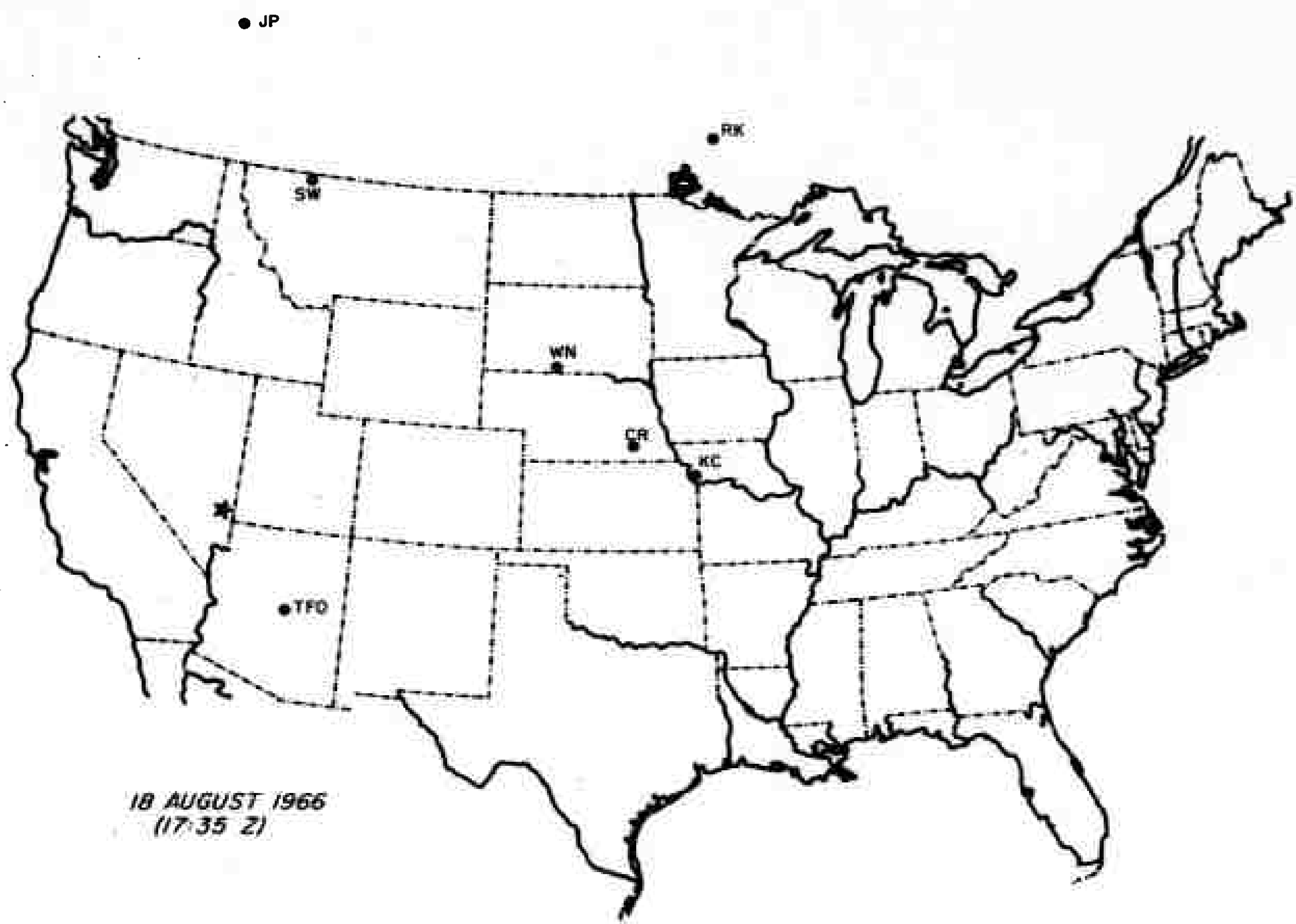

Figure 52b. Location of stations recording long period seismic energy from the southern Nevada earthquake of 18 August 1966 (17:35 Z).

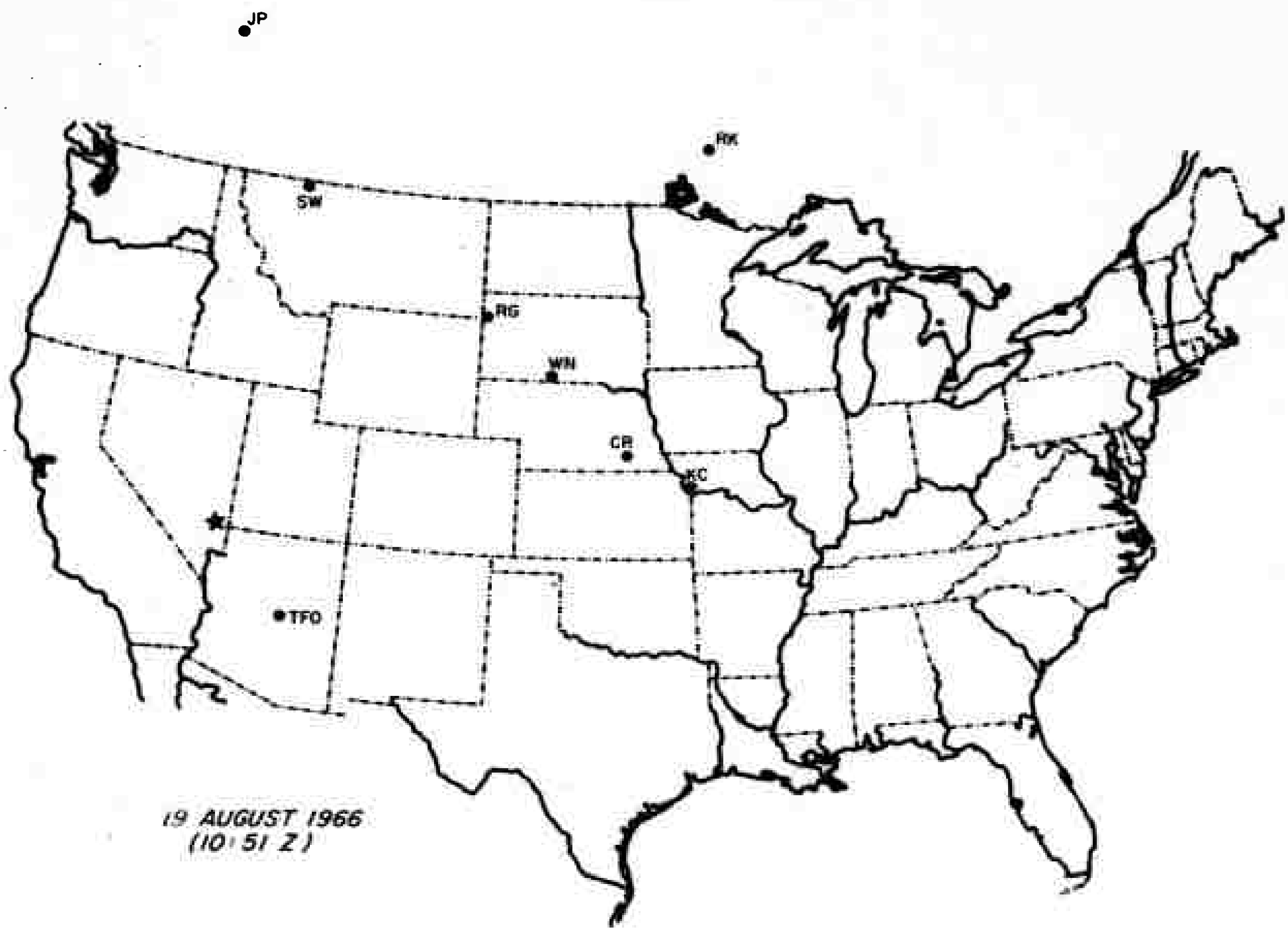

Figure 52c. Location of stations recording long period seismic energy from the southern Nevada earthquake of 19 August 1966 (10:51 Z).

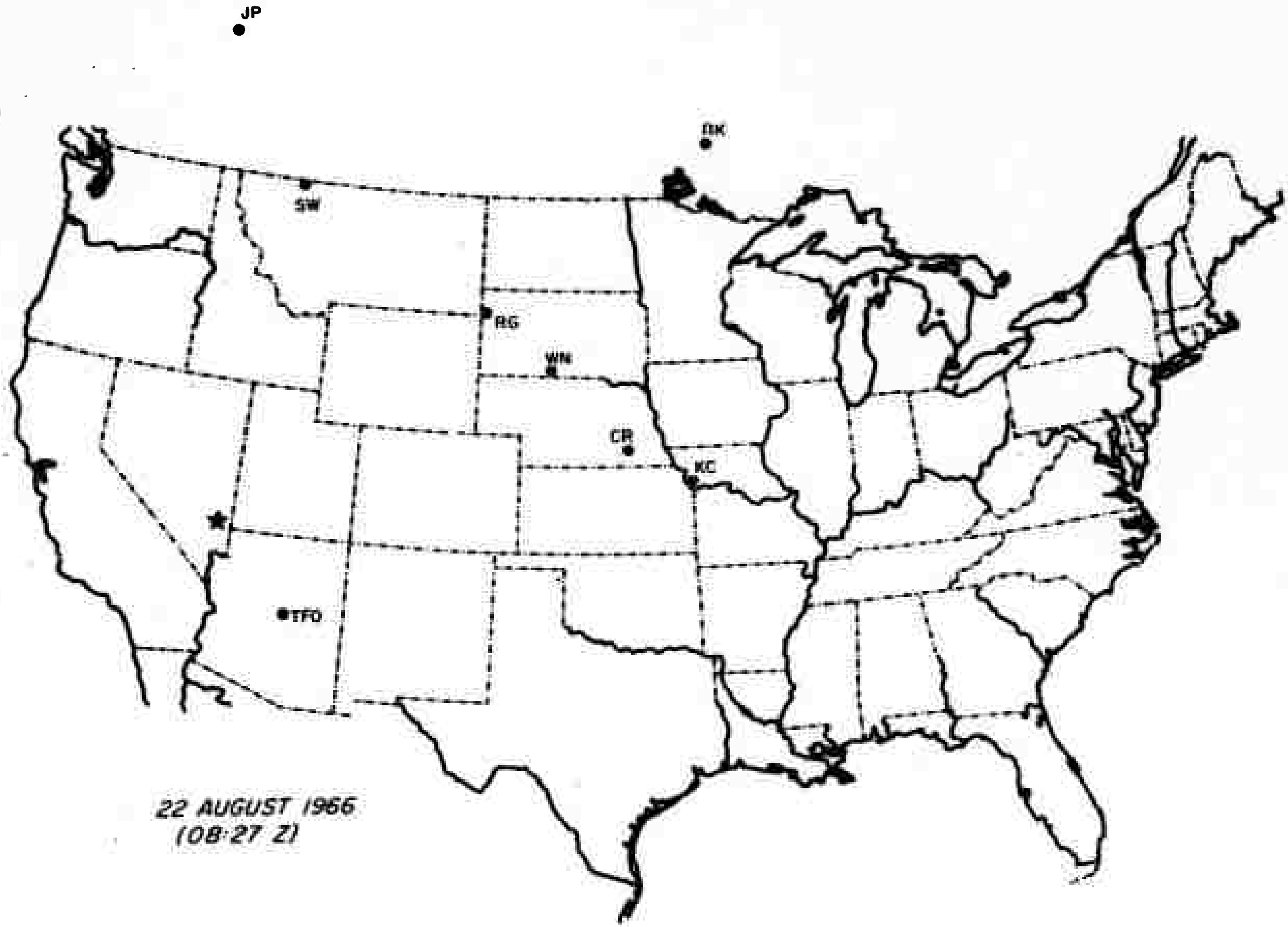

Figure 52d. Location of stations recording long period seismic energy from the southern Nevada earthquake of 22 August 1966 (08:27 Z).

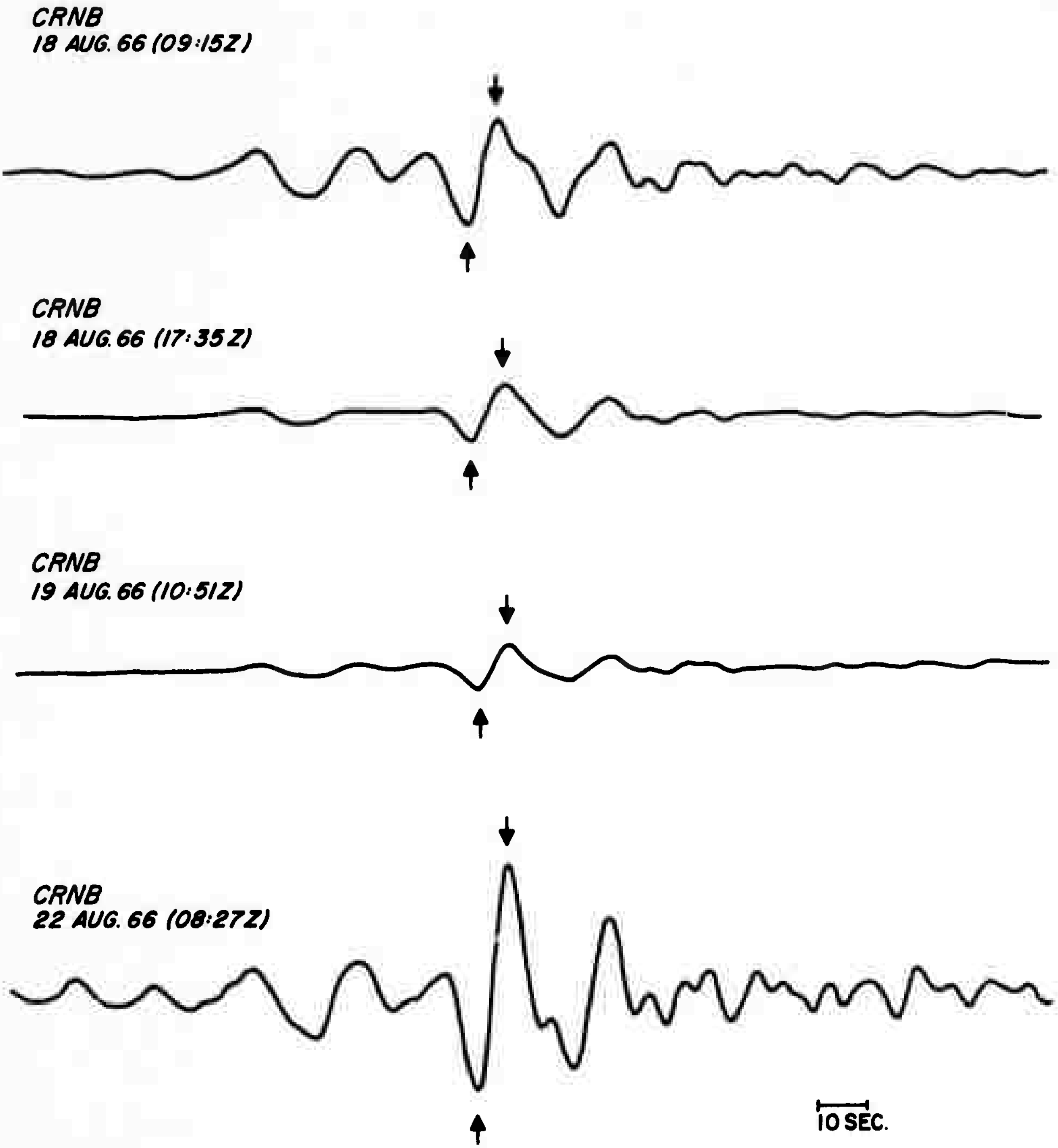

Figure 53. Rayleigh signals from four southern Nevada earthquakes recorded at CR-NB.

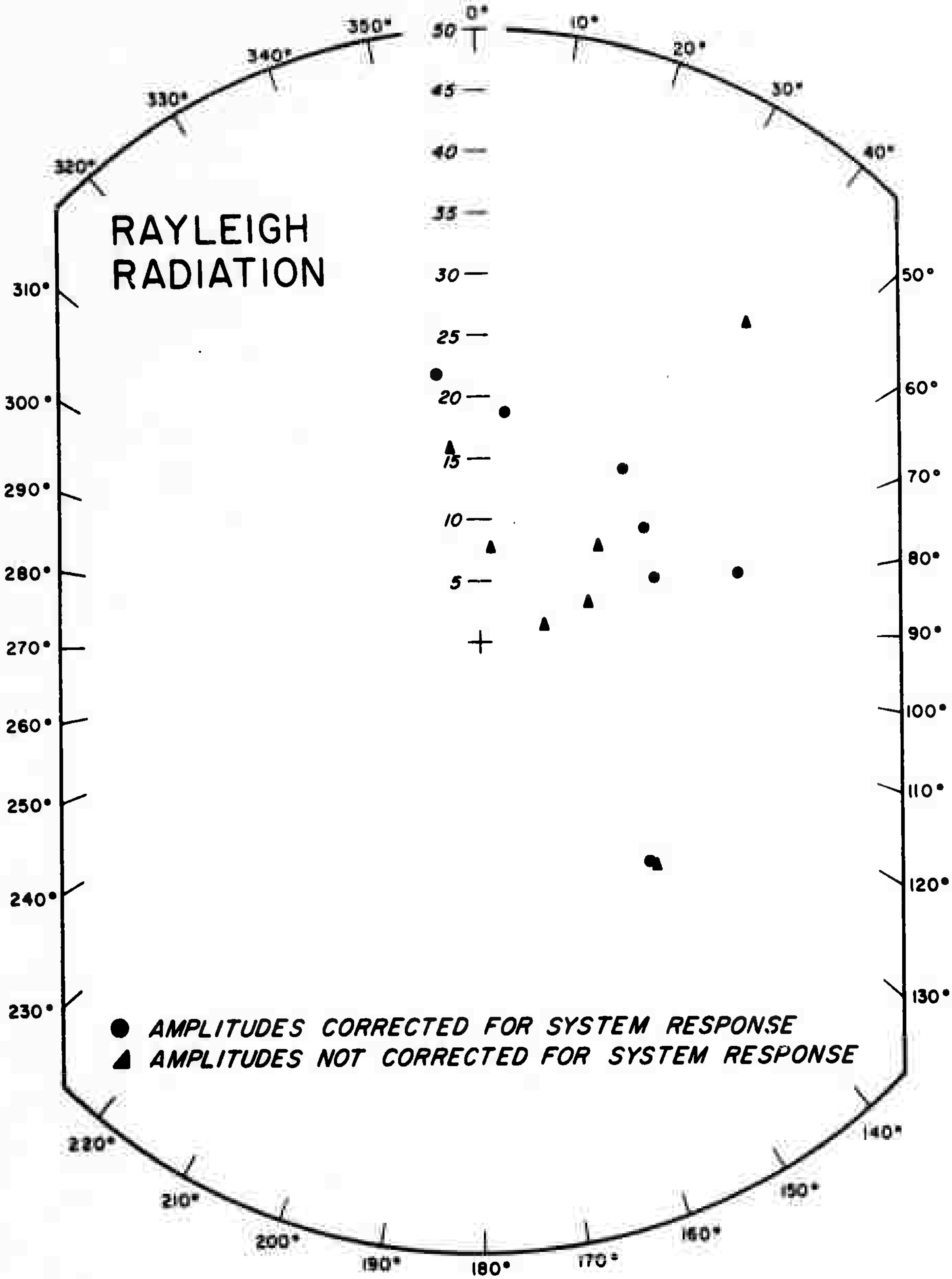

Figure 54. Rayleigh radiation pattern for the southern Nevada earthquake of 18 August 1966 (09:15Z).

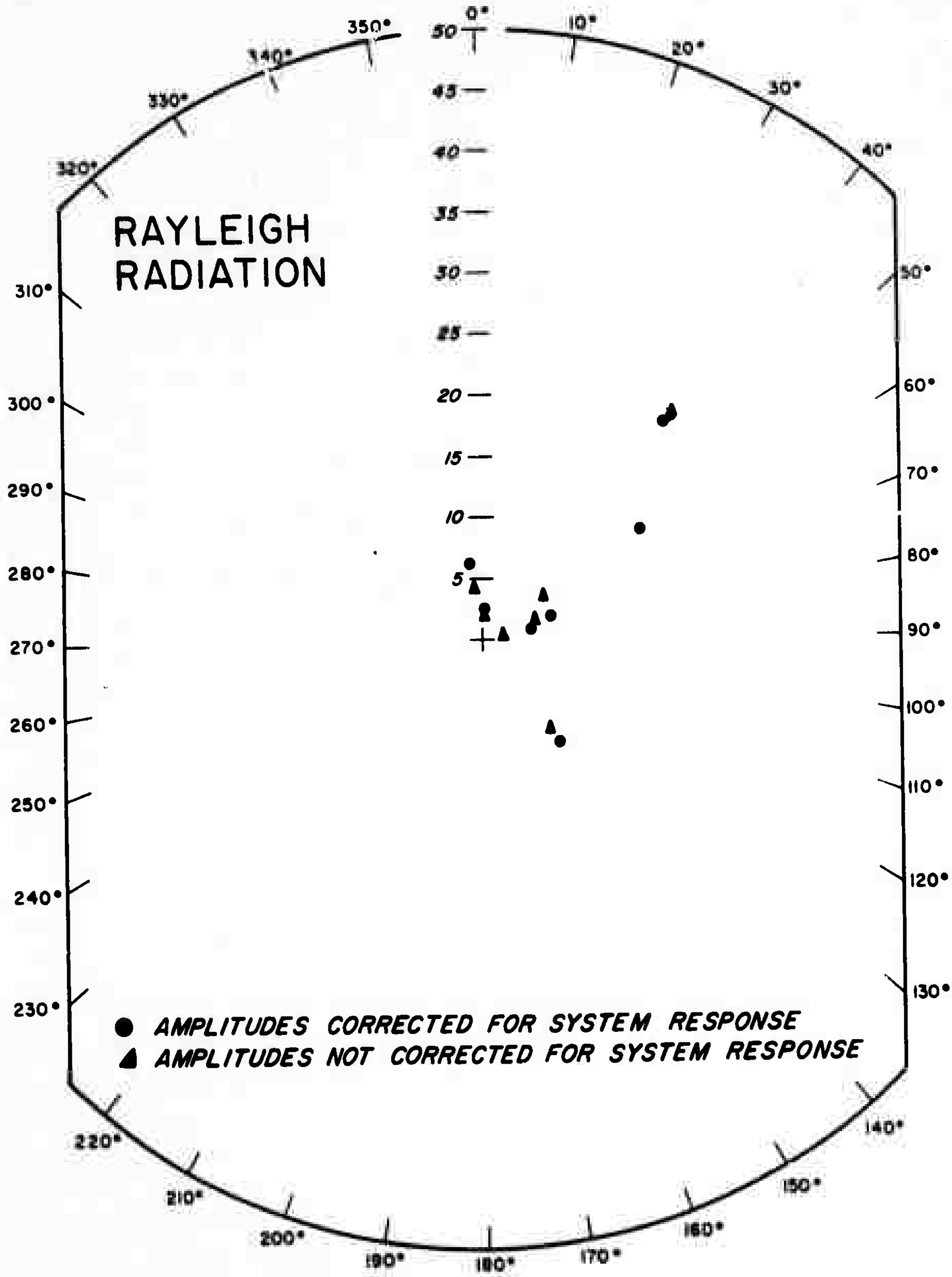

Figure 55. Rayleigh radiation pattern for the southern Nevada earthquake of 18 August 1966 (17:35Z).

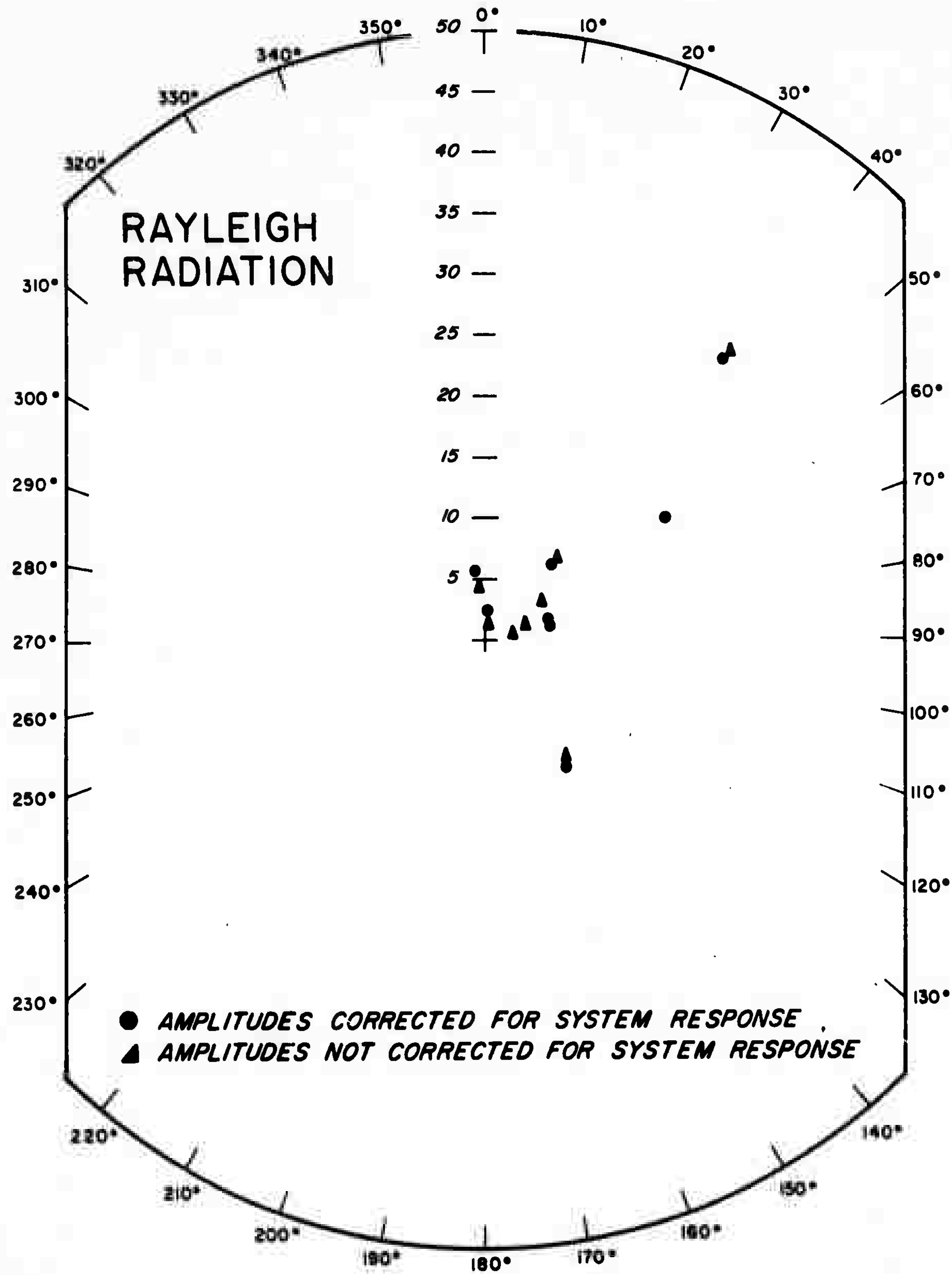

Figure 56. Rayleigh radiation pattern for the southern Nevada earthquake of 19 August 1966 (10:15Z).

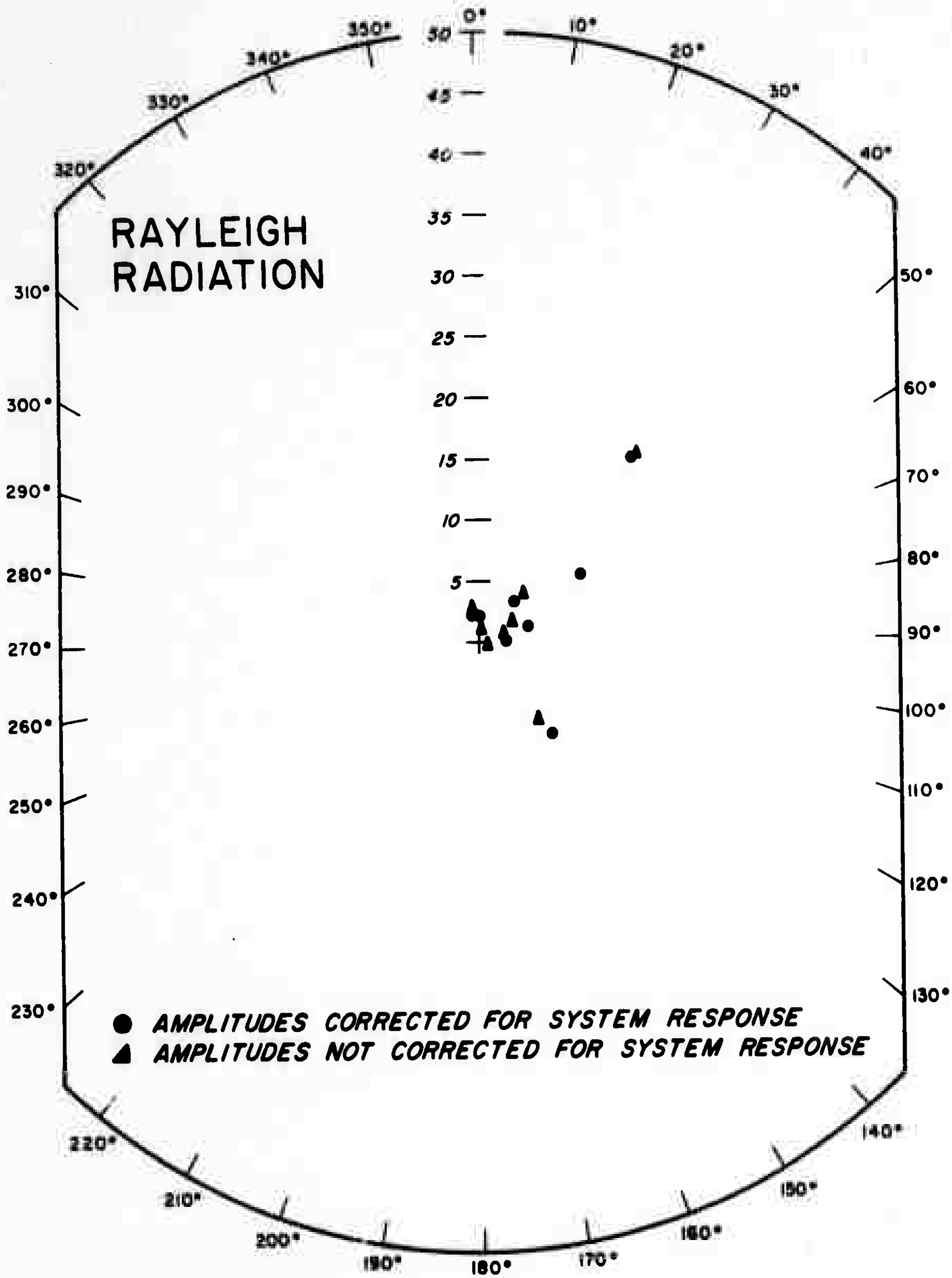

Figure 57. Rayleigh radiation pattern for the southern Nevada earthquake of 22 August 1966 (08:27Z).

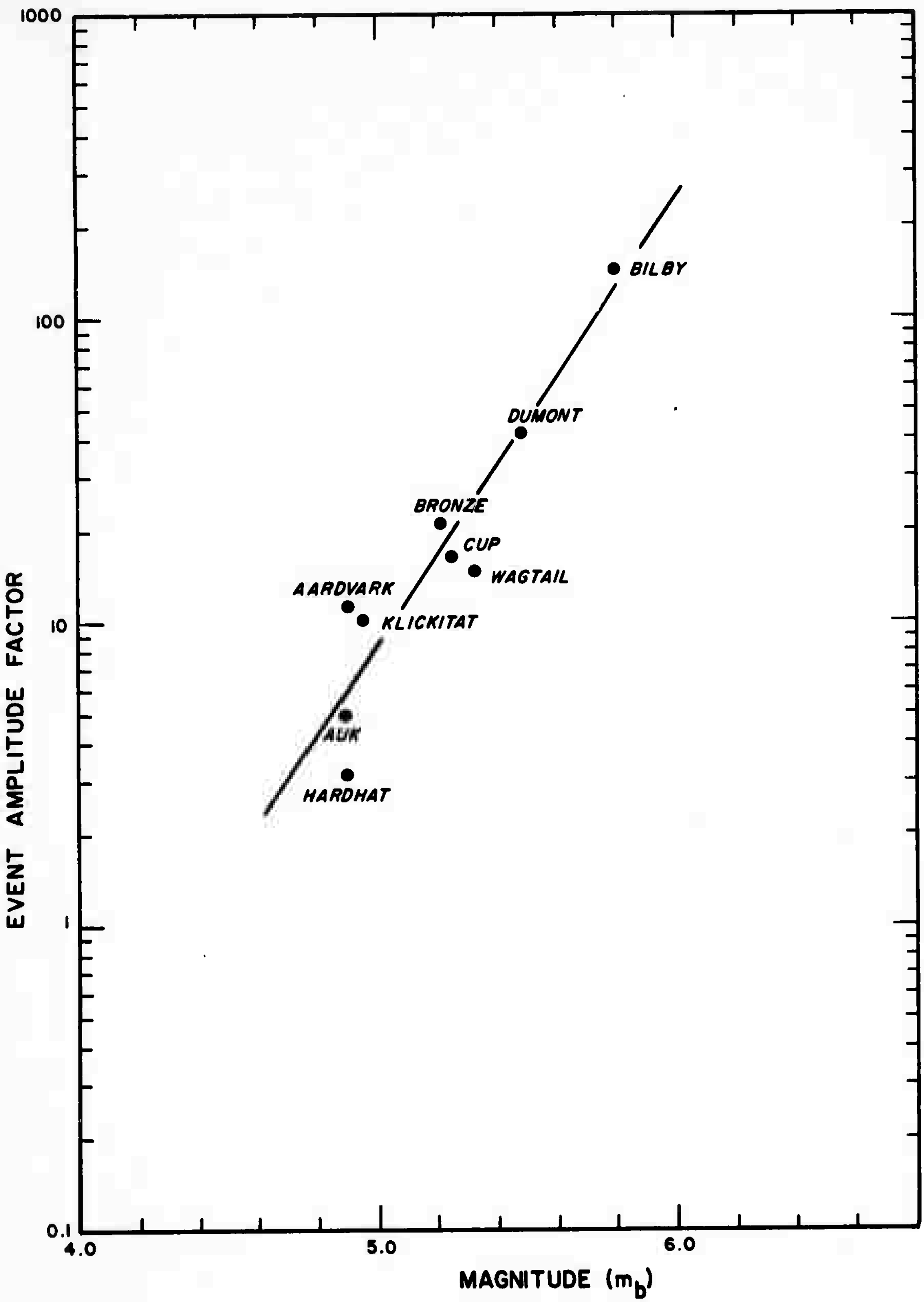

Figure 58. Event amplitude factors for Rayleigh waves as a function of body wave magnitude for some NTS explosion.

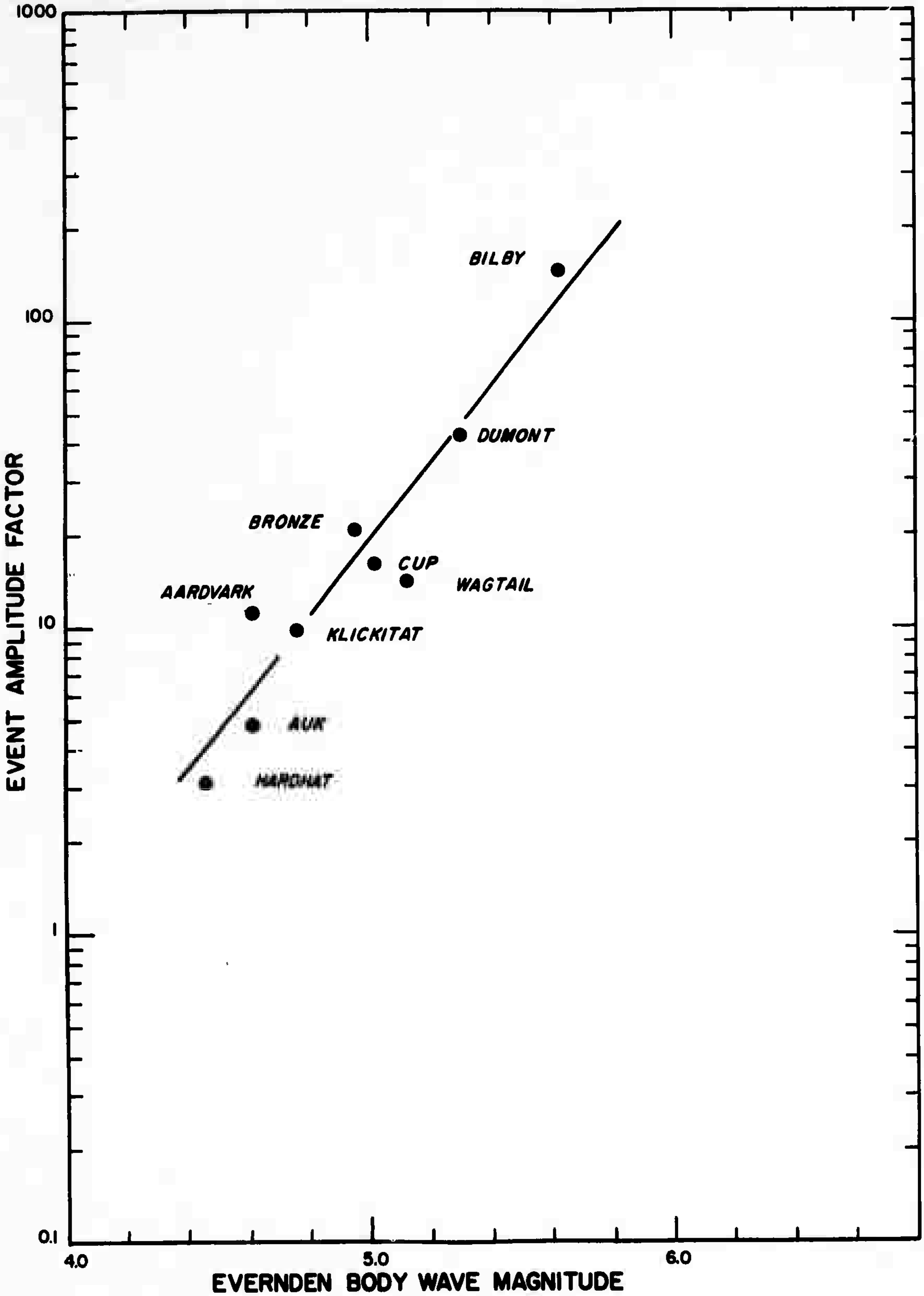

Figure 59. Event amplitude factors for Rayleigh waves as a function of Evernden's body wave magnitude for some NTS explosions.

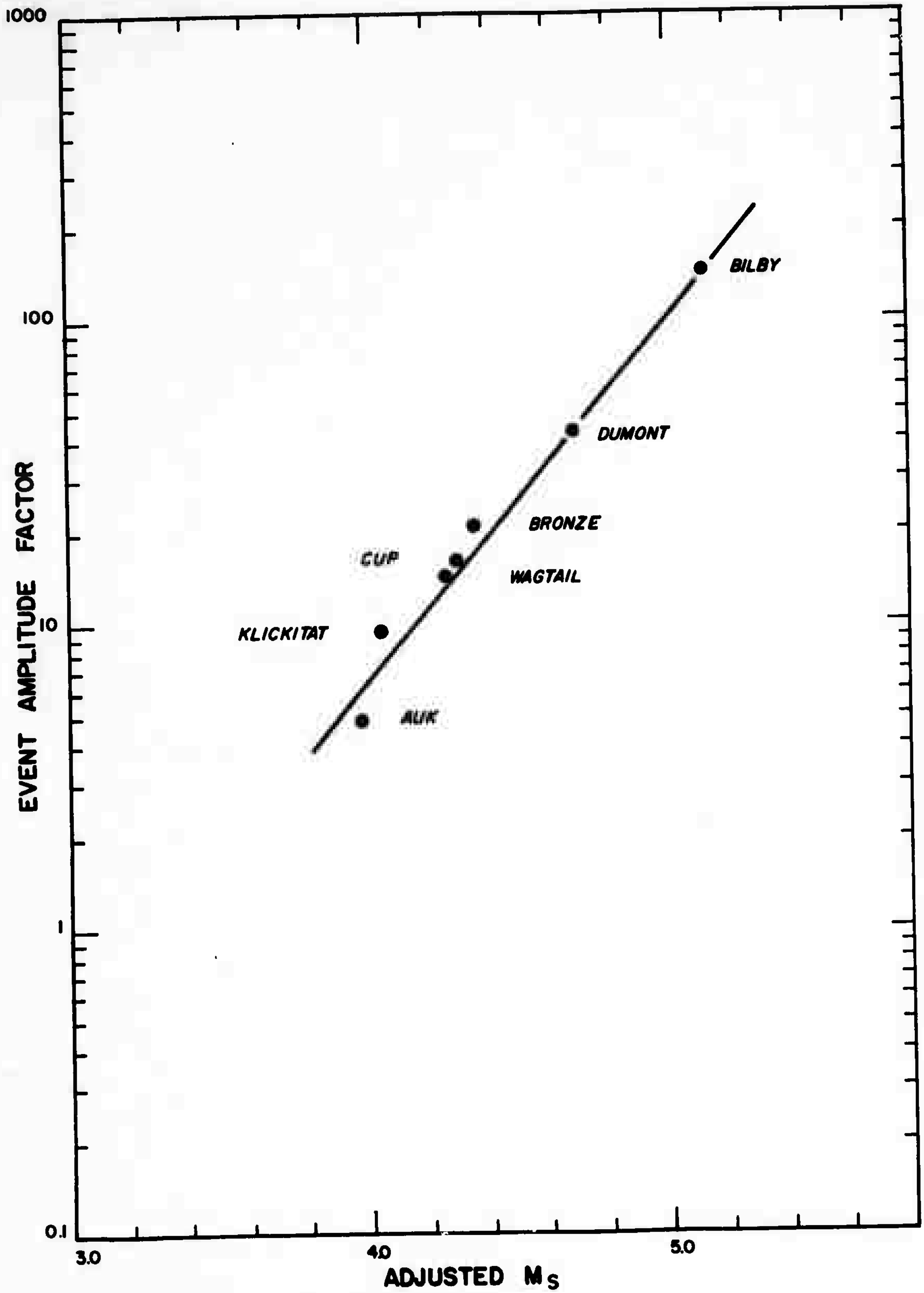

Figure 60. Event amplitude factors for Rayleigh waves as a function of the adjusted surface wave magnitude M_s.

APPENDIX

TABULATION OF LONG PERIOD DATA FOR SOME SOUTH NEVADA NUCLEAR EXPLOSIONS AND EARTHQUAKES

EVENT - AARDVARK

Station	2 x Magnification	Peak to Peak Amplitude (mm)	Period	Distance km	Azimuth Epicenter to Station (Deg)
DR-CO	24.20	28.5	14.0	733	84
HL-ID	23.00	25.0	11.0	746	11
PT-OR	15.96	30.5	12.0	979	347
LC-NM	21.40	46.5	10.5	1006	118
LP-TX	20.40	25.0	13.0	1755	115

EVENT - AUK

Station	2 x Magnification	Peak to Peak Amplitude (mm)	Period	Distance km	Azimuth Epicenter to Station (Deg)
SG-AZ	27.16	43.0	10.0	294	122
JR-AZ	38.60	65.0	14.0	440	123
LG-AZ	24.50	35.0	13.5	501	125
SN-AZ	25.04	25.5	10.0	530	131
HR-AZ	38.40	46.5	10.5	544	118
WO-AZ	42.00	56.0	12.0	544	115
NL-AZ	13.72	24.5	12.0	591	101
GE-AZ	26.06	29.0	10.0	618	125
DR-CO	12.20	10.0	14.0	730	84
LC-NM	24.00	22.5	10.5	1005	118
GV-TX	34.4	24.0	12.5	1794	99

Station	2 x Magnification	Peak to Peak Amplitude (mm)	Period	Distance km	Azimuth Epicenter To Station (deg)
CP-CL	2.13	67.0	10.5	482	184
MV-CL	4.00	124.0	10.5	520	299
BX-UT	2.70	104.0	15.5	586	93
DR-CO	4.02	99.5	15.5	732	84
HL-ID	5.38	81.0	11.0	747	11
RT-NM	3.59	68.5	13.5	1039	89
FR-MA	4.60	45.0	13.0	1282	35
TK-WA	7.60	87.5	14.5	1336	349
SK-TX	4.00	56.5	15.0	1426	94
DU-OK	2.16	20.5	16.5	1831	95
RK-ON	6.30	22.0	11.5	2343	42

EVENT - BILBY COLLAPSE

Station	2 x Magnification	Peak to Peak Amplitude (mm)	Period	Distance km	Azimuth Epicenter to Station (Deg)
CP-CL	21.30	56.0	12.0	482	184
MV-CL	37.20	95.0	12.0	520	299
BX-UT	27.00	61.5	15.5	586	93
DR-CO	40.20	69.0	15.0	732	84
HL-ID	53.80	111.5	14.0	747	11
RT-NM	35.90	47.5	16.0	1039	89
FR-MA	46.00	66.0	14.5	1282	35
TK-WA	76.40	76.0	16.0	1336	349
SK-TX	41.00	36.0	16.0	1426	94
DU-OK	21.60	13.0	16.5	1831	95

EVENT - CORDUROY COLLAPSE

Station	2 x Magnification	Peak to Peak Amplitude (mm)	Period	Distance km	Azimuth Epicenter to Station (Deg)
TFSO	6.00	14.8	14.0	538	125
SW-MA	9.60	11.3	11.5	1353	13
RG-SD	64.00	65.0	12.5	1377	46
WN-SD	46.00	52.5	18.0	1507	58
CR-NB	8.92	16.5	12.5	1706	71
KC-MO	9.36	12.0	13.0	1883	76

EVENT - BRONZE

Station	2 x Magnification	Peak to Peak Amplitude (mm)	Period	Distance km	Azimuth Epicenter to Station (Deg)
SG-AZ	18.46	111.5	9.5	297	122
JR-AZ	4.32	27.0	14.0	443	123
LG-AZ	18.24	125.0	13.5	504	125
TFSO	6.00	22.5	14.0	532	124
SN-AZ	5.40	27.0	11.0	533	131
WO-AZ	7.76	63.5	11.0	546	115
HR-AZ	5.66	36.5	9.5	546	118
NL2AZ	6.50	46.5	11.5	592	102
GE-AZ	7.80	32.8	12.0	621	125
HL2ID	8.50	23.0	13.0	731	10
LC-NM	15.20	67.0	10.0	1008	118
GV-TX	4.78	12.5	12.5	1796	99
RK-ON	46.00	30.5	12.0	2341	42

EVENT - DUMONT

Station	2 x Magnification	Peak to Peak Amplitude (mm)	Period	Distance km	Azimuth Epicenter to Station (Deg)
SW-MA	7.20	20.0	12.0	1359	13
RG-SD	19.52	72.0	12.5	1381	45
WN-SD	6.60	18.0	13.5	1510	58
CR-NB	8.92	50.0	11.5	1709	71
JP-AT	8.76	41.5	12.0	1762	355
KC-MO	7.92	35.0	14.0	1885	76

EVENT - CUP

Station	2 x Magnification	Peak to Peak Amplitude (mm)	Period	Distance km	Azimuth Epicenter to Station (Deg)
SG-AZ	2.90	16.5	9.5	300	123
JR-AZ	3.86	19.3	15.0	447	124
LG-AZ	2.12	9.5	14.0	508	125
TFSO	16.00	49.5	15.0	536	125
WO-AZ	10.50	41.3	10.5	550	116
HR-AZ	4.60	18.0	9.5	550	118
NL2AZ	4.10	15.0	11.0	594	103
HL2ID	8.36	21.5	13.0	726	10
LC-NM	14.12	43.0	9.5	1011	119
RK-ON	69.80	30.8	11.0	2337	42

EVENT - DUMONT COLLAPSE

Station	2 x Magnification	Peak to Peak Amplitude (mm)	Period	Distance km	Azimuth Epicenter to Station (Deg)
TFSO	8.00	13.8	15.0	535	124
SW-MA	79.00	70.5	14.0	1359	13
RG-SD	19.52	30.3	12.5	1381	45
WN-SD	66.00	94.3	18.0	1510	58
CR-NB	8.92	13.5	13.0	1709	71
JP-AT	8.76	8.0	12.5	1762	355
KC-MO	7.92	7.8	16.0	1885	76

EVENT - HALF BEAK COLLAPSE

Station	2 x Magnification	Peak to Peak Amplitude (mm)	Period	Distance km	Azimuth Epicenter to Station (Deg)
RG-SD	20.10	39.0	15.0	1381	47
WN-SD	68.00	86.0	18.0	1517	59
CR-NB	6.32	14.5	13.0	1722	72
JP-AT	8.54	13.0	13.0	1738	356
KC-MO	8.00	15.5	14.5	1900	.77

EVENT - KLICKITAT

Station	2 x Magnification	Peak to Peak Amplitude (mm)	Period	Distance km	Azimuth Epicenter to Station (Deg)
CP-CL	20.70	52.5	10.0	491	184
BX-UT	10.24	20.5	13.0	587	84
DR-CO	41.80	51.5	13.5	732	85
HL-ID	45.60	63.0	12.5	737	11
LC-NM	6.52	12.5	10.5	1011	119
RT-NM	34.40	28.0	13.0	1041	89
FR-MA	40.60	25.0	11.0	1275	36
SK-TX	29.60	17.8	15.5	1428	95

EVENT - HARDHAT

Station	2 x Magnification	Peak to Peak Amplitude (mm)	Period	Distance km	Azimuth Epicenter to Station (Deg)
HL-ID	21.80	9.5	16.0	729	11
DR-CO	47.00	25.5	13.0	734	85
PT-OR	12.32	4.9	14.0	961	347
LC-NM	37.00	30.5	11.5	1017	119
LP-TX	38.40	21.0	14.5	1765	116

EVENT - EARTHQUAKE 18 August 1966 (09:15)

Station	2 x Magnification	Peak to Peak Amplitude (mm)	Period	Distance km	Azimuth Epicenter to Station (Deg)
TFO	8.00	69.5	21.5	421	142
SW-MA	64.00	80.0	11.5	1308	7
WN-SD	7.10	16.0	25.0	1353	56
CR-NB	7.60	21.0	13.0	1538	71
KC-MO	7.98	10.0	11.0	1711	76
JP-AT	8.38	24.0	13.5	1762	351
RK-ON	9.84	17.5	21.0	2210	41

EVENT - WAGTAIL

Station	2 x Magnification	Peak to Peak Amplitude (mm)	Period	Distance km	Azimuth Epicenter to Station (Deg)
SG-AZ	3.20	14.0	9.5	295	122
JR-AZ	3.80	17.0	14.0	442	123
SN-AZ	3.34	11.0	10.0	531	131
HR-AZ	4.64	15.0	9.5	545	118
NL2AZ	16.04	80.0	11.0	591	102
HL2ID	6.84	11.2	13.0	735	10

EVENT - EARTHQUAKE 19 August 1966 (10:51)

Station	2 x Magnification	Peak to Peak Amplitude (mm)	Period	Distance km	Azimuth Epicenter to Station (Deg)
TFO	8.00	35.5	19.0	430	143
RG-SD	2.72	5.2	17.0	1238	42
SW-MA	68.80	15.0	12.0	1297	7
WN-SD	7.04	7.5	13.0	1346	57
CR-NB	8.18	8.3	13.0	1534	71
KC-MO	79.20	35.8	12.5	1708	77
JP-AT	7.92	6.8	14.0	1751	351
RK-ON	9.84	16.0	14.5	2202	41

EVENT - EARTHQUAKE 18 August 1966 (17:35)

Station	2 x Magnification	Peak to Peak Amplitude (mm)	Period	Distance km	Azimuth Epicenter to Station (Deg)
TFO	8.00	27.0	17.5	435	142
SW-MA	64.00	21.0	14.0	1298	7
WN-SD	7.10	8.0	14.0	1353	56
CR-NB	7.60	11.0	14.5	1543	71
KC-MO	81.00	28.2	12.5	1717	77
JP-AT	8.38	7.5	14.0	1750	351
RK-ON	9.84	12.5	15.0	2208	41

EVENT - EARTHQUAKE 22 August 1966 (08:27)

Station	2 x Magnification	Peak to Peak Amplitude (mm)	Period	Distance km	Azimuth Epicenter to Station (Deg)
TFO	8.00	24.0	17.5	427	141
RG-SD	22.40	26.0	18.5	1252	42
SW-MA	59.60	12.5	13.0	1309	7
WN-SD	7.58	4.5	13.0	1360	57
CR-NB	72.20	44.5	12.0	1546	71
KC-MO	79.20	15.0	12.5	1720	76
JP-AT	86.00	46.5	17.0	1761	351
RK-ON	9.02	9.5	14.5	2216	41